

# **Final Report for Hydro Research**

**Project Topic: Investigate the Performance and Cost Benefits of Using a Magnetically Geared Generator (MGG) for a Hydropower Generator**

Award covering period: 06/01/2017-05/31/2018

Student Name: Kang Li

Email: [kli10@uncc.edu](mailto:kli10@uncc.edu)

Advisor: Jonathan Bird

Email: [J.Bird@uncc.edu](mailto:J.Bird@uncc.edu)

## Table of Contents

1. Principles of Magnetic Gear .....	3
1.1 Co-axial flux focusing magnetic gear .....	3
1.2 Multi-stage Magnetic Gear Design .....	4
2. Summary of Design Analysis Completed .....	6
3. Ideal Stage 1 Magnetic Gear Design Analysis with a Pole Pair Combination of 11-71-60.....	7
4. Stage 1 Ideal Magnetic Gear Design with Extended Magnet .....	13
5. Flux Concentration Magnetic Gearbox Rotor Design Analysis .....	19
6. Ideal Stage 1 Magnetic Gear Design Analysis with a Pole Pair Combination of 12-78-66.....	23
7. Stage 1 Magnetic Gear Design with Extra Radial Flux .....	32
7.1 Initial design of the stage 1 magnetic gear .....	32
7.1.1 Force and deflection analysis .....	37
7.2 Final design of the stage 1 magnetic gear .....	44
7.2.1 Loss analysis.....	45
7.2.2 Force and deflection analysis .....	47
8. Stage 2 MG Design without Stator.....	55
8.1 Initial design of the stage 1 magnetic gear .....	55
8.1.1 Force and deflection analysis .....	64
8.1.2 Loss analysis.....	67
8.2 Final design of the stage 1 magnetic gear .....	70
8.2.1 Force and deflection analysis .....	72
9. Stage 2 MG Design with Stator .....	78
9.1 Fractional winding design for different number of slots .....	78
9.2 Winding function.....	83
9.3 Performance comparison between different stator designs.....	87
10. Cost of the Multistage Magnetic Gear .....	89
11. Scaling Analysis .....	91
12. Summary and Future Work.....	93

# Multi-stage Magnetic Gearbox design

## 1. Principles of Magnetic Gear

### 1.1 Co-axial flux focusing magnetic gear

The co-axial flux focusing magnetic gear (MG) is shown in Figure 1-1 which uses the flux focusing topology. The inner rotor (rotor 1) has  $p_1$  pole pairs with a rotational speed  $\omega_1$ . The cage rotor (rotor 2) has  $n_2$  pole pairs with a rotational speed  $\omega_2$ . The outer rotor (rotor 3) has  $p_3$  pole pairs with a rotational speed  $\omega_3$ .

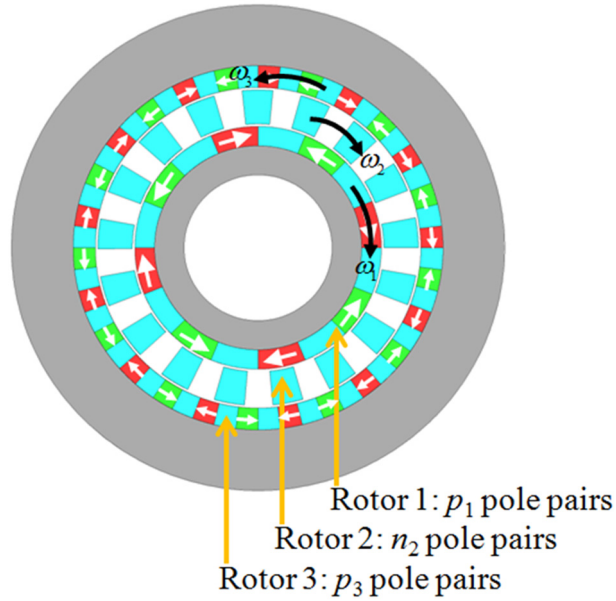


Figure 1-1. A co-axial MG with  $p_1 = 4$ ,  $n_2 = 17$  and  $p_3 = 13$ .

In order to make the MG to work, the angular velocity relationship must satisfy:

$$p_1\omega_1 + p_3\omega_3 = n_2\omega_2 \quad (1.1)$$

and

$$p_1 + p_3 = n_2 \quad (1.2)$$

The outer rotor is fixed as a stationary part ( $\omega_3 = 0$ ). Then equation (1.1) becomes:

$$p_1\omega_1 = n_2\omega_2 \quad (1.3)$$

The gear ratio,  $G_r$  can be calculated as:

$$G_{12} = \frac{\omega_1}{\omega_2} = \frac{n_2}{p_1} = \frac{p_1 + p_3}{p_1} \quad (1.4)$$

Neglecting losses the power relationship between rotors is:

$$T_1\omega_1 + T_2\omega_2 + T_3\omega_3 = 0 \quad (1.5)$$

where  $T_1$ ,  $T_2$  and  $T_3$  are the torque on rotor 1, rotor 2 and rotor 3, respectively. And the torque within the MG satisfies:

$$T_1 + T_2 + T_3 = 0 \quad (1.6)$$

The active region volumetric torque density of a rotary machine can be calculated by

$$T_v = \frac{T_2}{\pi r_{o3}^2 d} \quad (1.7)$$

where  $r_{o3}$  = outer radius of rotor 3 and  $d$  = axial length.

The mass torque density can be calculated by

$$T_m = \frac{T_2}{m_s + m_m} \quad (1.8)$$

where  $m_s$  = mass of steel and  $m_m$  = mass of magnets.

### 1.2 Multi-stage Magnetic Gear Design

The multi-stage magnetic gear (MSMG) is being designed to have a 59:1 gear ratio so that the performance of the MSMG can be directly compared with a 59:1 Nabtesco mechanical cycloidal gearbox which is shown in Figure 1-2 which is being used as the comparative gearbox.

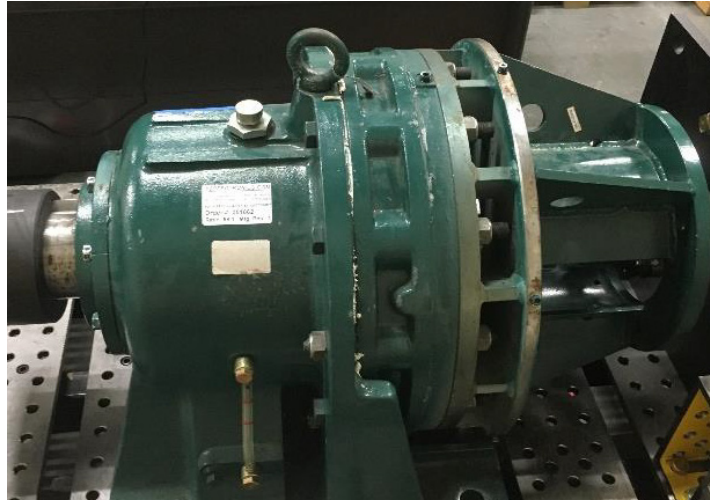


Figure 1-2. Sumitomo cyclo inline 59:1 ratio mechanical gearbox reducer model CHHJ-4225Y-59-320TC

Both of the stage 1 and stage 2 MGs use the same topology as shown in Figure 1-1. The pole pairs and rotational speed of the stage 2 MG are related by

$$p_4 + p_6 = n_5 \quad (1.9)$$

$$p_4\omega_4 + p_6\omega_6 = n_5\omega_5 \quad (1.10)$$

Similarly, the gear ratio of stage 2 is calculated by

$$G_{45} = \frac{n_5}{p_4} = \frac{\omega_4}{\omega_5} \quad (1.11)$$

Since rotor 1 and rotor 5 is connected, this gives

$$\omega_1 = \omega_5 \quad (1.12)$$

Therefore, the combined gear ratio of the MSMG is

$$G_r = G_{12}G_{45} = \frac{\omega_4}{\omega_2} = \frac{n_2n_5}{p_1p_4} \quad (1.13)$$

## **2. Summary of Design Analysis Completed**

The operating principles of MGs have been explained in section 1. In section 3, the ideal MG design will be discussed with a pole pair combination of 11-71-60. The parameter sweeping analysis has been conducted. In section 4, another design with extended magnets is discussed. The flux concentration topology will be discussed in section 5. In order to reduce the simulation time, especially when doing the loss analysis in 3-D, a new pole pair combination (12-78-66) has been chosen so that the MG can be simulated in a 1/6 model which is present in section 6. In section 7, a MG with extra radial flux will be introduced and the performance will be evaluated. The deflection and loss are also discussed. In section 8, the stage 2 MG will be discussed which uses a similar topology as stage 1 MG. The mechanical deflection of the rods and the efficiency will be calculated. In section 9, the stator will be added inside the stage 2 MG. The fractional winding distribution will be designed. The cost and scaling analysis are discussed in section 10 and section 11, respectively.

### 3. Ideal Stage 1 Magnetic Gear Design Analysis with a Pole Pair Combination of 11-71-60

In this section, a MG with pole pair combination ( $p_1 = 11$ ,  $n_2 = 71$  and  $p_3 = 60$ ) has been chosen and the performance has been evaluated and optimized. The outer radius of the outer rotor,  $r_{o3}$  is fixed at 270 mm and the inner radius of the inner rotor,  $r_{i1}$  is fixed at 100 mm which is shown in Figure 3-1 and the geometry parameters are described in Figure 3-2. The axial length  $d$  75 mm and the air gap  $g$  is 1 mm. A parameter sweeping analysis has been conducted for the outer radius of the inner rotor,  $r_{o1}$  and the radial length of the cage rotor,  $l_2$ . The material property is described in Table 3-I.

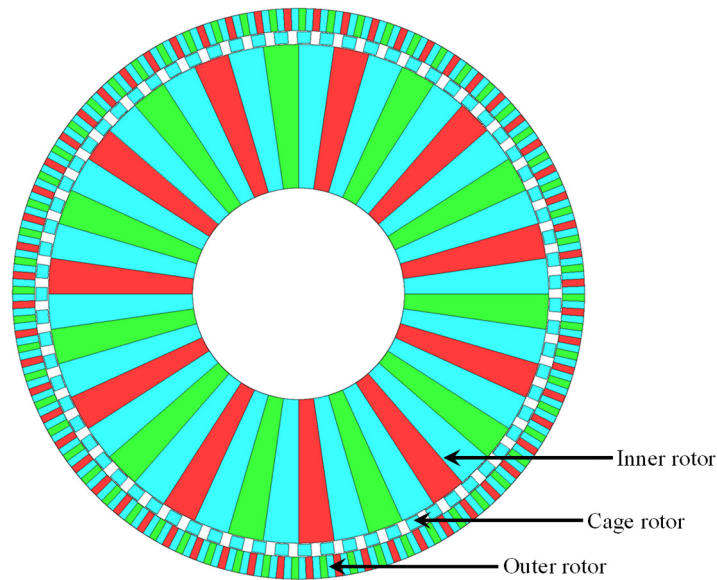


Figure 3-1. Stage 1 MG with  $r_{i1}$  fixed at 100 mm and  $r_{o3}$  fixed at 270 mm.

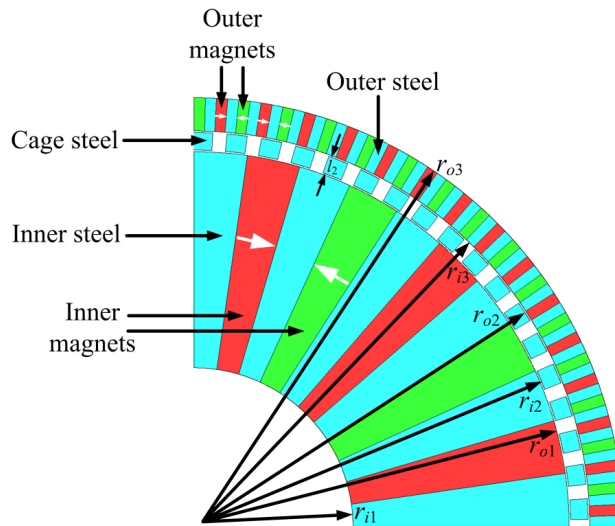
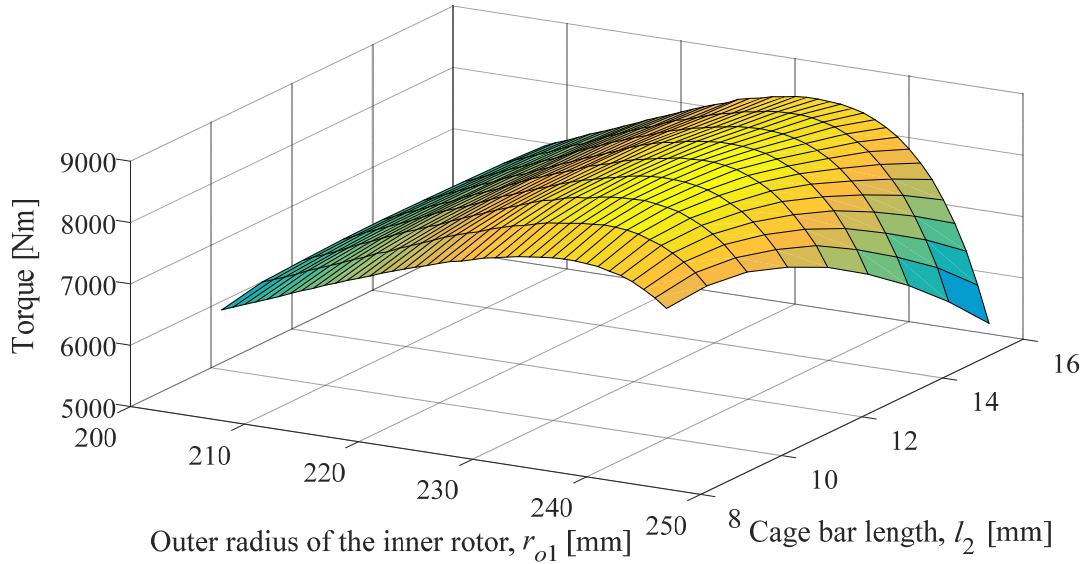


Figure 3-2. Geometry parameters for stage 1 MG.

**Table 3-I. Material properties.**

Description		Density [kg/m <sup>3</sup> ]	Conductivity [S/m]
Steel	Lamination, M 19 C5 G26	7850	0
Magnet	NdFeB, NMX40CH ( $B_r = 1.25$ T)	7600	625000

The  $r_{o1}$  and  $l_2$  are varied and the peak values of torque and torque densities are chosen which are shown in Figure 3-3-Figure 3-6.



**Figure 3-3. Parameter sweep for the torque value.**

Peak position:  $r_{i1} = 100$  mm,  $r_{o1} = 236$  mm,  $r_{i2} = 237$  mm,  $r_{o2} = 248$  mm,  $r_{i3} = 249$  mm,  $r_{o3} = 270$  mm. Peak value: 8816.29 Nm.

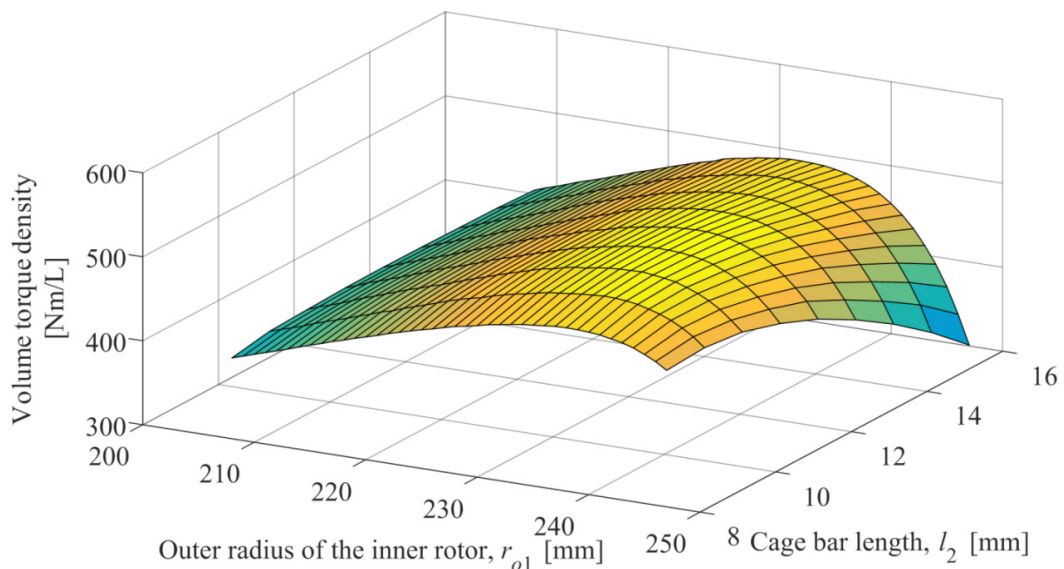


**Figure 3-4. Parameter sweep for the volume torque density.**

Peak position:  $r_{i1} = 100$  mm,  $r_{o1} = 236$  mm,  $r_{i2} = 237$  mm,  $r_{o2} = 248$  mm,  $r_{i3} = 249$  mm,  $r_{o3} = 270$  mm. Peak value: 513.27 Nm/L.

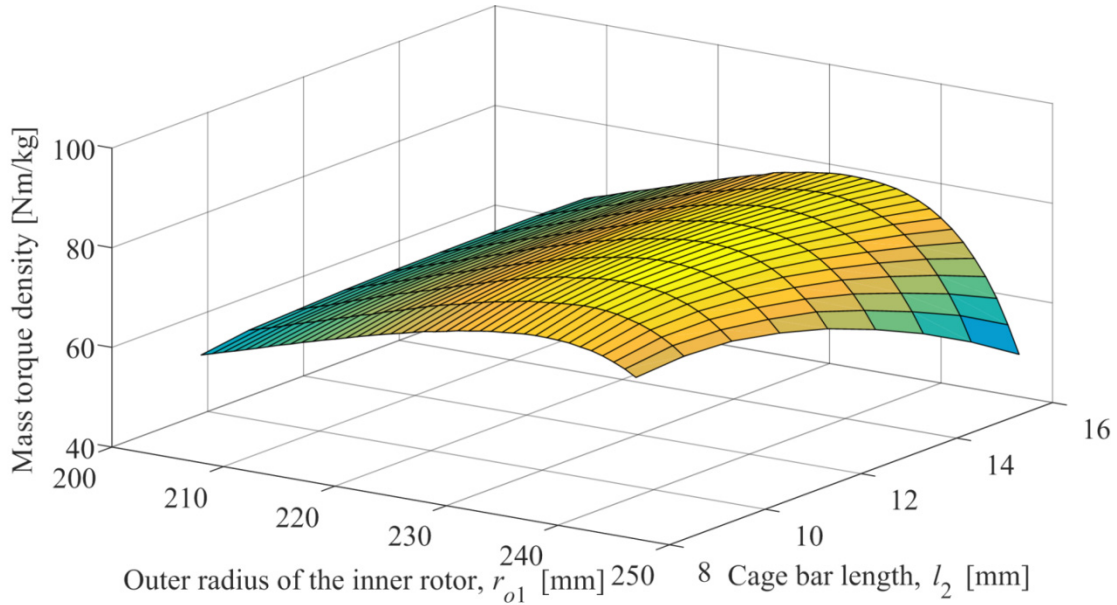


Figure 3-5. Parameter sweep for the mass torque density.

Peak position:  $r_{i1} = 100$  mm,  $r_{o1} = 236$  mm,  $r_{i2} = 237$  mm,  $r_{o2} = 248$  mm,  $r_{i3} = 249$  mm,  $r_{o3} = 270$  mm. Peak value: 80.99 Nm/kg.

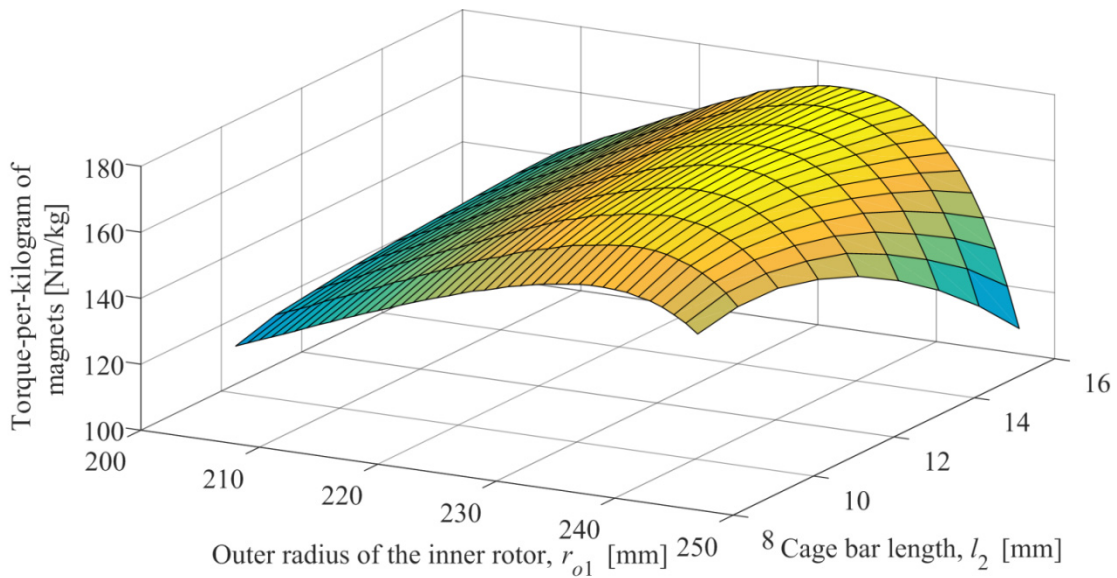


Figure 3-6. Parameter sweep for the torque-per-kilogram of magnet.

Peak position:  $r_{i1} = 100$  mm,  $r_{o1} = 237$  mm,  $r_{i2} = 238$  mm,  $r_{o2} = 250$  mm,  $r_{i3} = 251$  mm,  $r_{o3} = 270$  mm. Peak value: 174.86 Nm/kg.

The parameters are chosen so that the peak torque value is obtained. The torque plots are shown in Figure 3-7-Figure 3-9 when both of the cage and inner rotors are rotating. The torque ripples for the inner, cage and outer rotors are low.

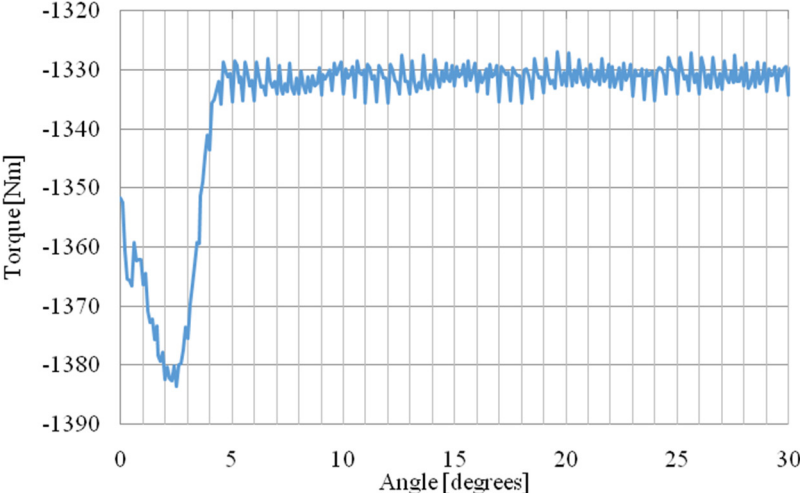


Figure 3-7. Torque on the inner rotor.

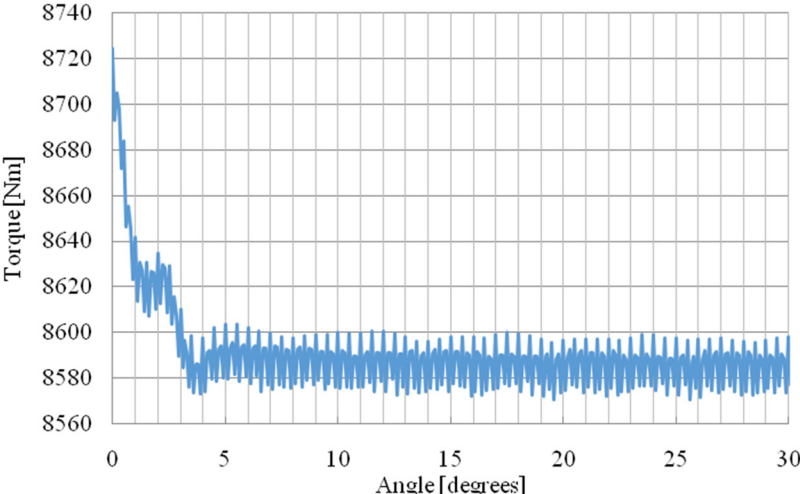


Figure 3-8. Torque on the cage rotor.

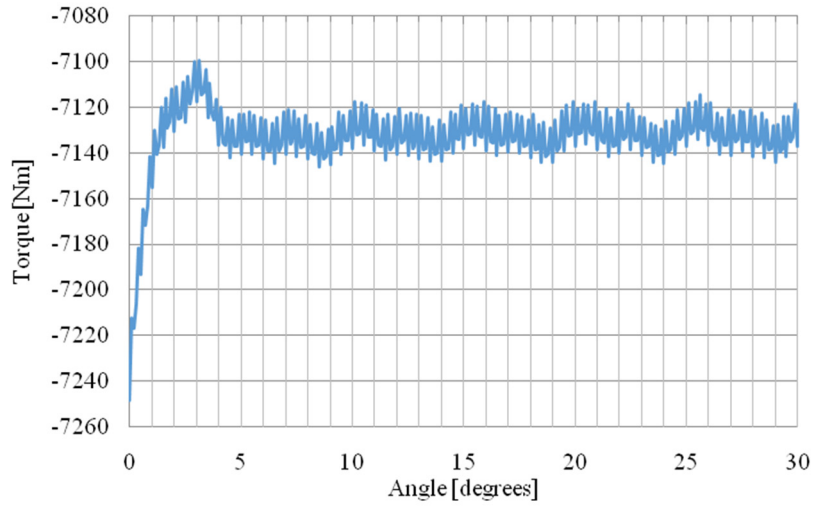


Figure 3-9. Torque on the outer rotor.

The mass and volume torque density plot is shown in Figure 3-10. It clearly shows that there is a limit for achieving high mass and volume torque densities.

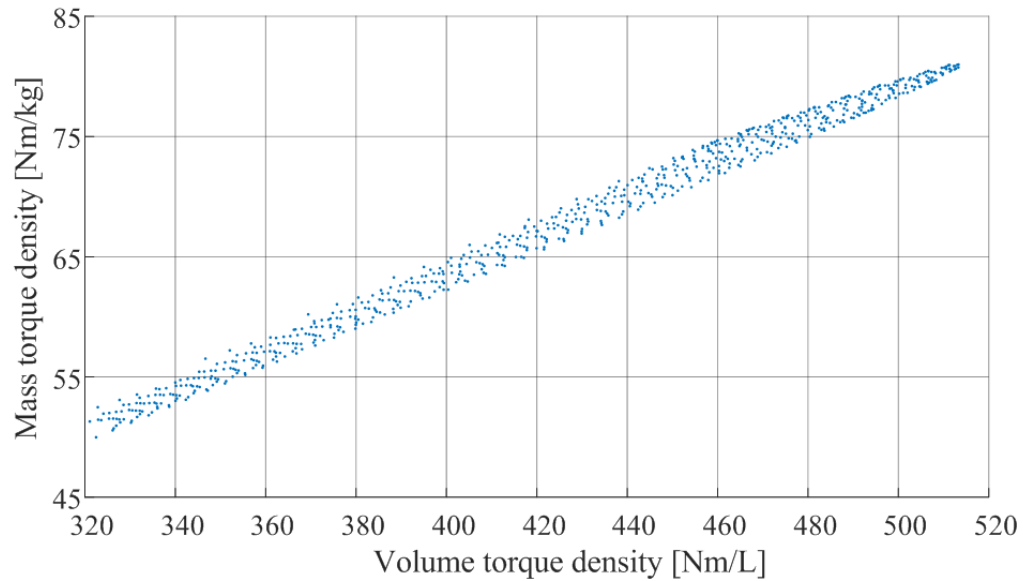


Figure 3-10. Mass and volume torque density when  $r_{f1} = 100$  mm.

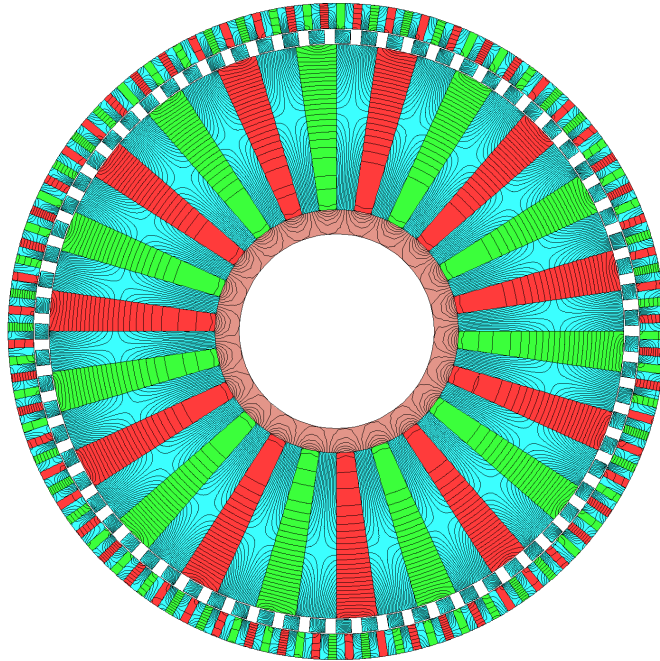


Figure 3-11. Magnetic flux lines.

#### 4. Stage 1 Ideal Magnetic Gear Design with Extended Magnet

In this section, a MG design with extended magnets is present. From Figure 3-11, a lot of the flux is going into the inner steels and then go radially inward which has no contribution to the torque. Therefore, the length of the inner and outer steels can be reduced which is shown in Figure 4-1. It can have two benefits:

- a. A higher torque can be achieved.
- b. The total mass can be reduced.

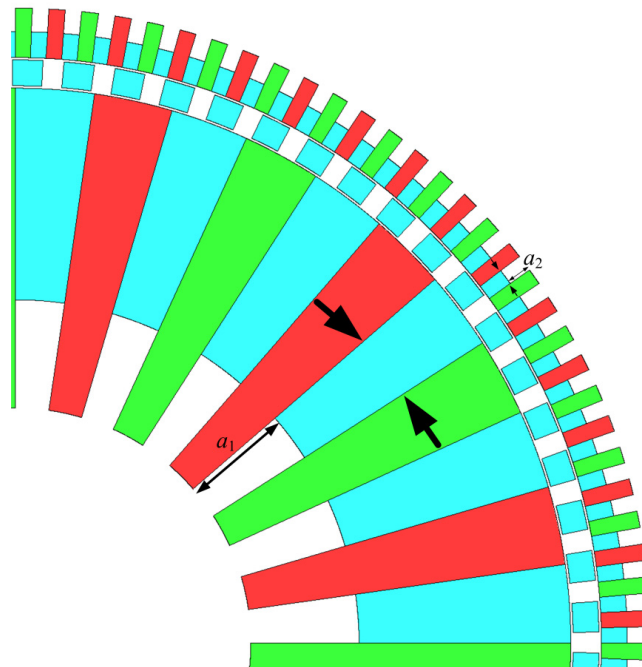


Figure 4-1. MG with reduced length of steel.

$a_1$  and  $a_2$  are the length of the inner and outer air region as shown in Figure 4-1. First,  $a_2$  is fixed at zero. The length of  $a_1$  is varied to obtain the peak torque which is shown in Figure 4-2. The peak torque is 9214.71 Nm when  $a_1 = 46$  mm. The new magnetic flux line plot is shown in Figure 4-3. It can be seen that more magnetic flux from the inner rotor is going radially outward.

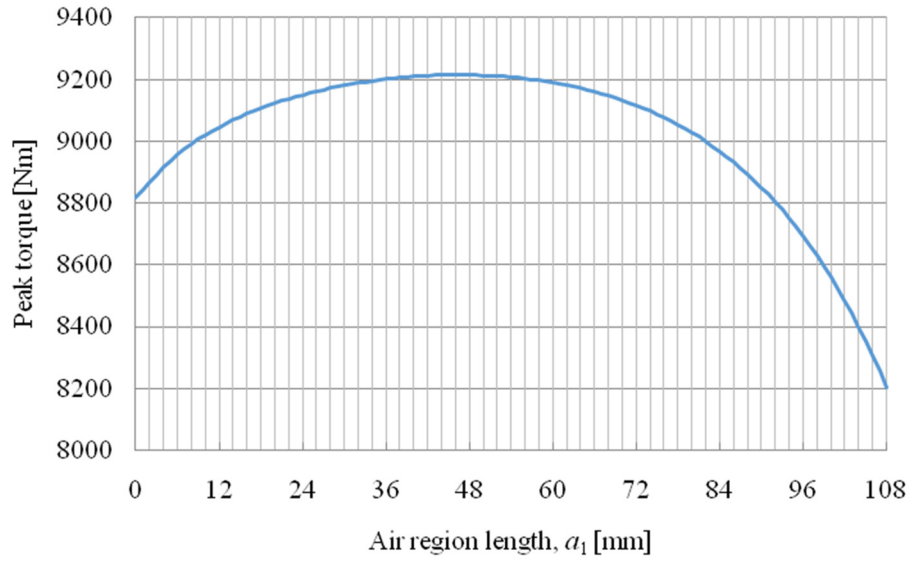


Figure 4-2. Peak torque with different values of  $a_1$ .

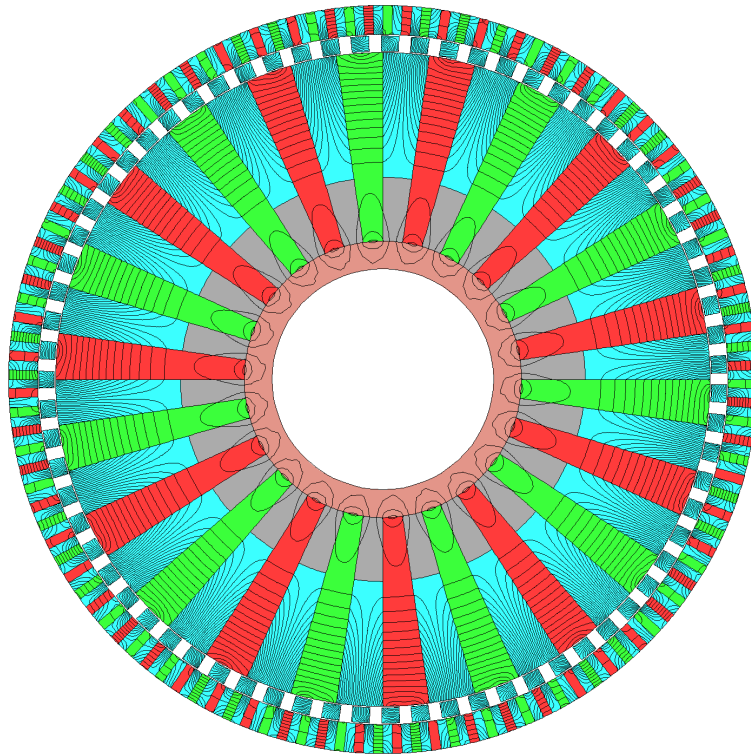


Figure 4-3. Magnetic flux lines with reduced length of steel when  $a_1 = 46$  mm.

Then  $a_2$  is varied with  $a_1$  fixed at 46 mm. The peak torque becomes 9550.51 Nm when  $a_2 = 5$  mm which is shown in Figure 4-4.

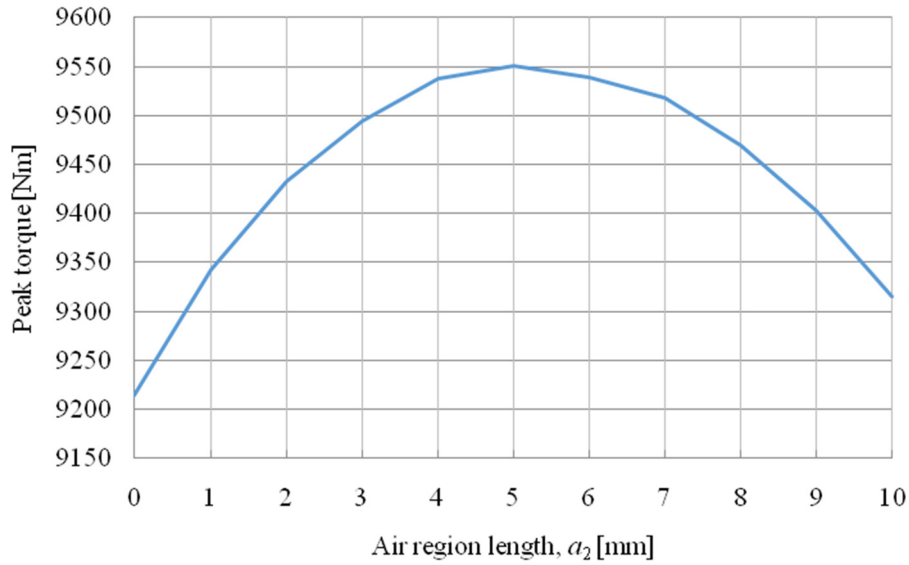


Figure 4-4. Peak torque with different values of  $a_2$ .

The Summary of the optimized design is shown in Table 4-I and Figure 4-6.

Table 4-I. Optimized parameters.

Description			Unit
Inner rotor	Inner radius, $r_{i1}$	100	mm
	Outer radius, $r_{o1}$	236	mm
	Pole pairs	11	-
	Air region length, $a_1$	46	mm
Cage rotor	Inner radius, $r_{i2}$	237	mm
	Outer radius, $r_{o2}$	248	mm
	Pole pairs	71	-
	Outer rotor	Inner radius, $r_{i3}$	249
	Outer radius, $r_{o3}$	270	mm
	Pole pairs	60	-
	Air region length, $a_2$	5	mm
Axial length, $d_1$		75	mm
Air gap, $g$		1	mm

The comparison for the designs without/with air regions is shown in Table 4-II and Figure 4-5.

Table 4-II. Performance comparison without/with air regions.

	Without air region	With optimized air region	Unit
Peak torque, $T_2$	8816.29	9550.51	Nm
Peak volume torque density, $T_{v1}$	513.27	556.30	Nm/L
Peak mass torque density, $T_{m1}$	80.99	99.58	Nm/kg

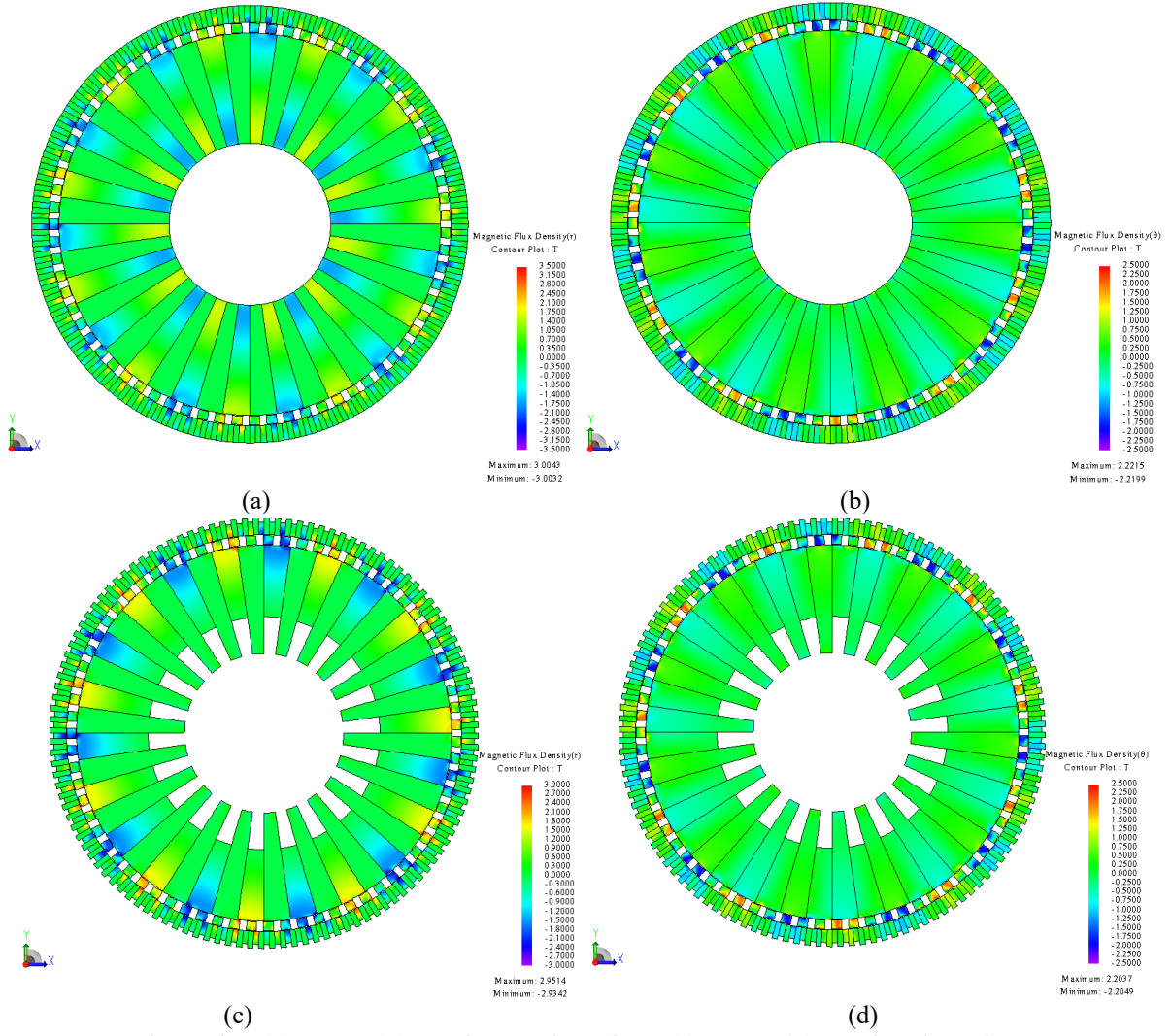


Figure 4-5. (a)  $B_r$  and (b)  $B_\theta$  without air regions. (c)  $B_r$  and (d)  $B_\theta$  with air regions.

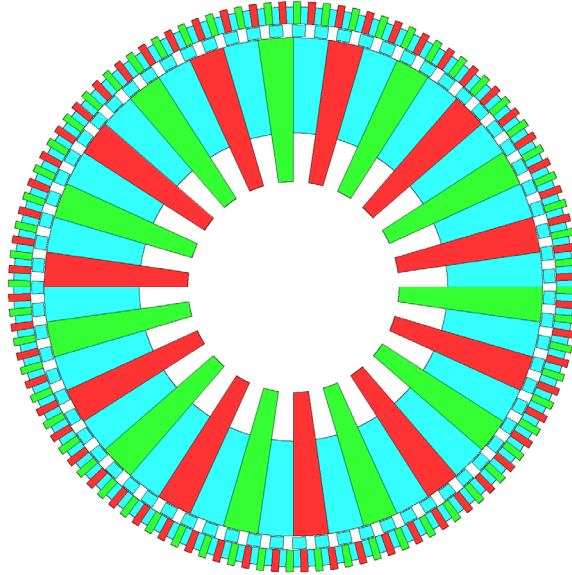


Figure 4-6. Optimized design with air regions.

The torque plots are shown in Figure 4-7-Figure 4-9 when the cage rotor is rotating at 33 RPM and the inner rotor is rotating at 213 RPM.

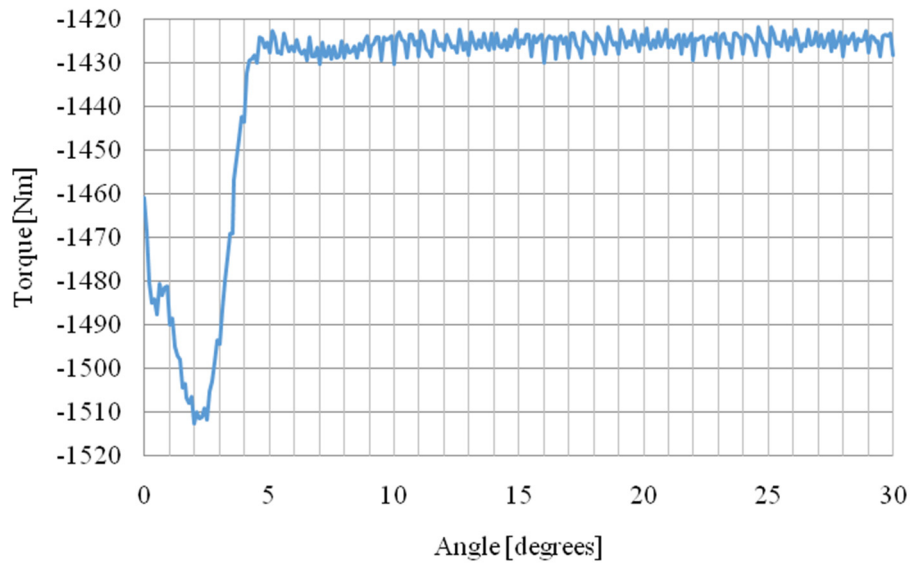


Figure 4-7. Torque on the inner rotor.

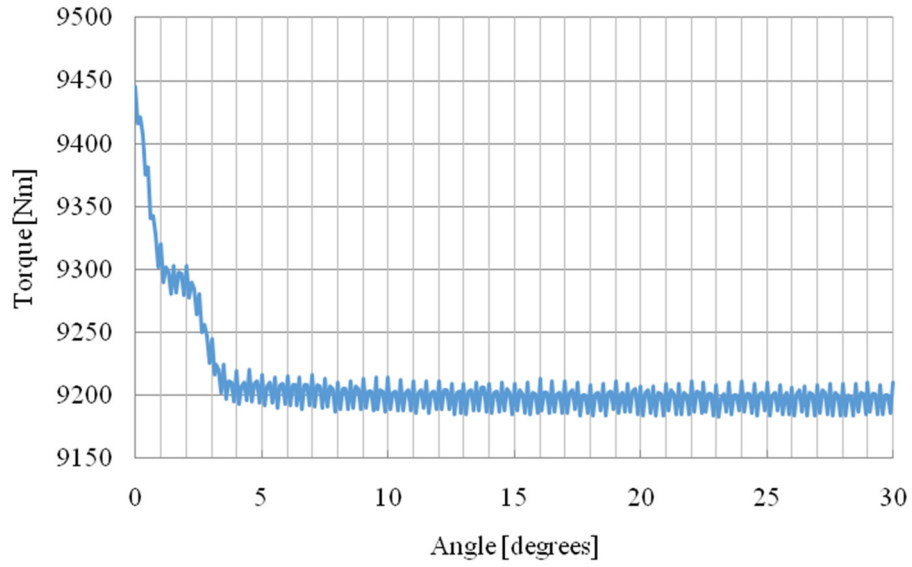


Figure 4-8. Torque on the cage rotor.

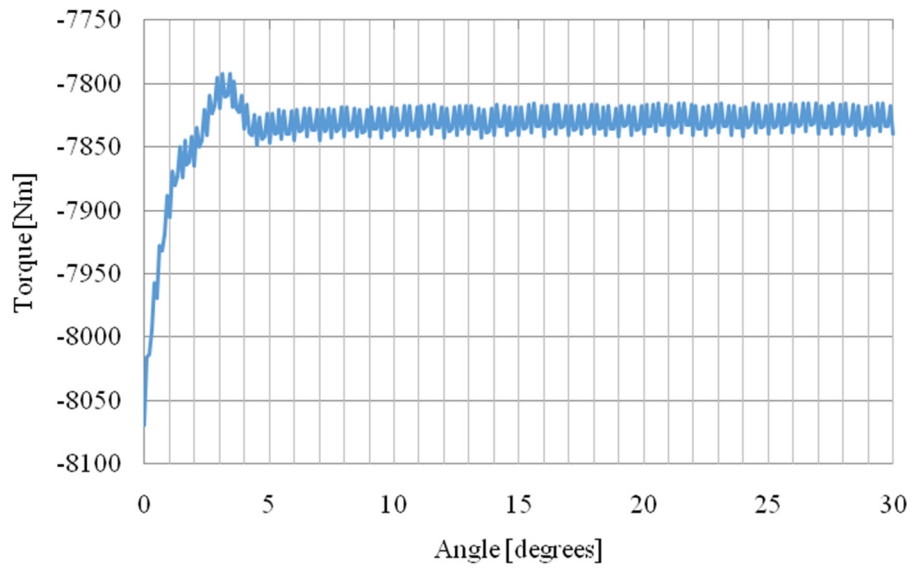


Figure 4-9. Torque on the outer rotor.

## 5. Flux Concentration Magnetic Gearbox Rotor Design Analysis

In this section, MGs with flux concentration topology will be discussed. In the previous design,  $r_{i1}$  is 100 mm which will result in very long inner magnets. These magnets will be too large and will not be properly used. Therefore, a second design typology was investigated with magnets that are the same length as the steel poles.  $r_{i1}$  is initially increased to 150 mm. Then  $r_{o1}$  and  $l_2$  are varied in order to obtain the peak torque value. Then  $r_{i1}$  is increased and the process is repeated. The results are shown in Figure 5-1.

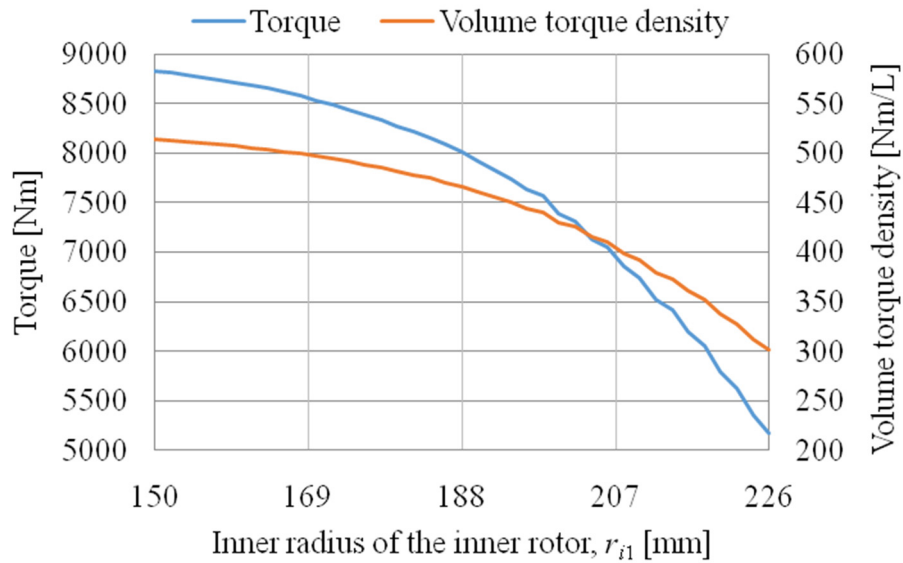


Figure 5-1. The values of torque and torque density when  $r_{i1}$  is varied.

The goal is to design a MG which has a volume torque density over 300 Nm/L. Now the volume torque density is chosen to be larger than 350 Nm/L (because after adding magnet retaining lips, the torque will decrease):  $r_{i1} = 218$  mm,  $r_{o1} = 247$  mm,  $r_{i2} = 248$  mm,  $r_{o2} = 255$  mm,  $r_{i3} = 256$  mm,  $r_{o3} = 270$  mm. These parameters give a peak torque value of 6052.94 Nm (352.39 Nm/L). After adding the retaining lips and 1 mm bridges as shown in Figure 5-2, the volume torque density becomes 216.17 Nm/L which is too low.

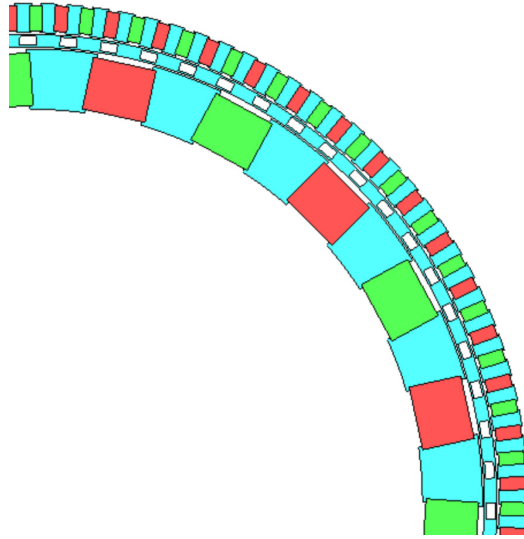


Figure 5-2. MG with magnet retaining lips and bridges.

Radial magnetized magnets have been added to increase the torque. The width of the radial magnets has been fixed at 20 mm and the length has been varied. The peak torque occurs when  $l_m = 24$  mm which gives a volume torque density of 228.00 Nm/L which is shown in Figure 5-3.

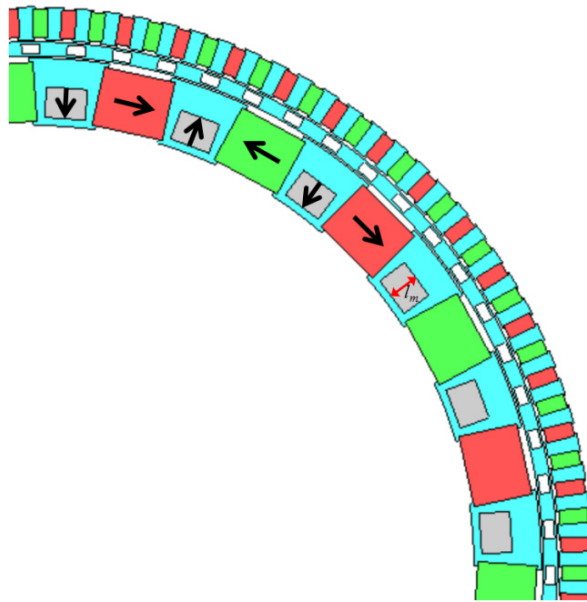


Figure 5-3. MG with radially magnetized magnets in the inner rotor.

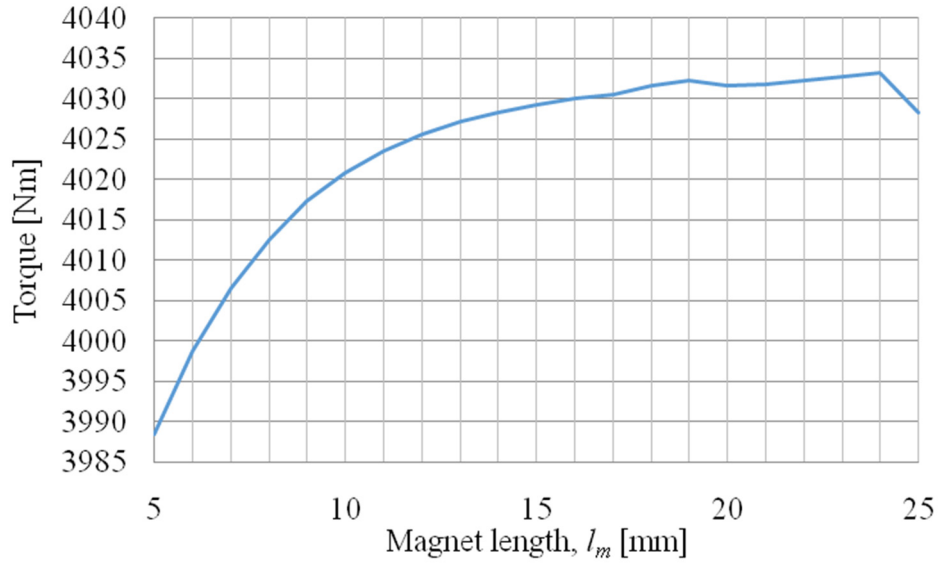


Figure 5-4. The torque values with different  $l_m$ .

In the previous design shown in Figure 5-3, the radial length of the cage rotor was only 7 mm which was shown to be too small to prevent large mechanical deflections from occurring. Therefore,  $l_2$  is fixed at 15 mm.  $r_{i1}$  and  $r_{o1}$  are varied. The peak torque values are shown in Figure 5-5. The volume torque density is chosen to be larger than 400 Nm/L:  $r_{i1} = 194$  mm,  $r_{o1} = 237$  mm,  $r_{i2} = 238$  mm,  $r_{o2} = 253$  mm,  $r_{i3} = 254$  mm,  $r_{o3} = 270$  mm. With these parameters, a peak torque value of 6932.29 Nm (403.59 Nm/L) is achieved.

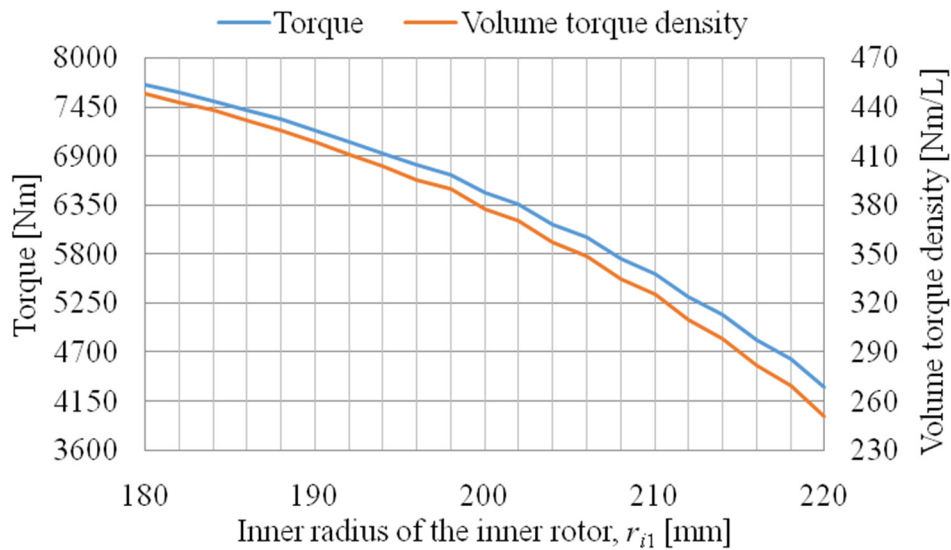


Figure 5-5. The values of torque and torque density when  $r_{i1}$  is varied.

Magnet retaining lips and 1 mm bridges have been added. The torque becomes 5272.41 Nm which gives a volume torque density of 298.06 Nm/L.

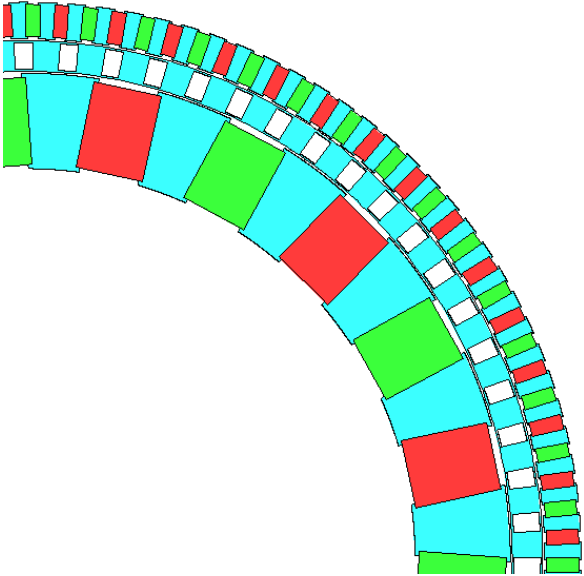


Figure 5-6. MG with modified geometry parameters.

Radial magnetized magnets have been added to increase the torque. The width of the radial magnets has been fixed at 16 mm and the length has been varied. The peak torque occurs when  $l_m = 25$  mm which gives a volume torque density of 311.08 Nm/L (with a torque value of 5502.78 Nm). This optimized geometry is shown in Figure 5-7.

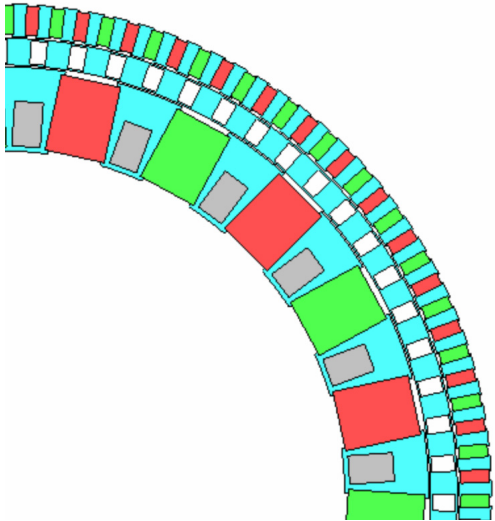


Figure 5-7. Optimized geometry with radial magnets.

## 6. Ideal Stage 1 Magnetic Gear Design Analysis with a Pole Pair Combination of 12-78-66

Conducting the parameter sweeping analysis is very time consuming. Therefore, in this section, a pole pair combination of 12-78-66 has been chosen so that the MG can be modeled with 1/6 of its geometry due to symmetric. The geometry is shown in Figure 6-1 and

Table 6-I.

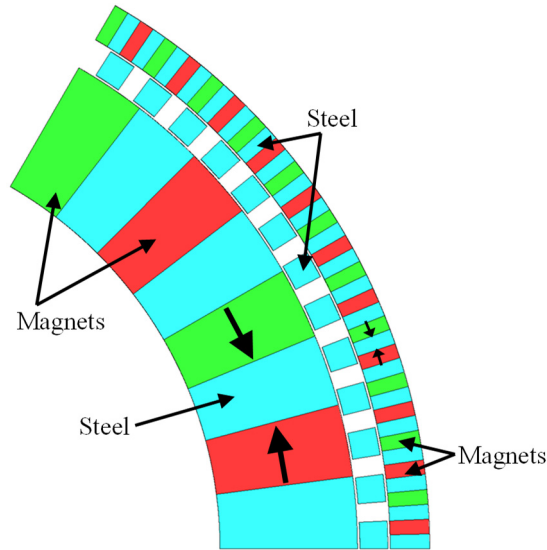


Figure 6-1. 1/6 model of stage 1 MG with a pole combination of 12-78-66.

Table 6-I. Parameters for stage 1 MG.

Description		Value	Unit
Inner rotor	Inner radius, $r_{i1}$	varied	mm
	Outer radius, $r_{o1}$	varied	mm
	Pole pairs	12	-
Cage rotor	Inner radius, $r_{i2}$	varied	mm
	Outer radius, $r_{o2}$	varied	mm
	Pole pairs	78	-
Outer rotor	Inner radius, $r_{i3}$	varied	mm
	Outer radius, $r_{o3}$	270	mm
	Pole pairs	66	-
Air gap, $g$		1	mm
Axial length, $d_1$		75	mm

The mass and volume torque density plot is shown in Figure 6-2-Figure 6-4 when  $r_{i1} = 220$  mm,  $r_{i1} = 200$  mm and  $r_{i1} = 180$  mm. For different values of  $r_{i1}$ , the torque density values are clearly grouped. The parameters for each  $r_{i1}$  when the peak torque occurs are shown in Table 6-II.

From the figure as shown below, it can be seen that:

- For one value of  $l_2$ , the line looks quite linear.
- All the lines seem parallel to each other.
- When  $l_2$  is increasing, the lines are shifted in  $y$ -direction, which means the two boundaries of the plot are the maximum value of  $l_2$  and the minimum value of  $l_2$ .
- When  $l_2$  is increased from 5 mm to 12 mm, the peak value is increasing and then decreasing.

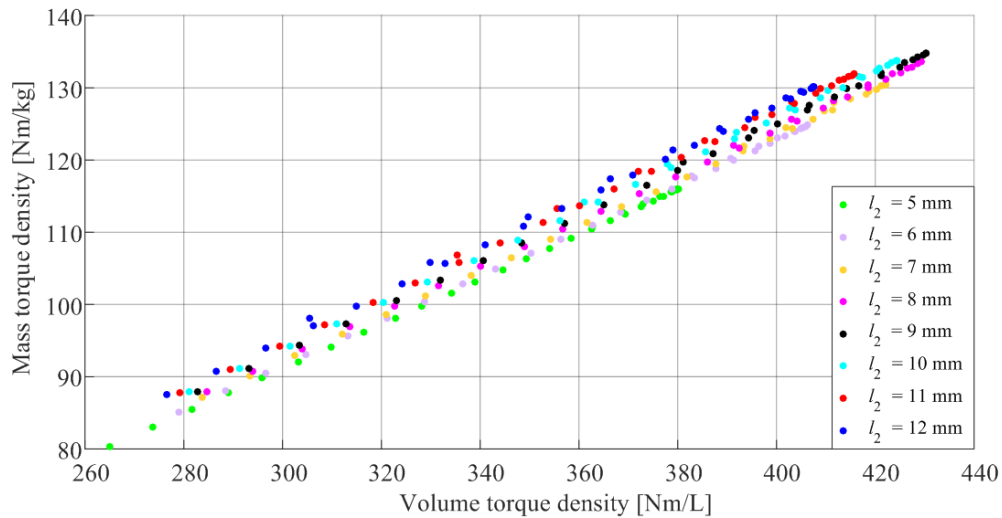


Figure 6-2. Mass and volume torque densities when  $r_{i1} = 200$  mm.

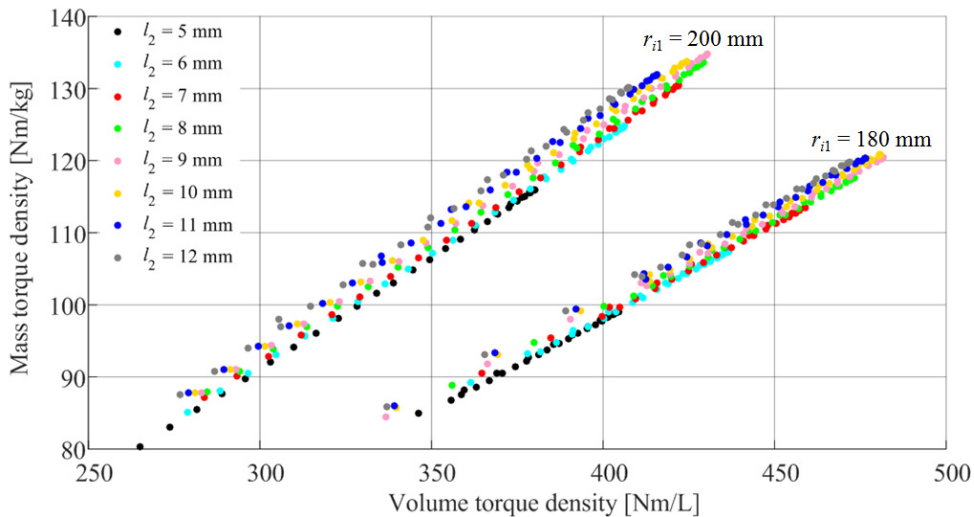


Figure 6-3. Mass and volume torque densities when  $r_{i1} = 200$  mm and  $r_{i1} = 180$  mm.

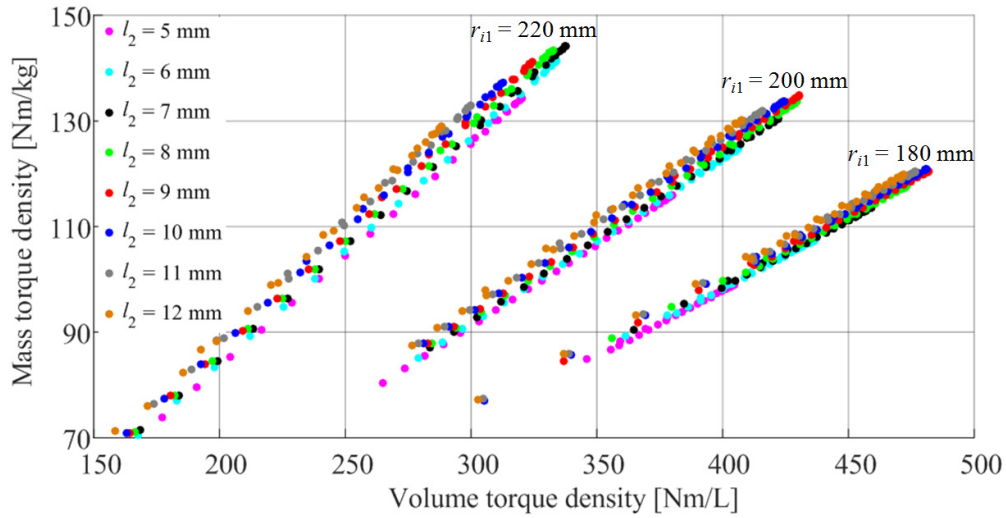


Figure 6-4. Mass and volume torque densities when  $r_{i1} = 220$  mm,  $r_{i1} = 200$  mm and  $r_{i1} = 180$  mm.

Table 6-II. Parameters of the MG after parameter sweeping.

Description		Value (peak torque) ( $r_{i1} = 180$ mm)	Value (peak torque) ( $r_{i1} = 200$ mm)	Value (peak torque) ( $r_{i1} = 220$ mm)	Unit
Inner rotor	Inner radius, $r_{i1}$	180	200	220	mm
	Outer radius, $r_{o1}$	240	243	247	mm
	Pole pairs	12			-
Cage rotor	Inner radius, $r_{i2}$	241	244	248	mm
	Outer radius, $r_{o2}$	250	253	255	mm
	Pole pairs	78			-
Outer rotor	Inner radius, $r_{i3}$	251	254	256	mm
	Outer radius, $r_{o3}$	270	270	270	mm
	Pole pairs	66			-
Torque, $T_2$		8275.263	7390.943	5800.268	Nm
Air gap, $g$		1			mm
Axial length, $d_1$		75			mm

The inner radius of the inner rotor  $r_{i1}$  was varied from 150 mm to 240 mm. At each value of  $r_{i1}$ , the peak torque was obtained. The torque density plots are shown in Figure 6-5 and Figure 6-6.

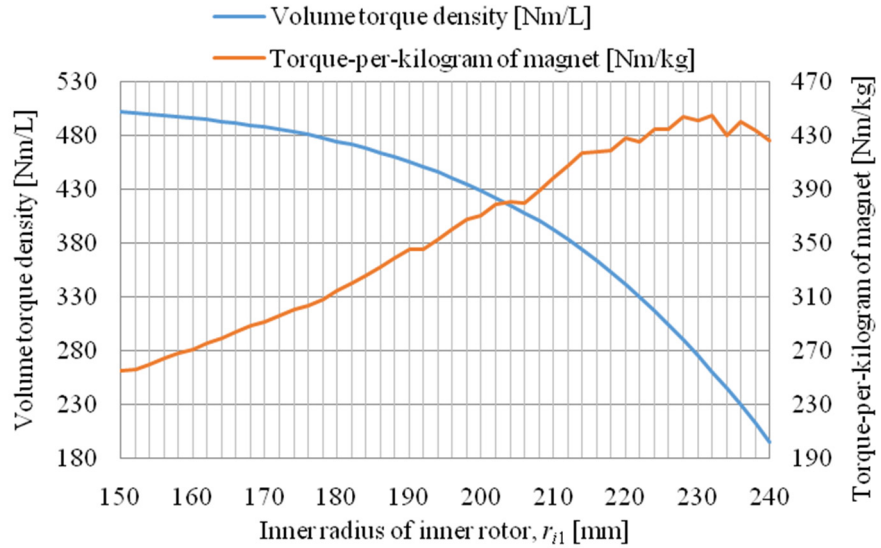


Figure 6-5. Values of volume and mass torque densities when  $r_{i1}$  is varied.

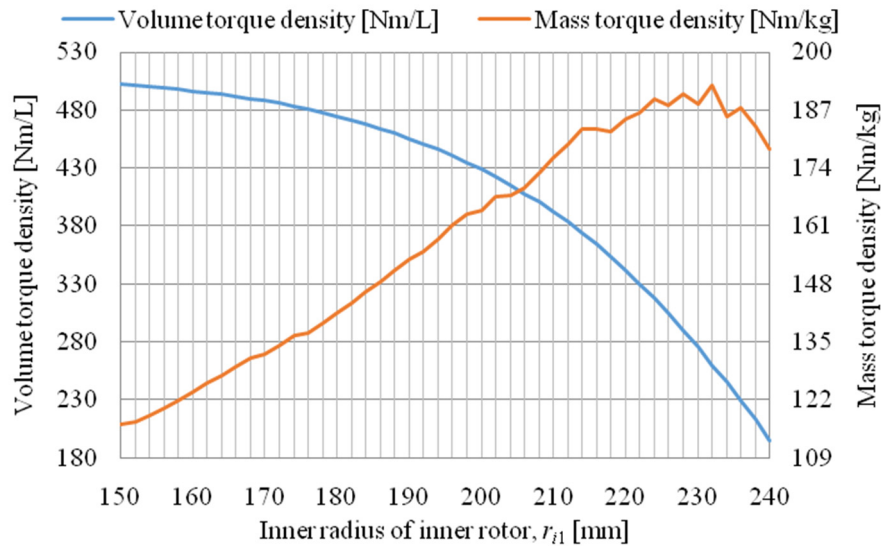


Figure 6-6. Values of volume and mass torque densities when  $r_{i1}$  is varied.

The parameters are chosen as shown in Table 6-III in order to get a relatively high mass and volume torque density. The magnetic flux lines are shown in Figure 6-7.

Table 6-III. Geometry parameters.

Description		Value	Unit
Inner rotor	Inner radius, $r_{i1}$	180	mm
	Outer radius, $r_{o1}$	239	mm
Cage rotor	Inner radius, $r_{i2}$	240	mm
	Outer radius, $r_{o2}$	252	mm
Outer rotor	Inner radius, $r_{i3}$	253	mm
	Outer radius, $r_{o3}$	270	mm

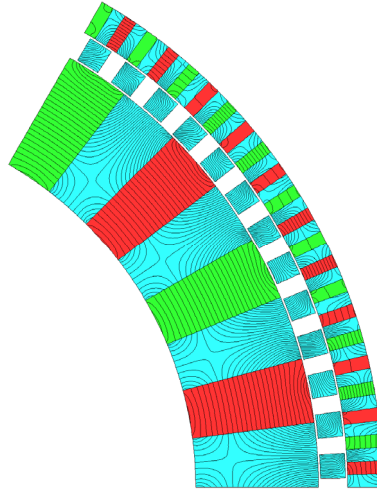


Figure 6-7. Magnetic flux lines.

The torque plots are shown in Figure 6-8-Figure 6-10 when the cage rotor is rotating at 80 RPM and the inner rotor is rotating at 520 RPM. The inner, cage and outer rotors have low torque ripples which are 4.18%, 0.87% and 0.27%, respectively.

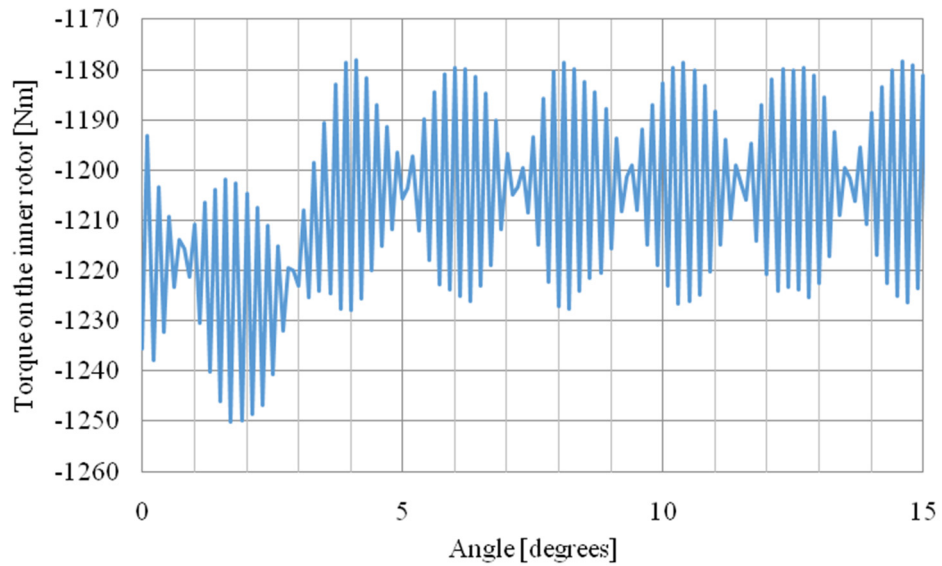


Figure 6-8. Torque on the inner rotor.

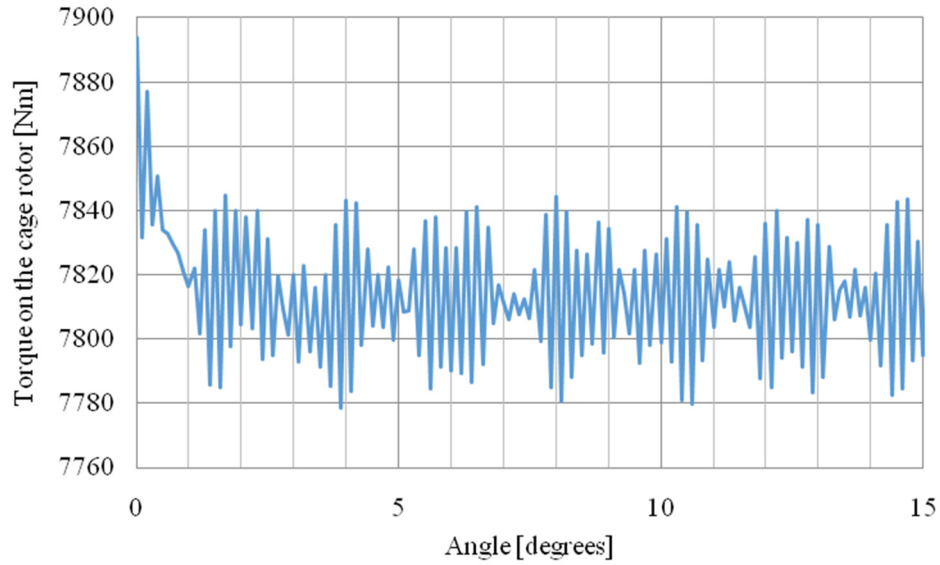


Figure 6-9. Torque on the cage rotor.

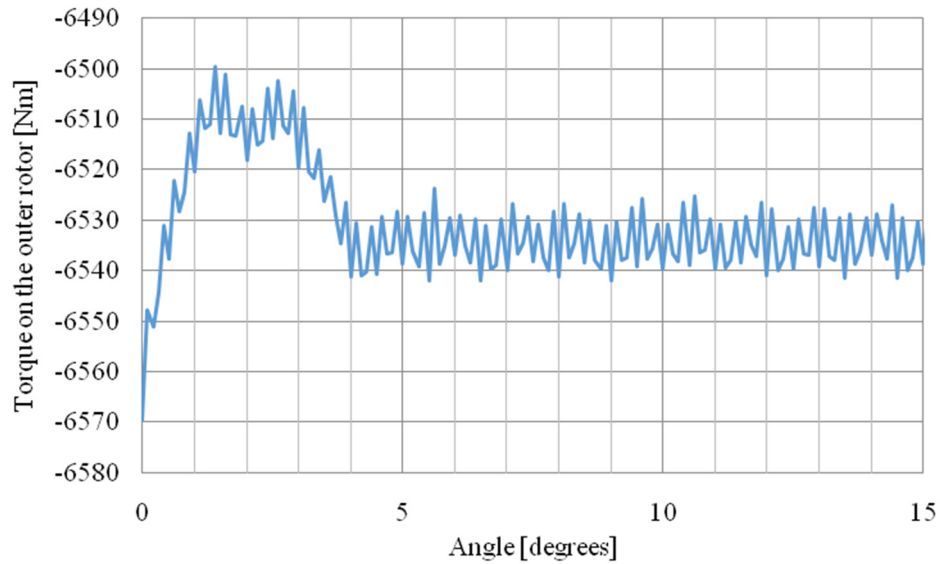


Figure 6-10. Torque on the inner rotor.

The radial length of the cage steel is  $l_2 = 12$  mm in the design shown in Figure 6-7. In order to make it mechanically strong,  $l_2$  is increased so that the cage bar will have smaller deflection. Therefore,  $r_{i1}$  was fixed at 180 mm and  $l_2$  was fixed at  $l_2 = 15$  mm. Then  $r_{o1}$  was varied from 220 mm to 250 mm. The peak torque occurs when  $r_{o1} = 236$  mm which is shown in Figure 6-11. The corresponding volume and mass torque densities are 434.85 Nm/L and 112.13 Nm/kg, respectively. And the modified design is shown in Figure 6-12.

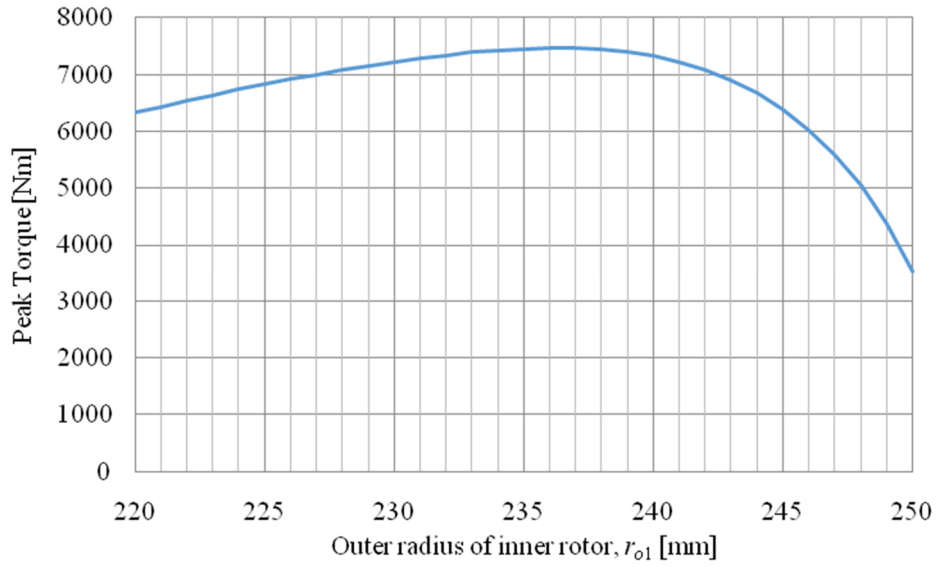


Figure 6-11. Peak torque when  $r_{o1}$  is varied.

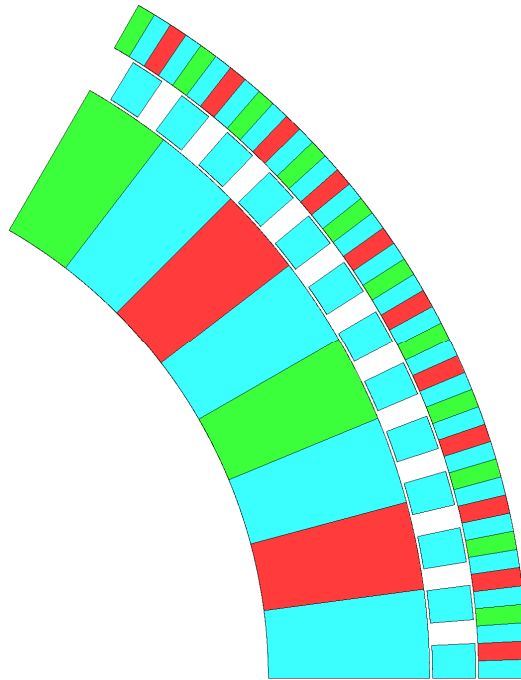
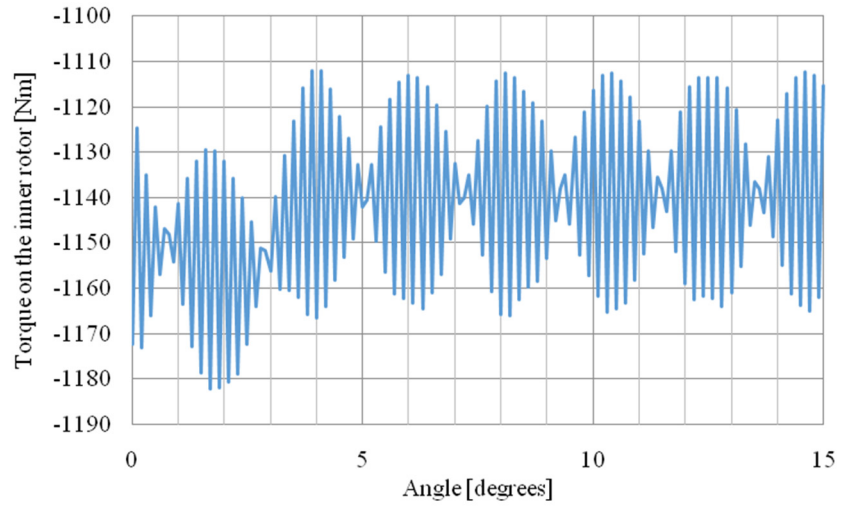
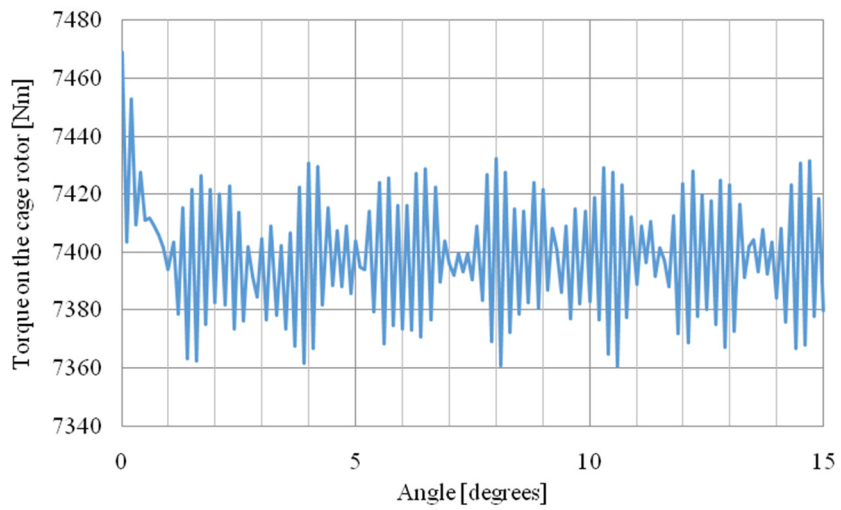


Figure 6-12. MG with modified parameters.

The torque plots are shown in Figure 6-13-Figure 6-15 when the cage rotor is rotating at 80 RPM and the inner rotor is rotating at 520 RPM. The inner, cage and outer rotors have low torque ripples which are 6.61%, 1.47% and 0.97%, respectively.



**Figure 6-13. Torque on the inner rotor.**



**Figure 6-14. Torque on the cage rotor.**

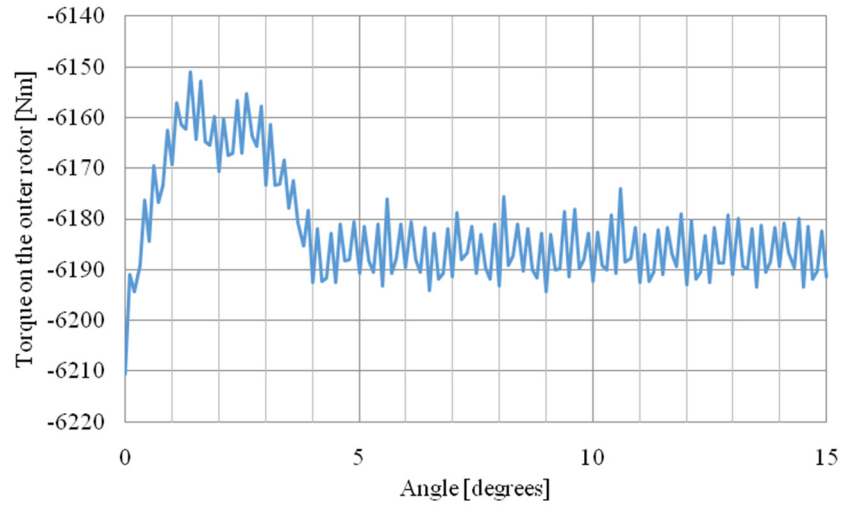


Figure 6-15. Torque on the outer rotor.

## 7. Stage 1 Magnetic Gear Design with Extra Radial Flux

### 7.1 Initial design of the stage 1 magnetic gear

In this section, a new MG design with extra radial flux is introduced which can increase the torque value. Rods and magnet retaining lips have been added to mechanically assemble it as shown in Figure 7-1. The material of the yellow rods is non-magnetic and the material of the green rods is 416 steel. The peak torque value of this design is 6113.37 Nm. In order to increase the torque, 6 mm by 6 mm radially magnetized magnets are used for the outer rotor as shown in Figure 7-2. After adding the radial magnets, the torque value is increased to 6482.89 Nm.

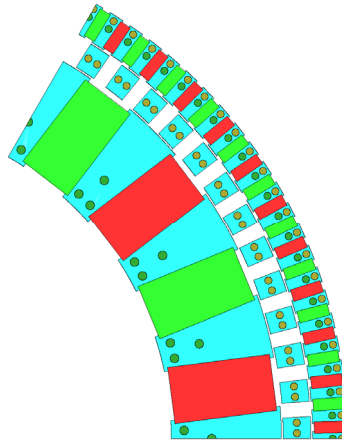


Figure 7-1. MG with plastic rods (yellow), steel rods (green).

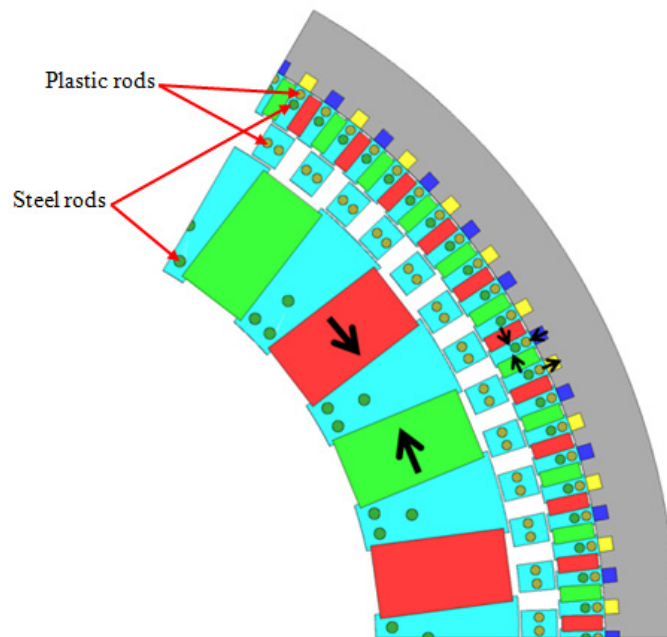


Figure 7-2. MG with plastic rods (yellow), steel rods (green) and radial magnets at the outer rotor.

The radially magnetized magnets have also been used for the inner rotor to increase the torque further which is shown in Figure 7-3. The width of the magnets has been fixed at 14 mm and the length is varied. The results are shown in Figure 7-4. It can be seen that the torque will only be increased by a small amount by increasing the length of the magnets. Considering the cost and performance, the length of the magnets can be chosen as 5mm which gives a torque value of 6607.93 Nm. The design is shown in Figure 7-5.

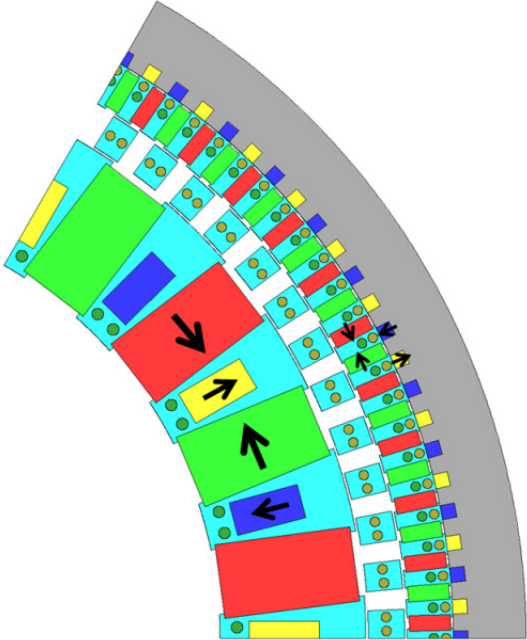


Figure 7-3. MG with plastic rods (yellow), steel rods (green) and radial magnets at the inner and outer rotors.

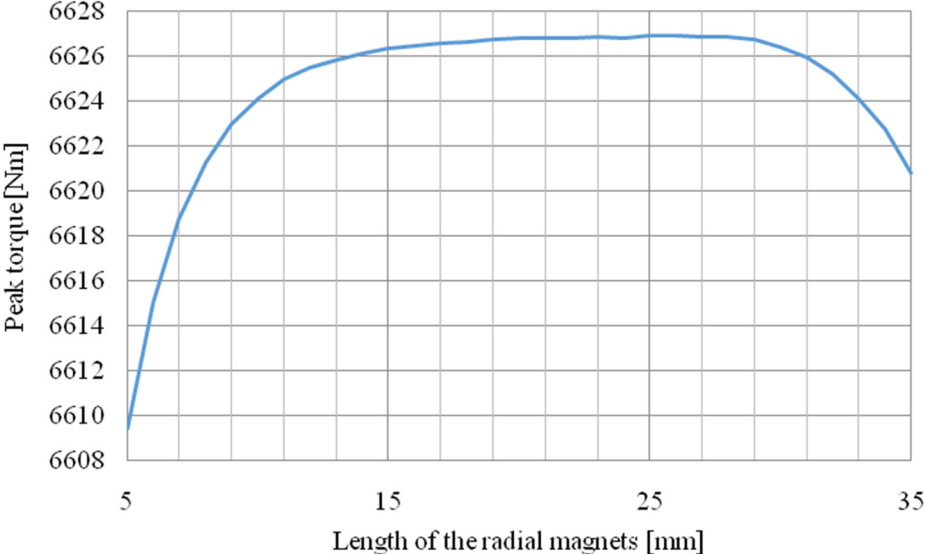


Figure 7-4. The peak torque with different length of the inner radial magnets.

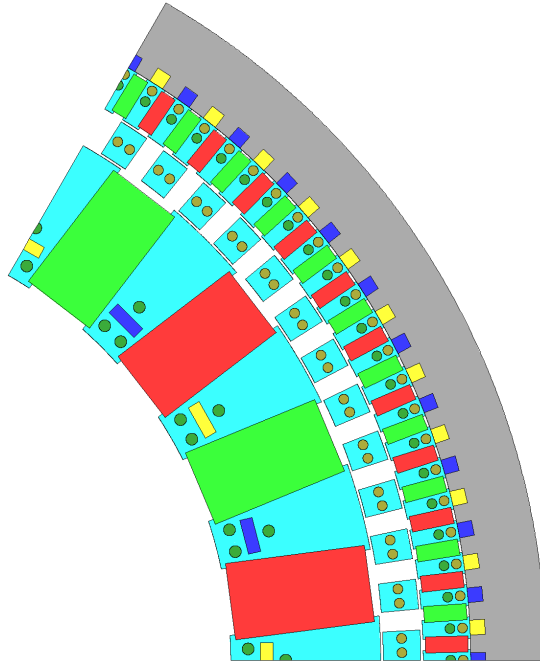


Figure 7-5. 5 mm radial length of the inner radial magnets.

The inner steel parts have been modified to achieve a higher torque. The radial length of the magnets has also been varied which is shown in Figure 7-6 and Figure 7-7. The peak torque occurs when the radial length of the magnets is 17 mm. The peak torque is 6957.52 Nm.

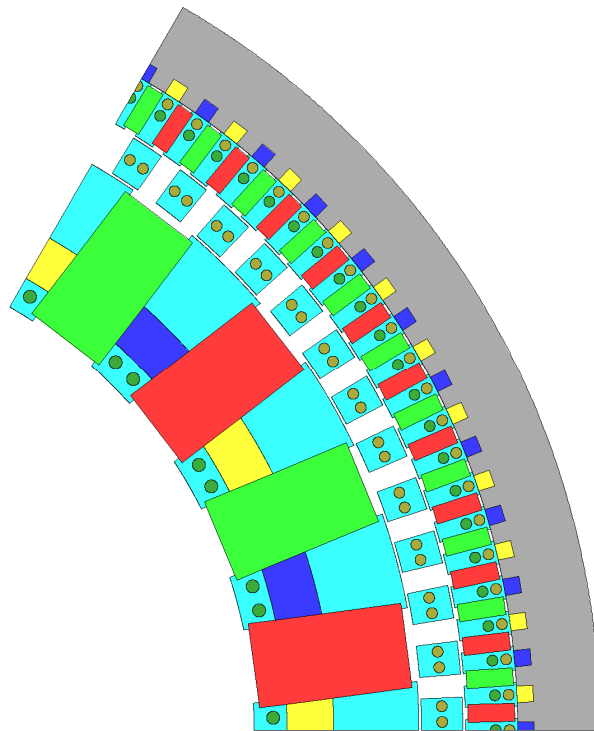


Figure 7-6. Modified structure of the inner steel.

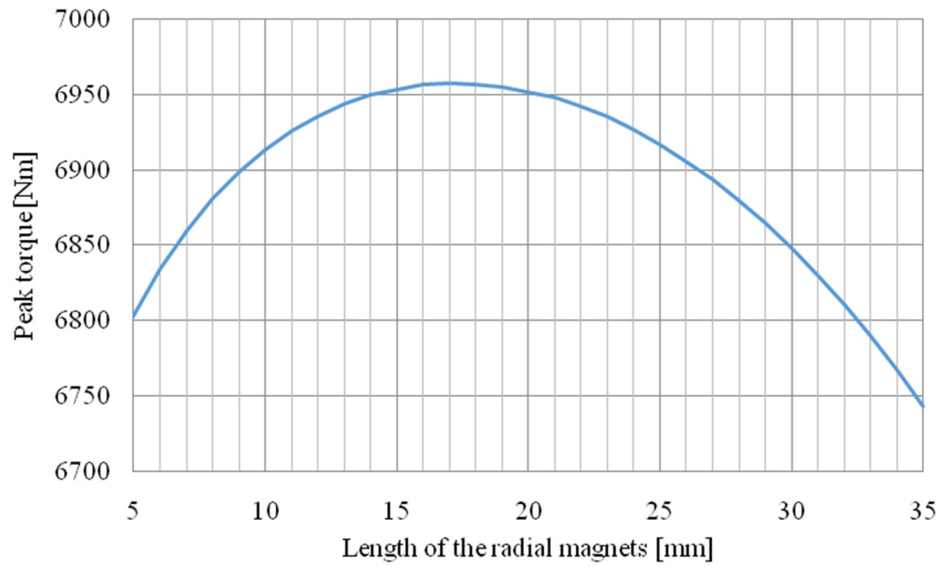


Figure 7-7. The peak torque with different length of the inner radial magnets.

The modified design with all the mechanical supporting rods is shown in Figure 7-8. The torque plots when both the inner and cage rotors are rotating are shown in Figure 7-9-Figure 7-11. The torque ripples of the inner, cage and outer rotors are 1.36%, 0.32% and 0.16%, respectively. The calculated volume torque density is 376 Nm/L.

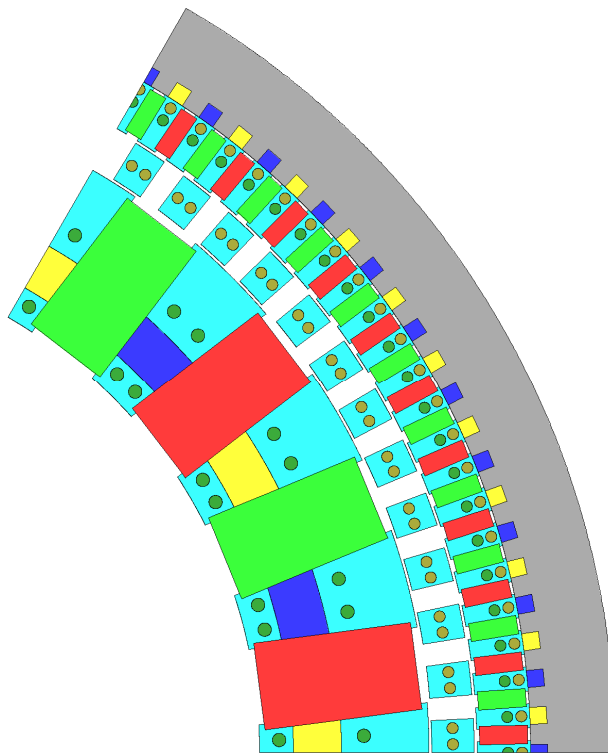


Figure 7-8. Geometry of the stage 1 MG.

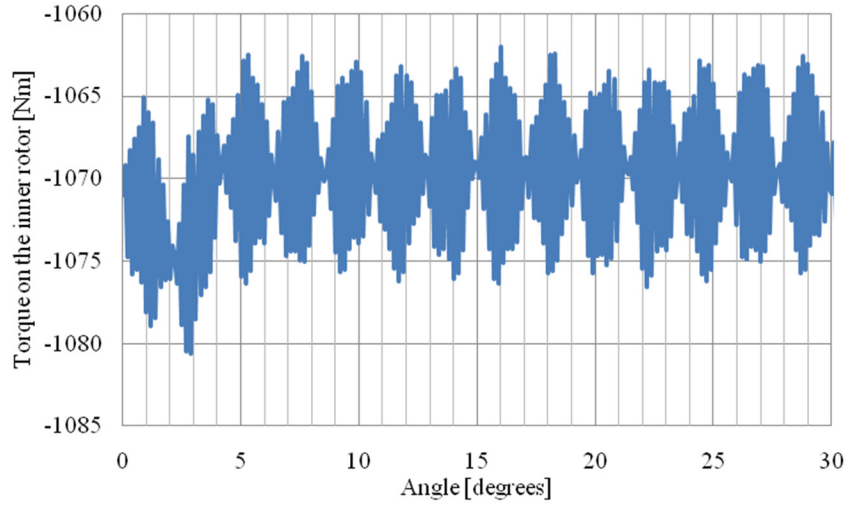


Figure 7-9. Torque on the inner rotor.

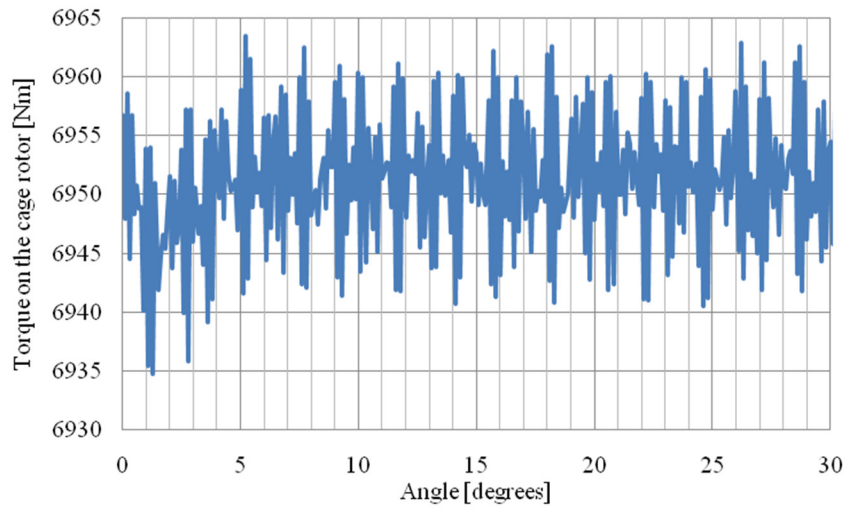


Figure 7-10. Torque on the cage rotor.

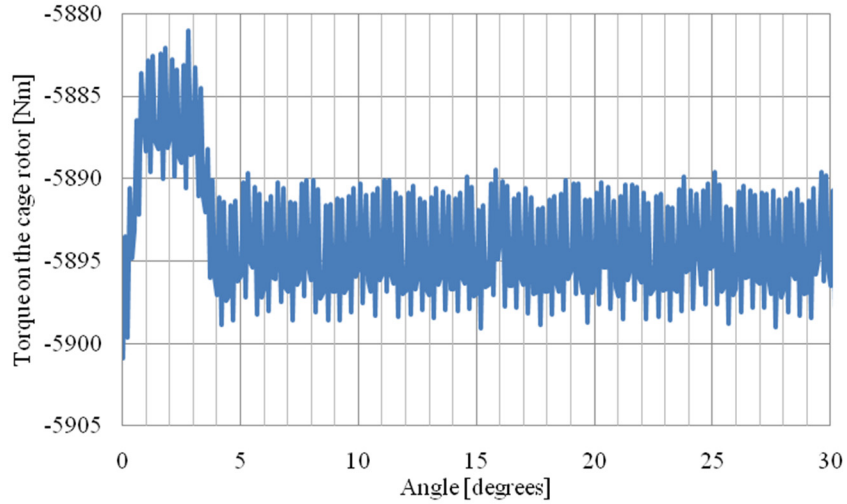


Figure 7-11. Torque on the outer rotor.

### 7.1.1 Force and deflection analysis

In order to make sure that the rods are not deflected too much so that the three rotors will not touch each other, the magnetic forces have been calculated on the inner, cage and outer steel pieces as shown in Figure 7-12. Since all the magnetic force are applied on the rods, then the deflection of the rods has also been calculated to make sure that the air gap between each rotor is still maintained. The radial and tangential forces on the steel pieces are present in Figure 7-13-Figure 7-16.

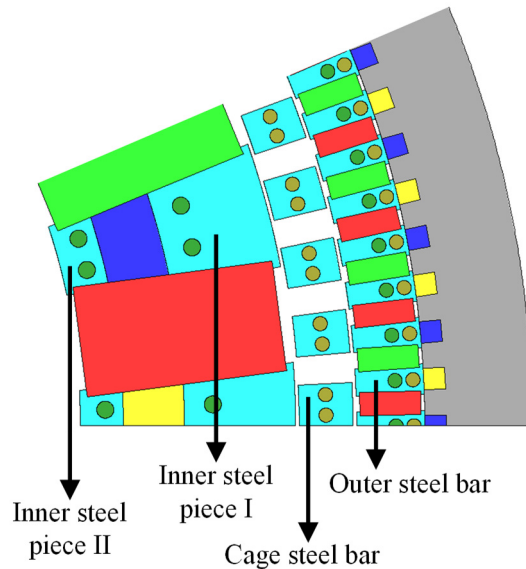


Figure 7-12. Forces to be calculated on each part.

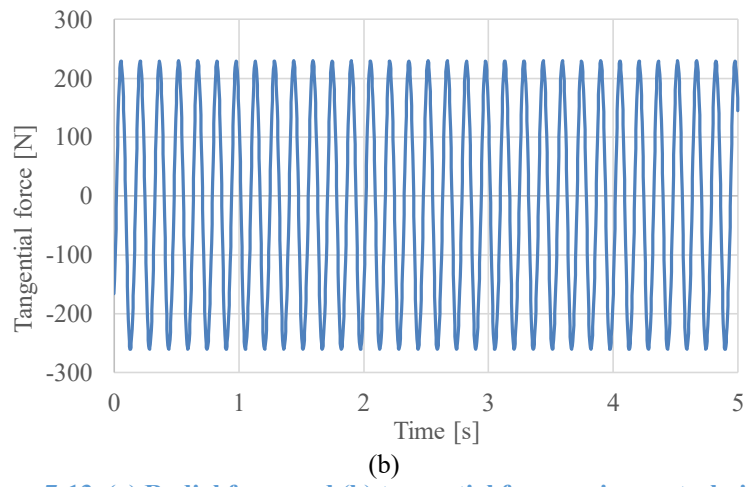
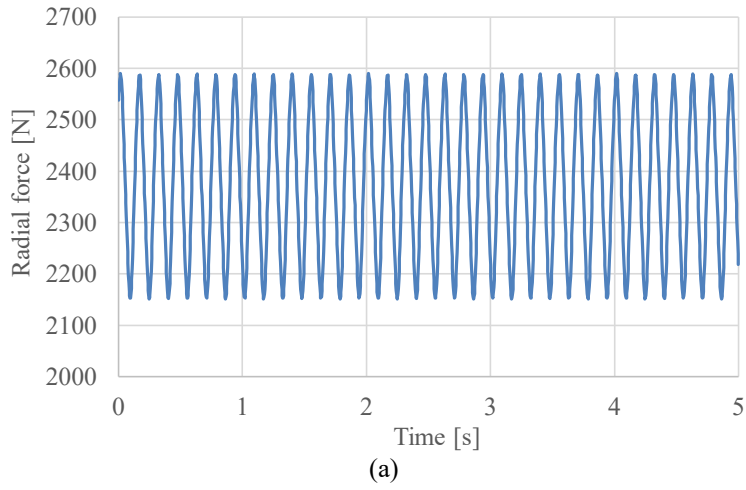
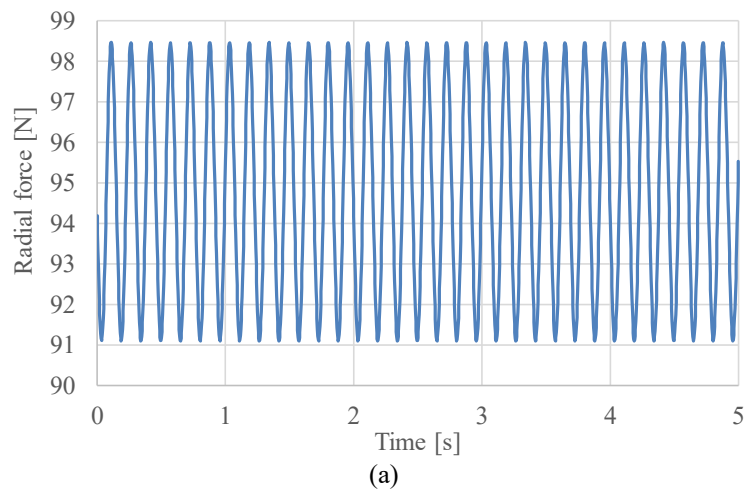
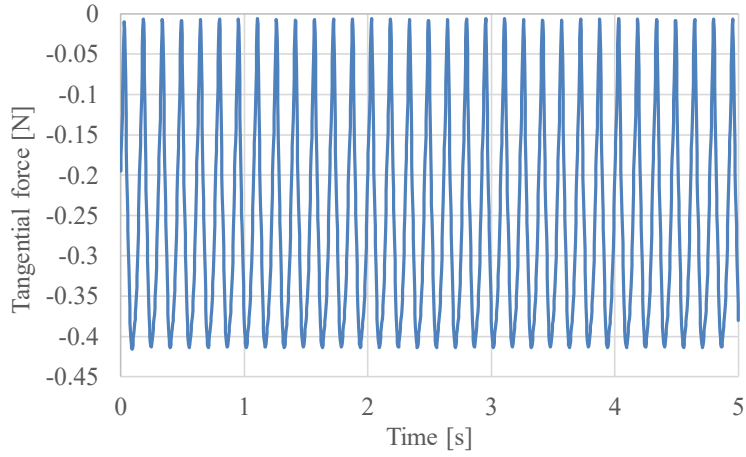


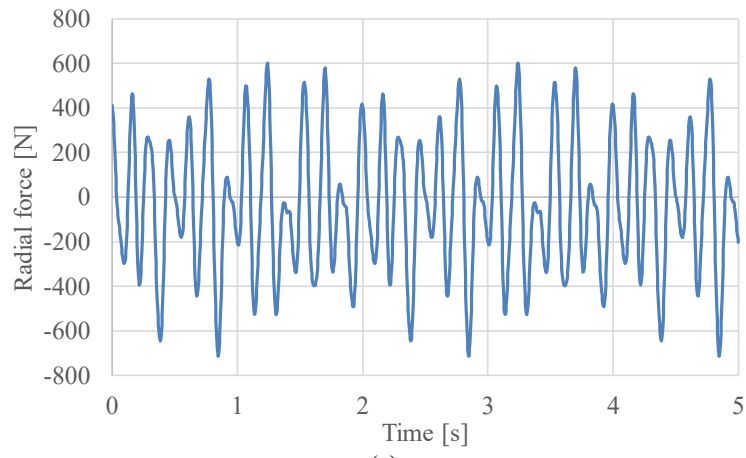
Figure 7-13. (a) Radial force and (b) tangential force on inner steel piece I.



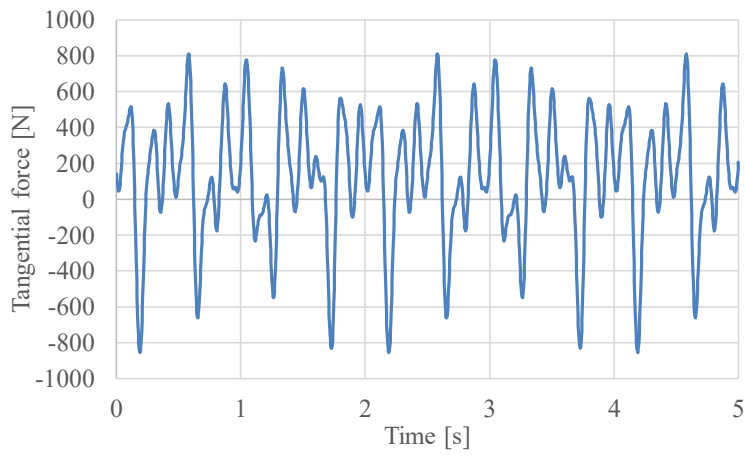


(b)

Figure 7-14. (a) Radial force and (b) tangential force on inner steel piece II.

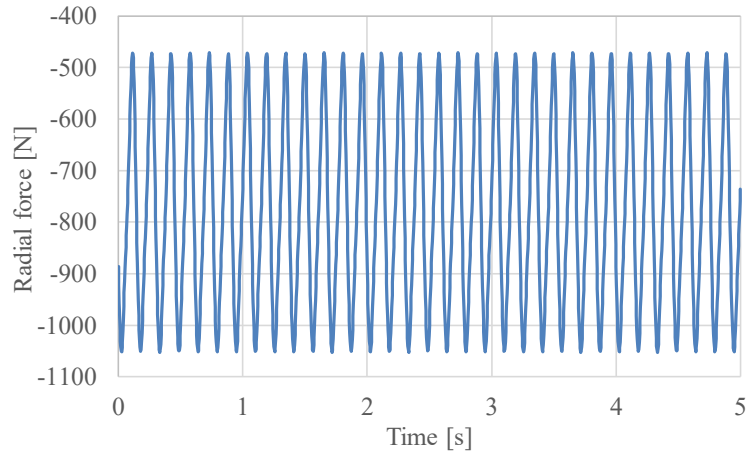


(a)

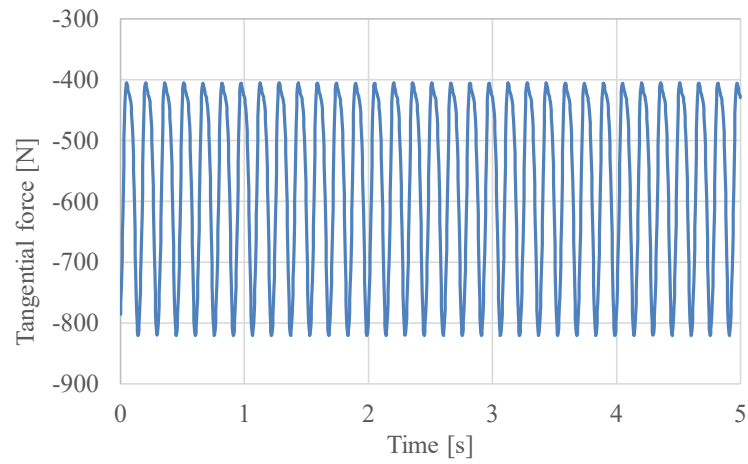


(b)

Figure 7-15. (a) Radial force and (b) tangential force on cage steel bar.



(a)



(b)

**Figure 7-16. (a) Radial force and (b) tangential force on outer steel bar.**

The mechanical deflection has been calculated based on the radial and tangential magnetic force values. The deflection of the rods on the inner, cage and outer rotors is shown in Figure 7-17- Figure 7-19 when the lamination steel was considered to have Young's modulus of 190 Gpa (when the lamination steel is considered as solid steel).

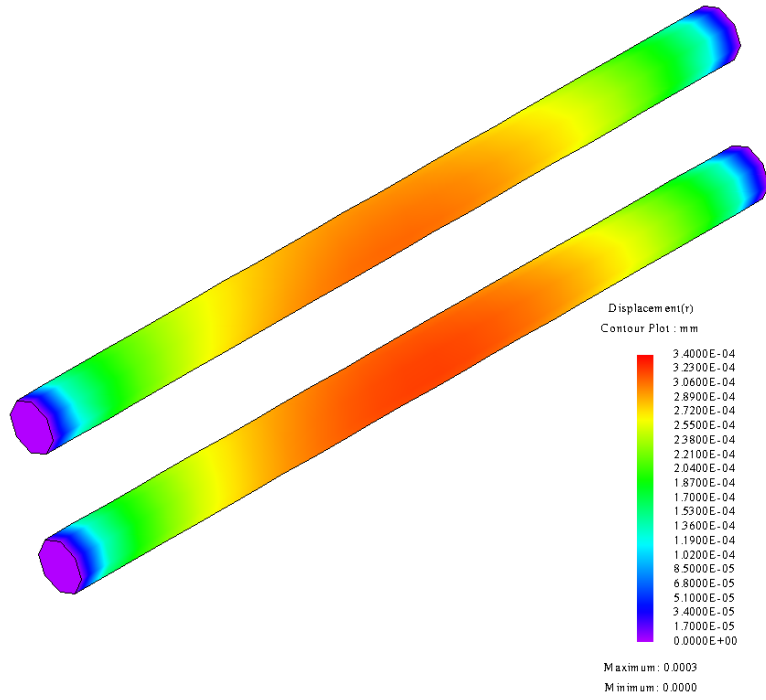


Figure 7-17. Deflection of the inner rod.

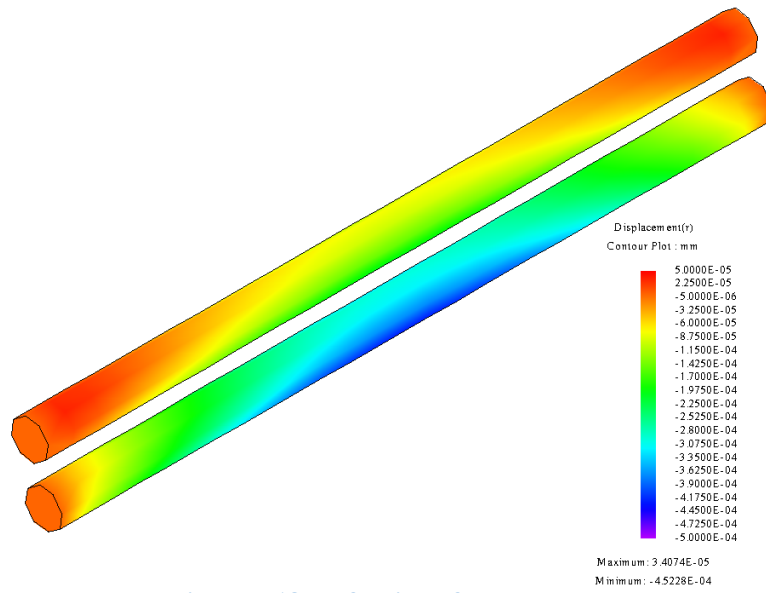


Figure 7-18. Deflection of the cage rod.

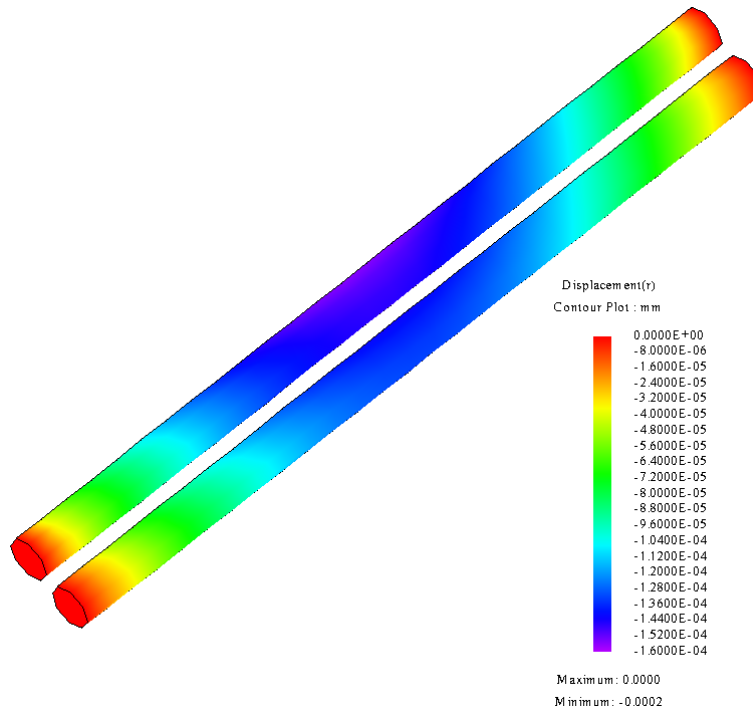


Figure 7-19. Deflection of the outer rod.

When the lamination steel was considered to provide no support (very small Young's modulus), the deflection of the rods on the inner, cage and outer rotors is shown in Figure 7-20-Figure 7-22. In real cases, the deflection will be smaller than these values.

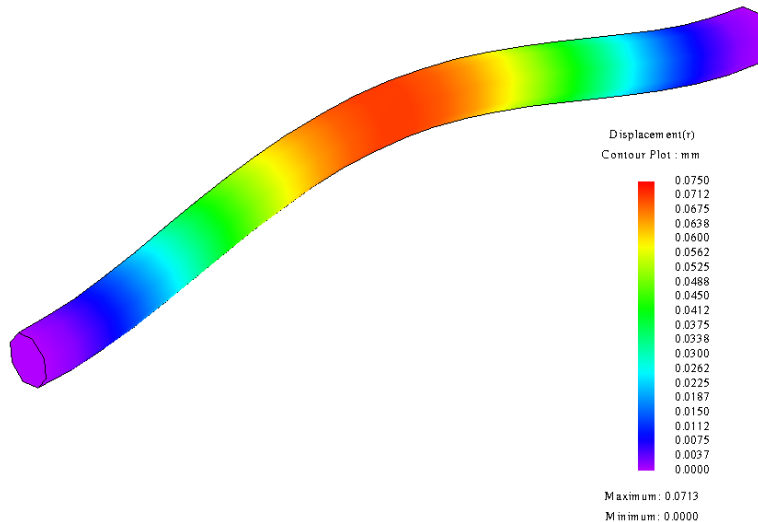
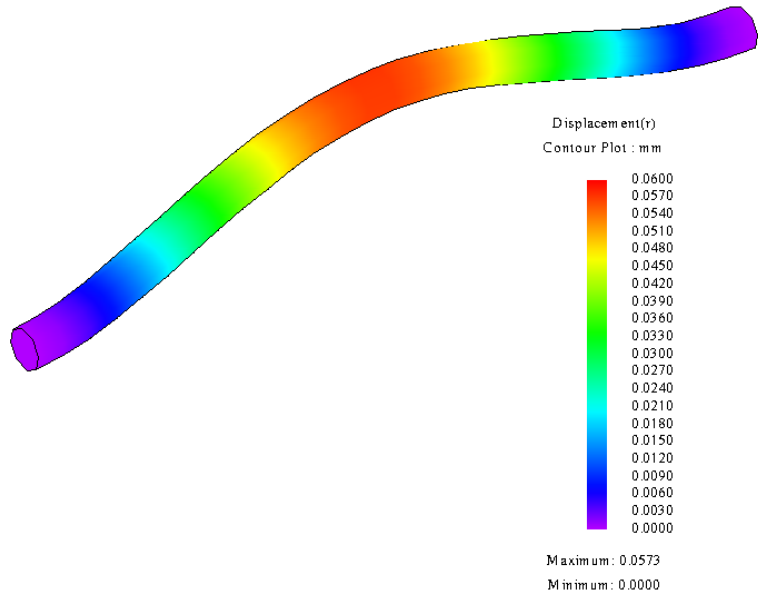
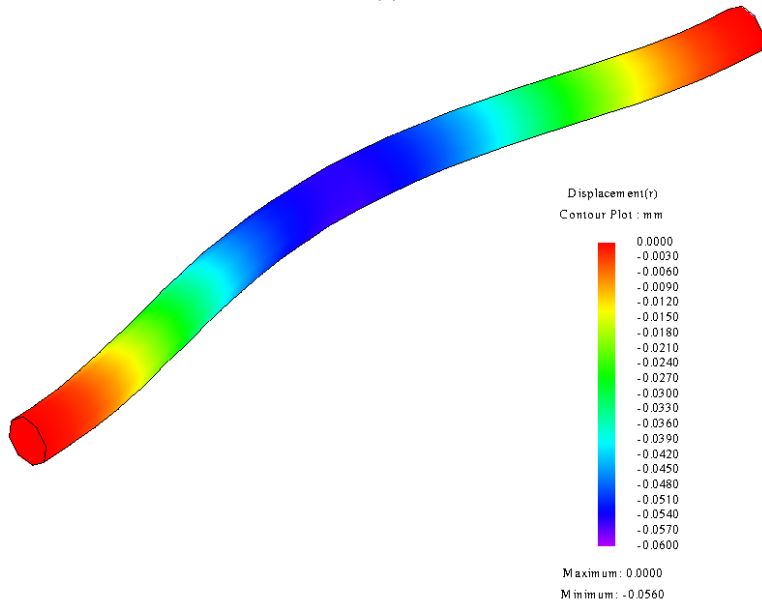


Figure 7-20. Deflection of the inner rod.



(a)



(b)

Figure 7-21. Deflection of the cage rod (a) deflected outward and (b) deflected inward.

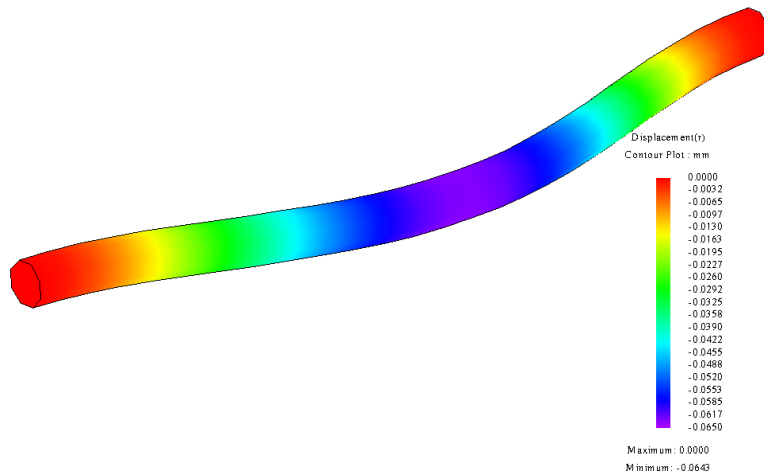


Figure 7-22. Deflection of the outer rod.

### 7.2 Final design of the stage 1 magnetic gear

The volume torque density of the design shown in Figure 7-1 is calculated to be 345.6 Nm/L while the volume torque density of the design shown in Figure 7-2 is 350.9 Nm/L. Adding those extra outer radial magnets only gives a 1.5% improvement of the volume torque density. Therefore, the design shown in Figure 7-8 is modified. The radial length of the inner radial magnets has been varied again in order to achieve peak torque which is shown in Figure 7-23. The peak torque occurs when the radial length of the radial magnets is 17 mm as shown in Figure 7-24. The final design with all the supporting rods and magnet retaining lips is shown in Figure 7-25.

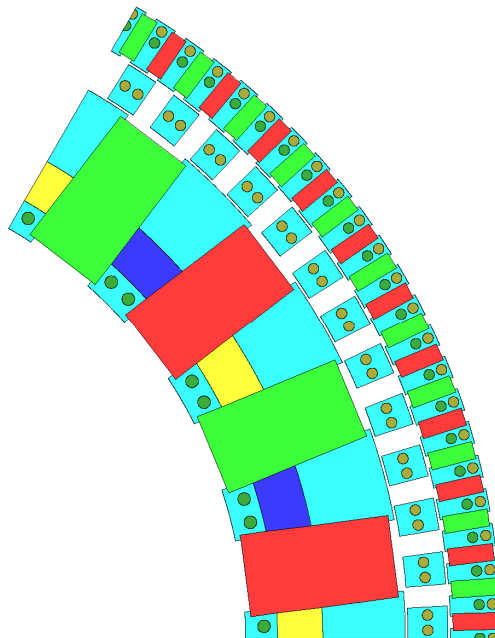


Figure 7-23. Parameter sweep for the stage 1 MG.

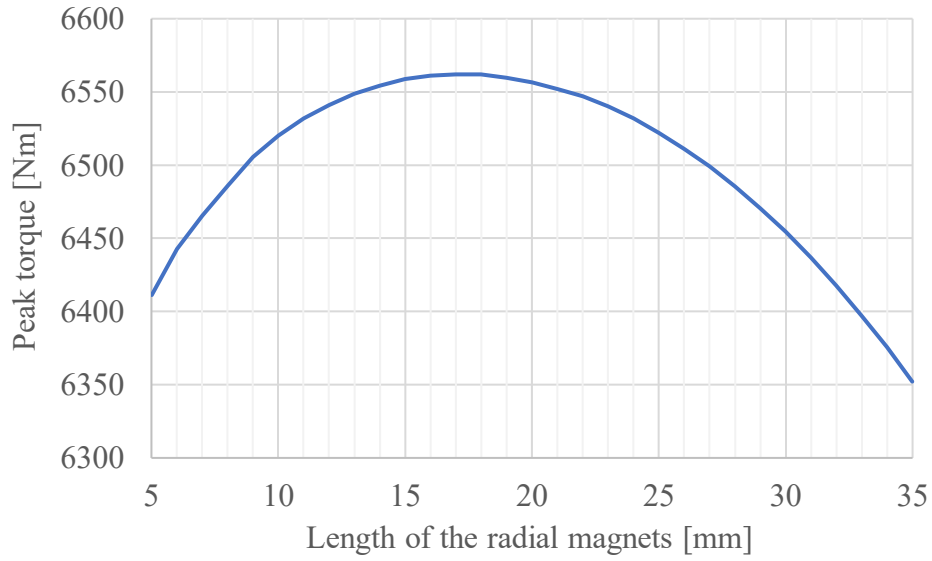


Figure 7-24. The peak torque with different length of the inner radial magnets.

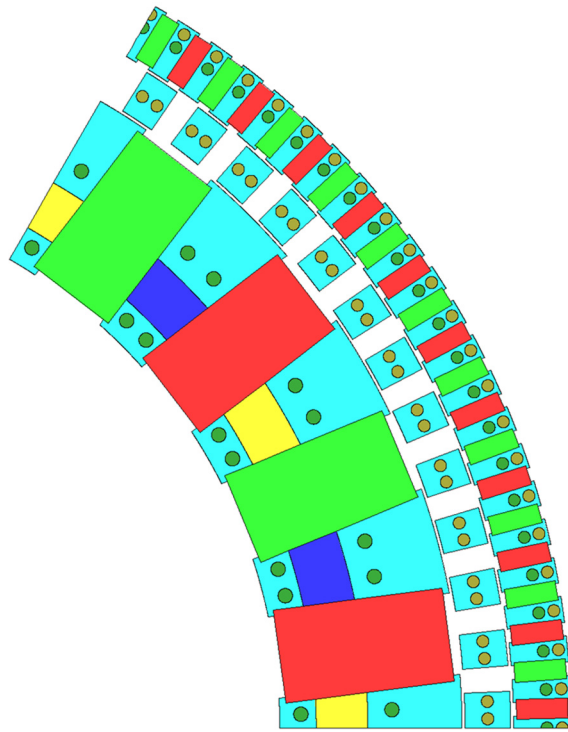


Figure 7-25. Final design of the stage 1 MG.

### 7.2.1 Loss analysis

When the cage rotor has an angular speed of 80 RPM and the inner rotor has an angular speed of 520 RPM, the total loss as a function a time is plotted in Figure 7-26. The loss was calculated in a

2-D model and the efficiency is calculated to be 95%. The contour plot of the loss and current density is shown in Figure 7-27. It can be seen that most of the losses are on the outer steel rods and magnets because of the large number of pole pairs. One approach to reduce the losses on the outer rotor is to use axially segmented magnets.

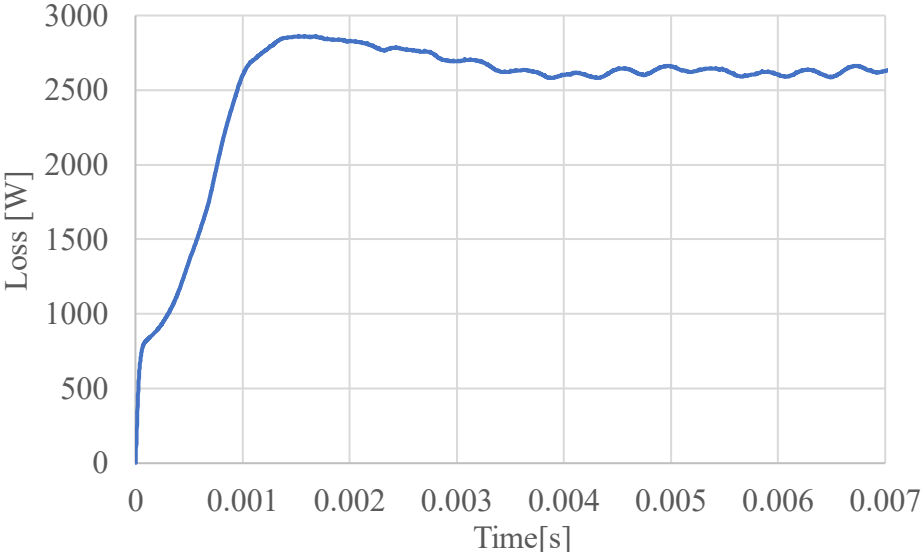
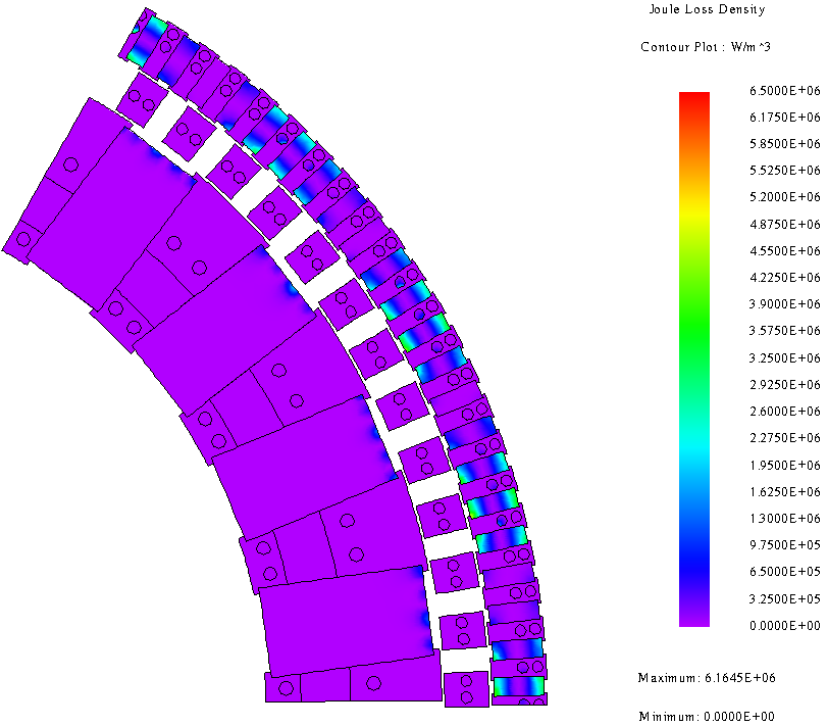


Figure 7-26. Eddy current losses for stage 1 MG when the cage rotor has an angular speed of 80 RPM and the inner rotor has an angular speed of 520 RPM.



(a)

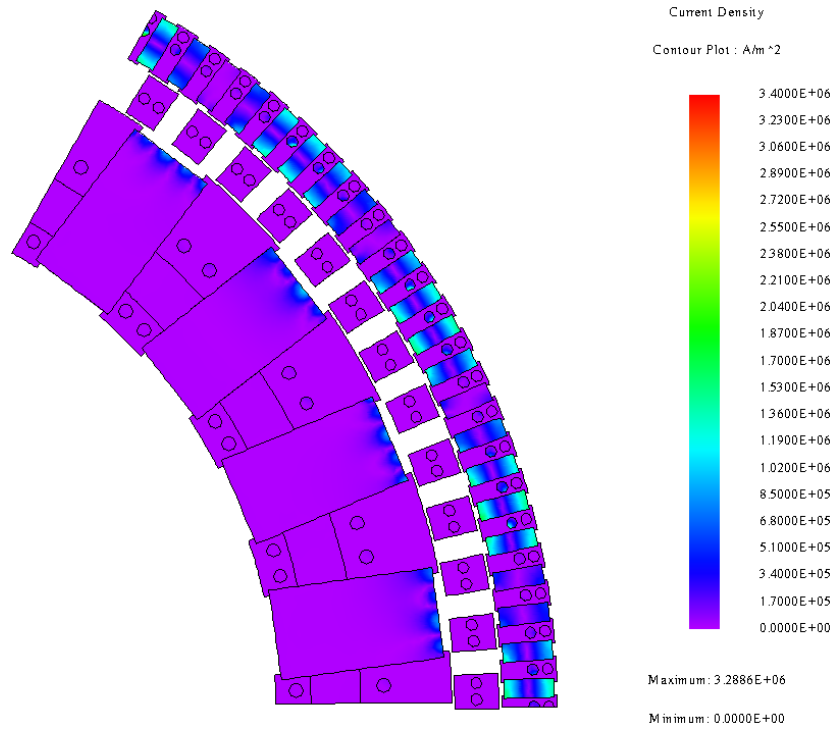
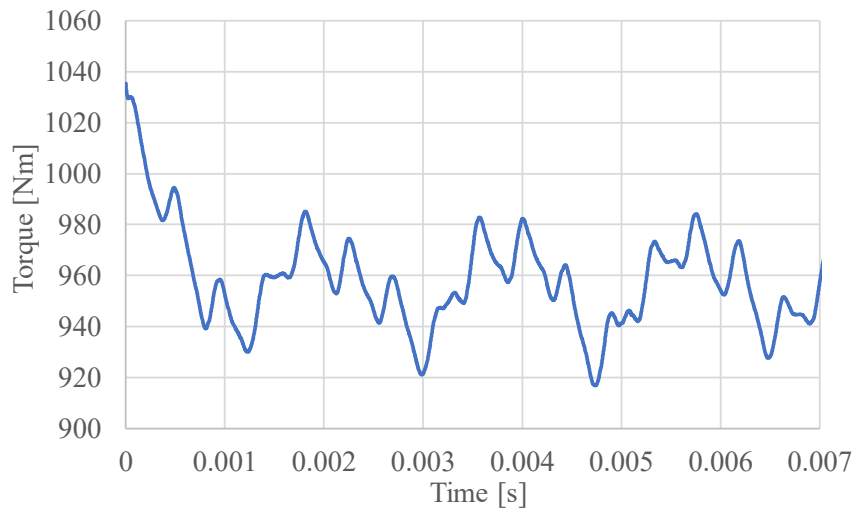


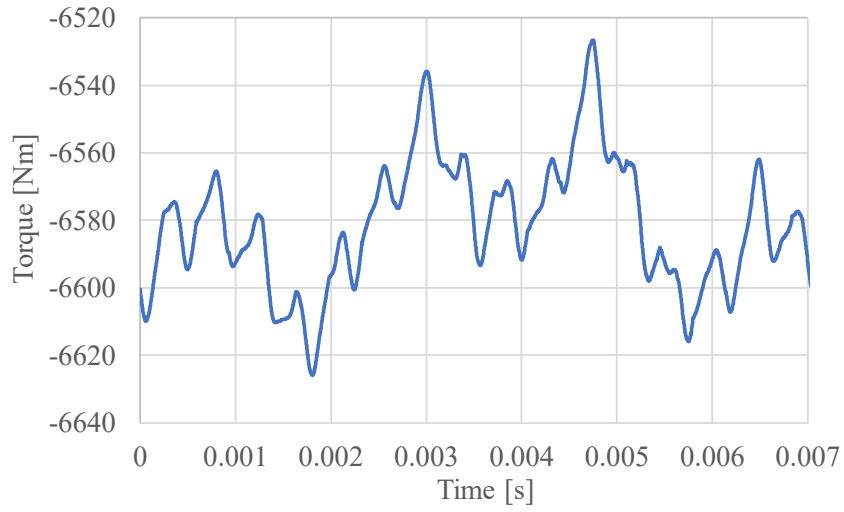
Figure 7-27. Contour plot of the (a) loss density and (b) current density.

### 7.2.2 Force and deflection analysis

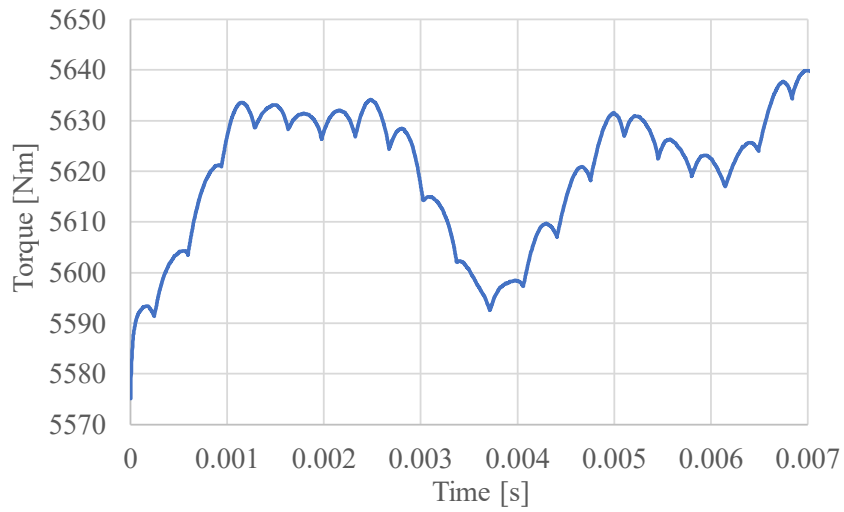
The torque plots for the final design are shown in Figure 7-28. The radial and tangential forces have been calculated on each piece of single lamination which is shown in Figure 7-29. The force values as a function of time are shown in Figure 7-30-Figure 7-33.



(a)



(b)



(c)

Figure 7-28. Torque on the (a) inner rotor (b) cage rotor and (c) outer rotor.

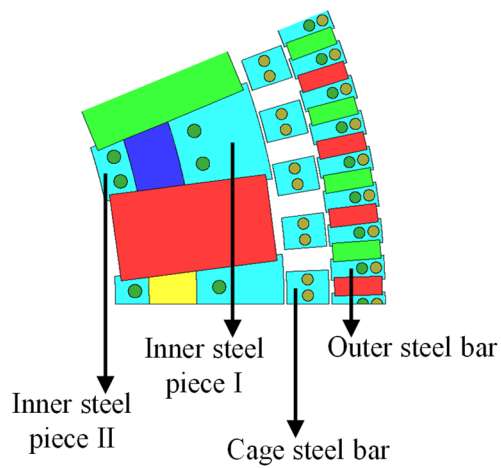
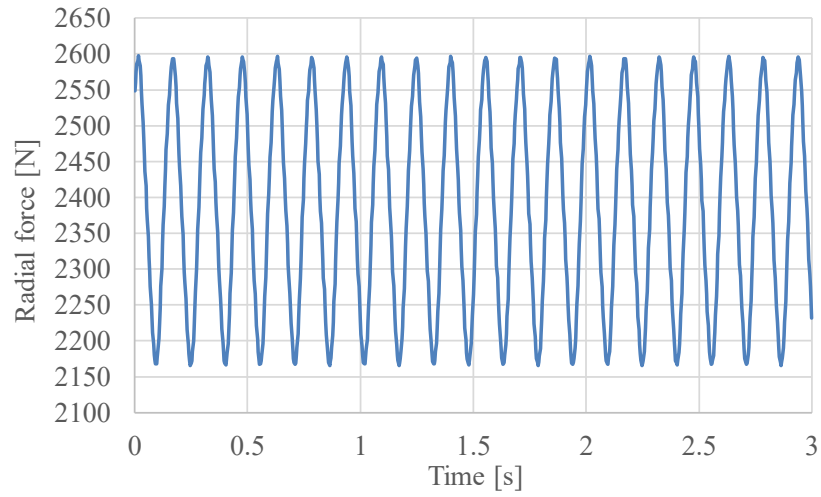
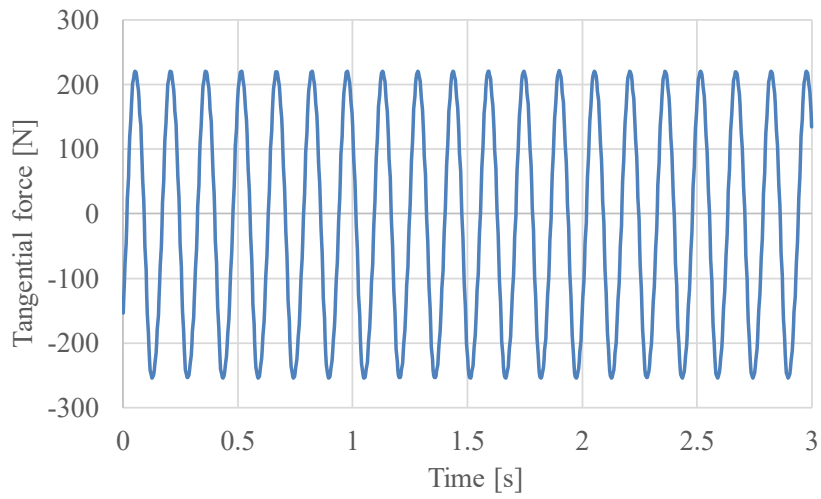


Figure 7-29. Forces to be calculated on each part.

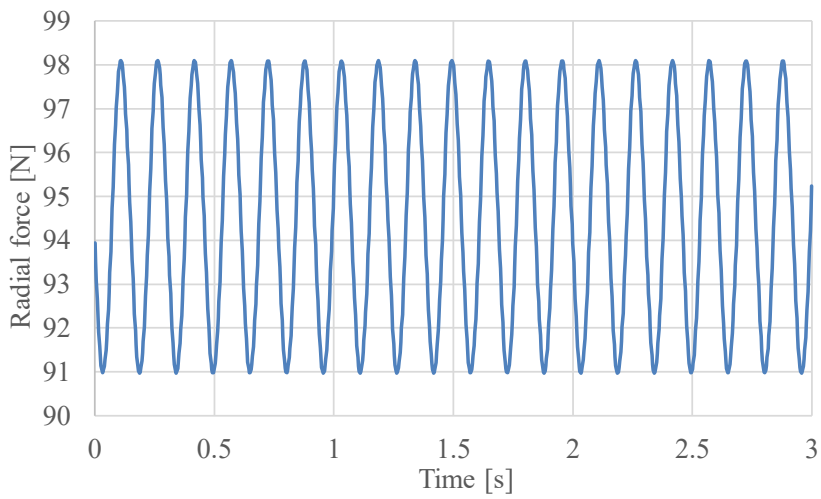


(a)

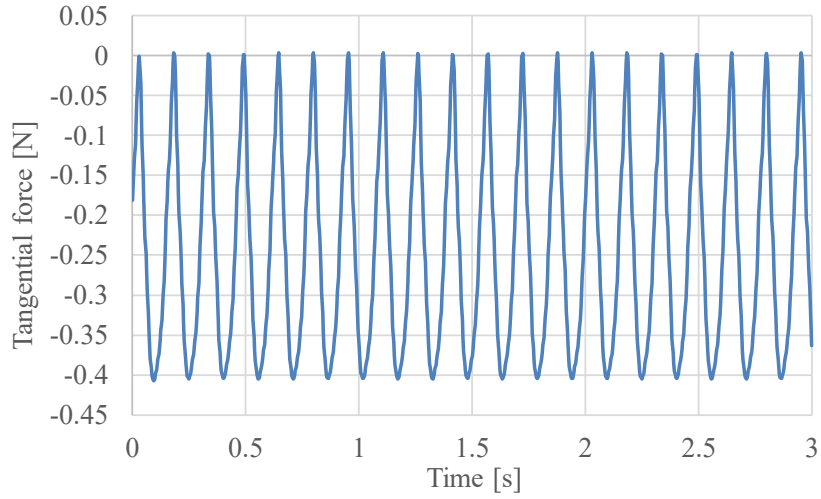


(b)

**Figure 7-30. (a) Radial force and (b) tangential force on inner steel piece I.**

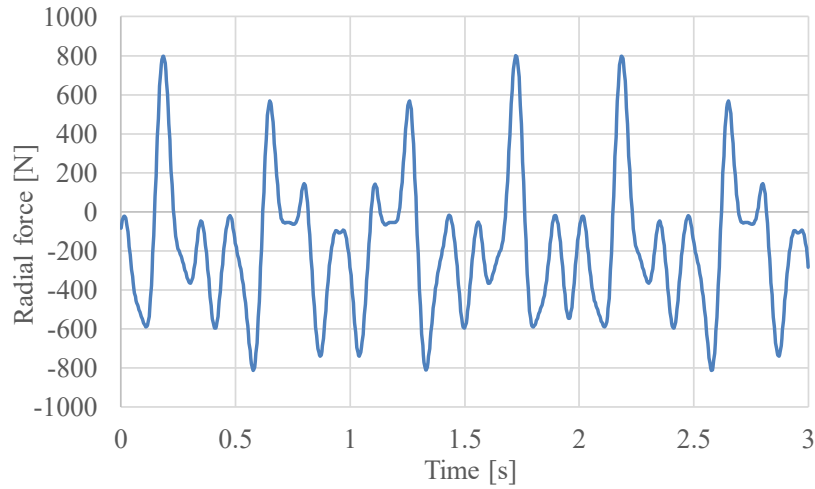


(a)

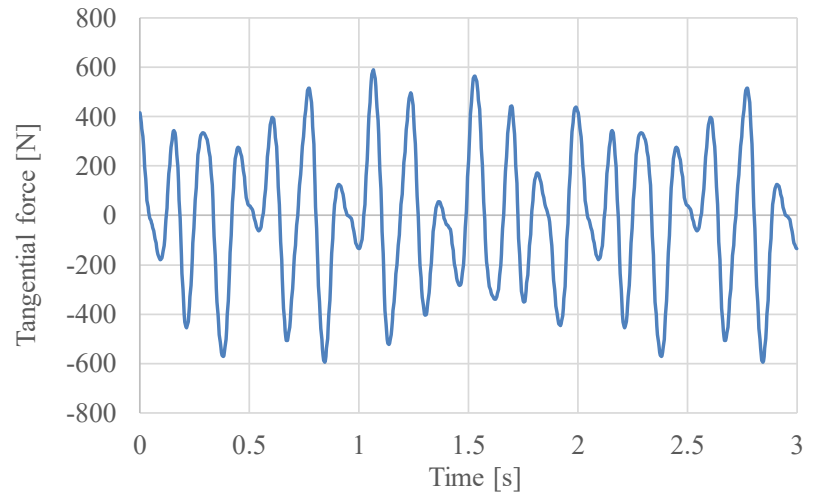


(b)

Figure 7-31. (a) Radial force and (b) tangential force on inner steel piece II.

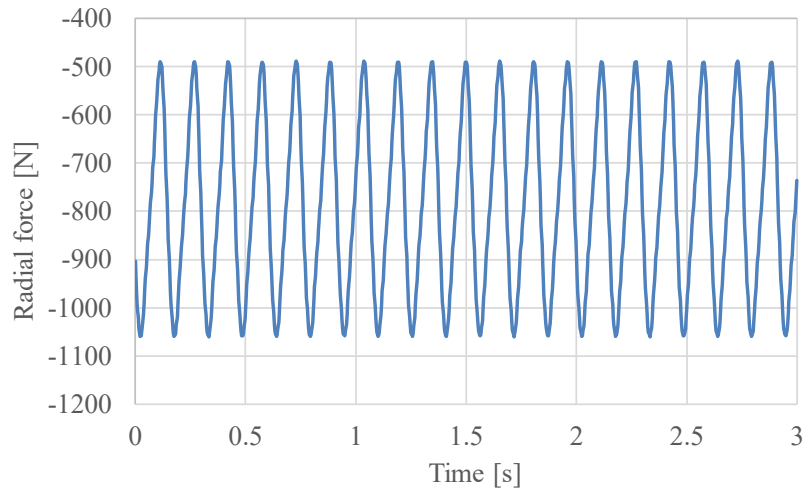


(a)

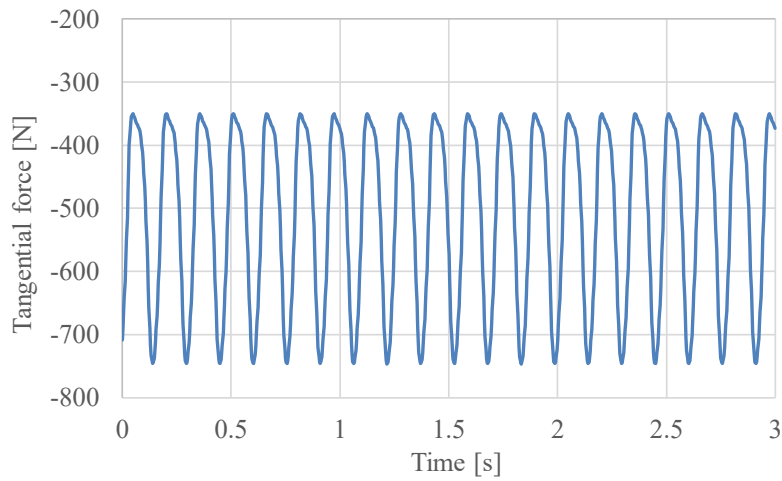


(b)

Figure 7-32. (a) Radial force and (b) tangential force on cage steel bar.



(a)



(b)

**Figure 7-33. (a) Radial force and (b) tangential force on outer steel bar.**

Based on the force values, the deflection of the rods has been calculated which are shown in Figure 7-34-Figure 7-36. The maximum deflection of the rods is 0.11 mm which is acceptable compared to the 1 mm air gap. When calculating the deflection, the lamination steels are assumed to provide no support which means the real deflection will be even smaller. Therefore, the air gap will be maintained between each rotor. The final geometry parameters are described in Table 7-I and the calculated volume torque density is 370.84 Nm/L.

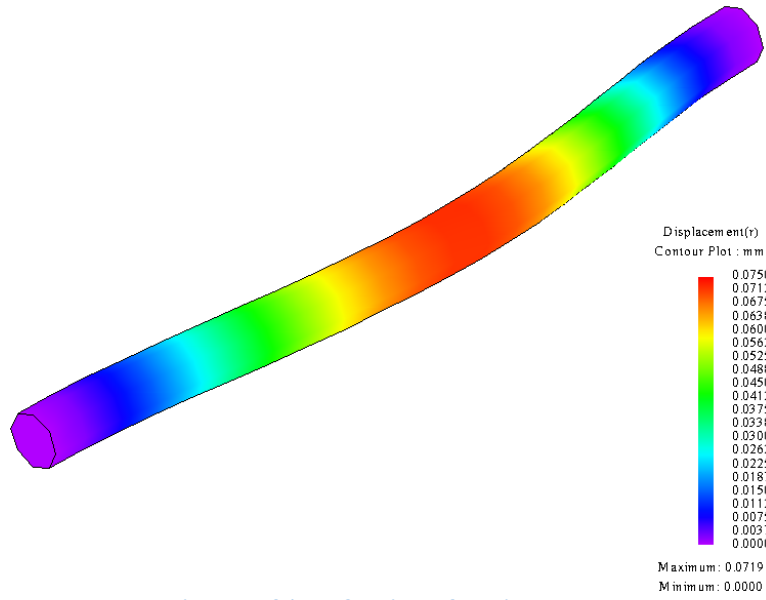
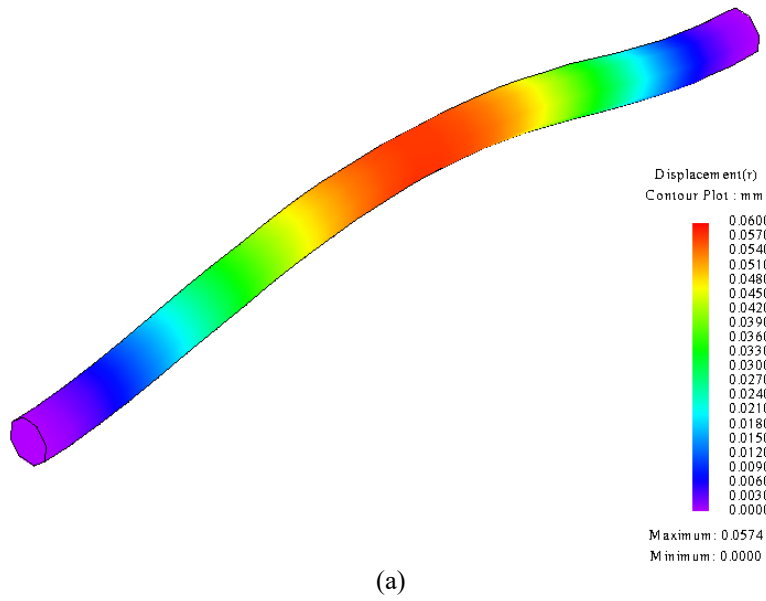
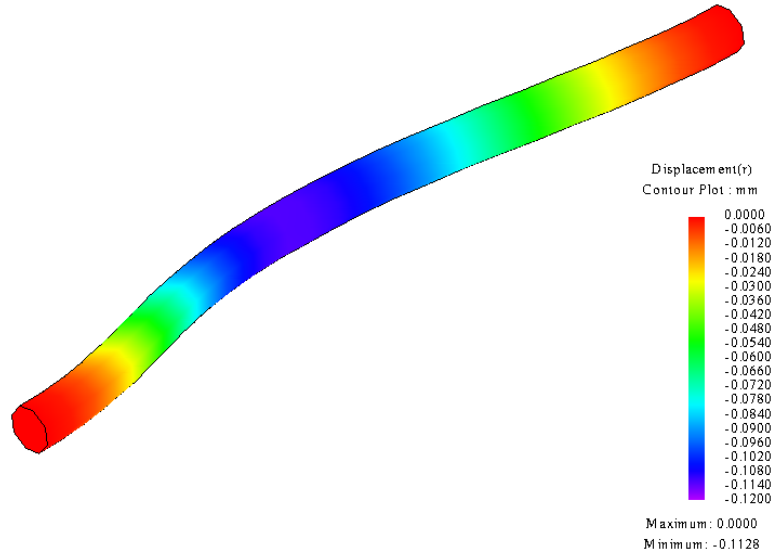


Figure 7-34. Deflection of the inner rod.





(b)

Figure 7-35. Deflection of the cage rods when (a) deflected outward and (b) deflected inward.

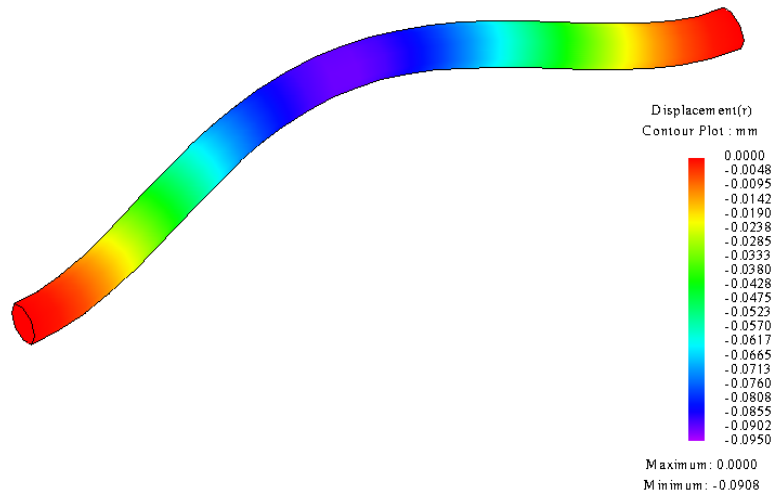


Figure 7-36. Deflection of the outer rods.

**Table 7-I. Final geometry parameters of stage 1 MG.**

Description		Unit	
Inner rotor	Inner radius, $r_{i1}$	178	mm
	Outer radius, $r_{o1}$	238	mm
	Pole pairs	12	-
	Radial length of the radial magnets	17	mm
Cage rotor	Inner radius, $r_{i2}$	239	mm
	Outer radius, $r_{o2}$	254	mm
	Pole pairs	78	-
Outer rotor	Inner radius, $r_{i3}$	255	mm
	Outer radius, $r_{o3}$	274	mm
	Pole pairs	66	-
Axial length, $d_1$		75	mm
Air gap, $g$		1	mm

## 8. Stage 2 MG Design without Stator

### 8.1 Initial design of the stage 1 magnetic gear

The gear ratio of the stage 1 MG is calculated to be  $G_{12} = 78/12=6.5$ . In order to obtain a 59:1 gear ratio, the stage 2 MG was designed to have  $p_4 = 6$  (inner rotor),  $n_5 = 54$  (cage rotor) and  $p_6 = 48$  (outer rotor). Therefore, the overall gear ratio of the MSMG is:

$$G_r = G_{12}G_{45} = \frac{78}{12} \cdot \frac{54}{6} = 58.5 \quad (2.1)$$

The inner radius of the inner rotor was fixed at 155 mm so that a stator could be put inside it. The radial length of the cage rotor was fixed at 15 mm so that the steel could provide enough mechanical support to prevent deflection. The radial length of the inner and the outer magnets has been varied. The radial length of the inner magnets was varied from 35 mm to 60 mm and the radial length of the outer magnets was varied from 10 mm to 40 mm. The parameter sweep result is shown in Figure 8-1.

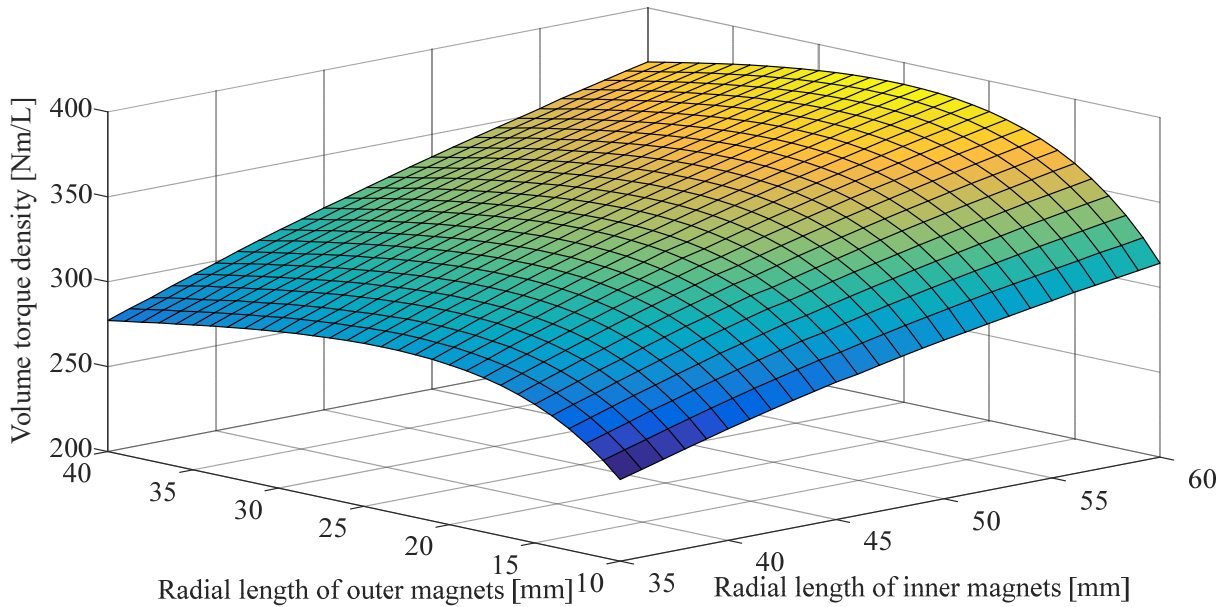


Figure 8-1. Parameter sweep for stage 2 MG.

It can be seen that with the radial length of the inner magnets increasing, the peak torque density is also increasing. The radial length of the inner magnets was chosen to be 45 mm because it could provide relatively high torque value and was not too large to assemble. The peak volume torque density was 339.4 Nm/L when the radial length of the outer magnets is 24 mm. The corresponding torque value was 2322.3 Nm. The geometry parameters are shown in Table 8-I.

**Table 8-I. Geometry parameters of stage 2 MG.**

Description			Unit
Inner rotor	Inner radius, $r_{i4}$	155	mm
	Outer radius, $r_{o4}$	200	mm
	Pole pairs	6	-
Cage rotor	Inner radius, $r_{i5}$	201	mm
	Outer radius, $r_{o5}$	216	mm
	Pole pairs	54	-
Outer rotor	Inner radius, $r_{i6}$	217	mm
	Outer radius, $r_{o6}$	241	mm
	Pole pairs	48	-
Axial length, $d_2$		37.5	mm
Air gap, $g$		1	mm

Magnet retaining lips and rods have been added to the inner and outer rotors. Plastic square bars have been added to the cage rotor. Using plastic bars can reduce the eddy current loss and increase the efficiency. The design is shown in Figure 8-2 with a peak torque of 2109.17 Nm. Radial magnets were added to the inner rotor as shown in Figure 8-3 which gave a torque value of 2126.92 Nm. The inner magnets have also been modified in order to achieve a higher torque value which are shown in Figure 8-4 and Figure 8-5. The corresponding torque was 2155.76 Nm and 2021.19 Nm, respectively.

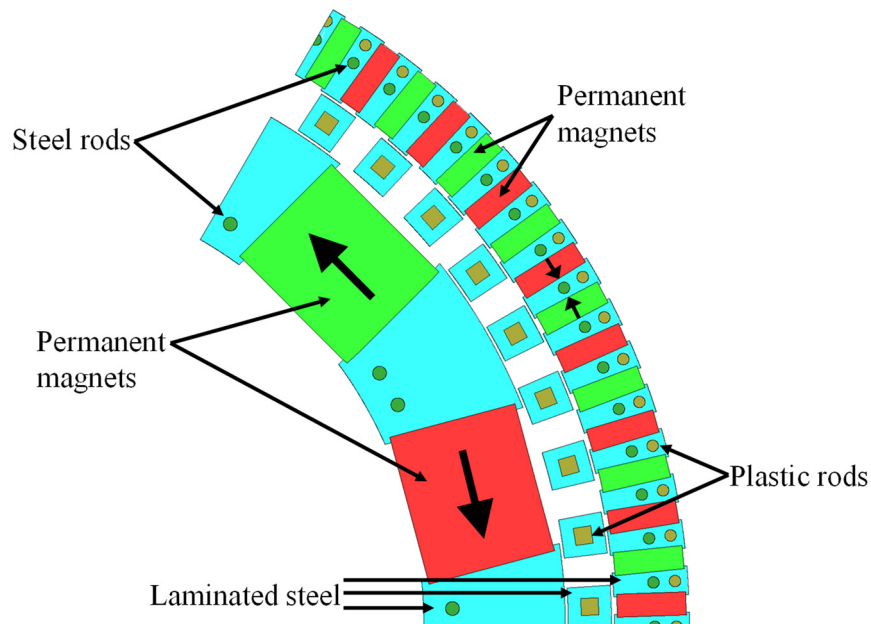


**Figure 8-2. Initial design of stage 2 MG.**

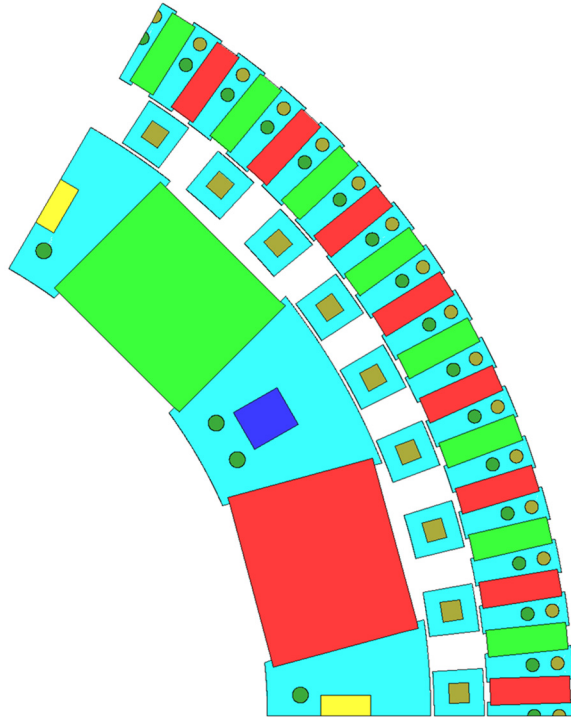


Figure 8-3. Modified inner rotor of stage 2 MG.

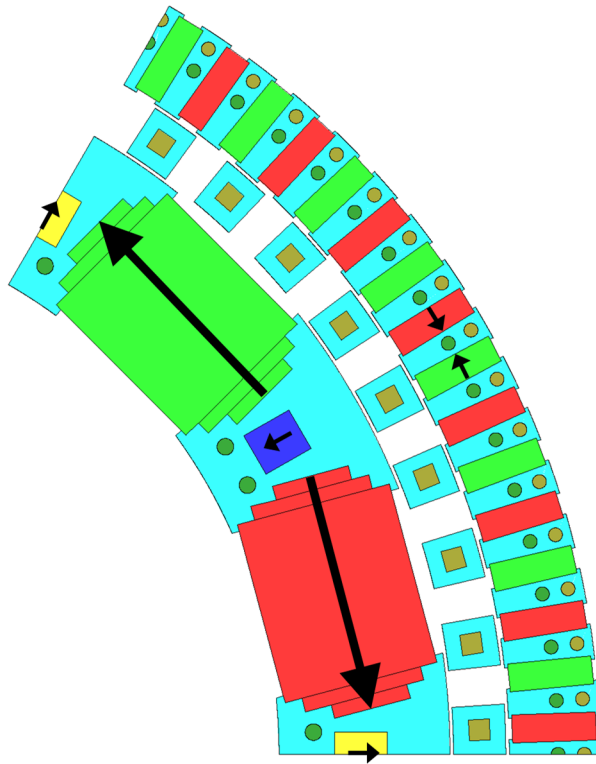


Figure 8-4. Modified inner rotor of stage 2 MG.

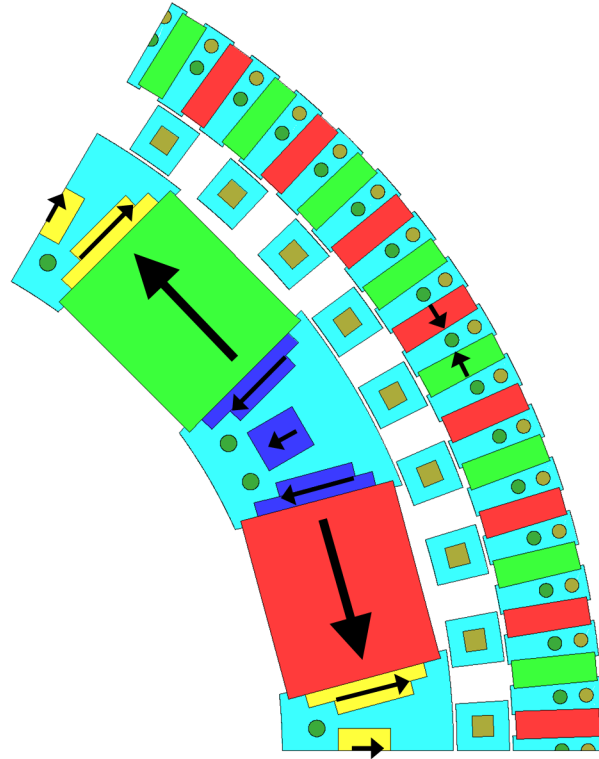


Figure 8-5. Modified inner rotor of stage 2 MG.

Since the previous designs did not show much improvement, new shapes of inner radial magnets were designed as shown in Figure 8-6. The radial length of the inner radial magnets has been varied from 5 mm to 20 mm and the result is shown in Figure 8-7. In order to save enough space for the inner rods, the inner radial magnets should not be longer than 20 mm. Therefore, the torque became 2309.0 Nm with radial length of 20 mm. 4.5 mm by 5 mm radial magnets were used on the outer rotor to increase the torque which is shown in Figure 8-8 with the peak torque of 2438.0 Nm. The modified geometry is shown in Table 8-II. When the cage rotor and the inner rotor was rotating with 520 RPM and 4680 RPM, the torque on the three rotors is shown in Figure 8-9.

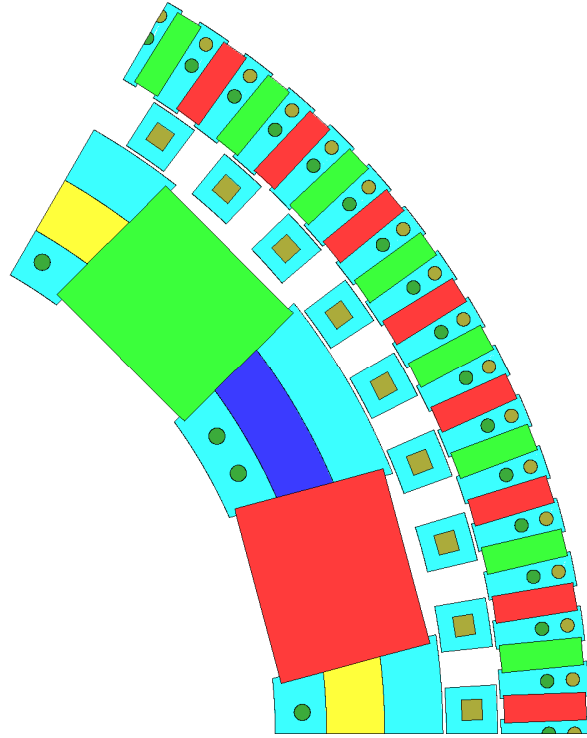


Figure 8-6. Modified inner rotor of stage 2 MG.

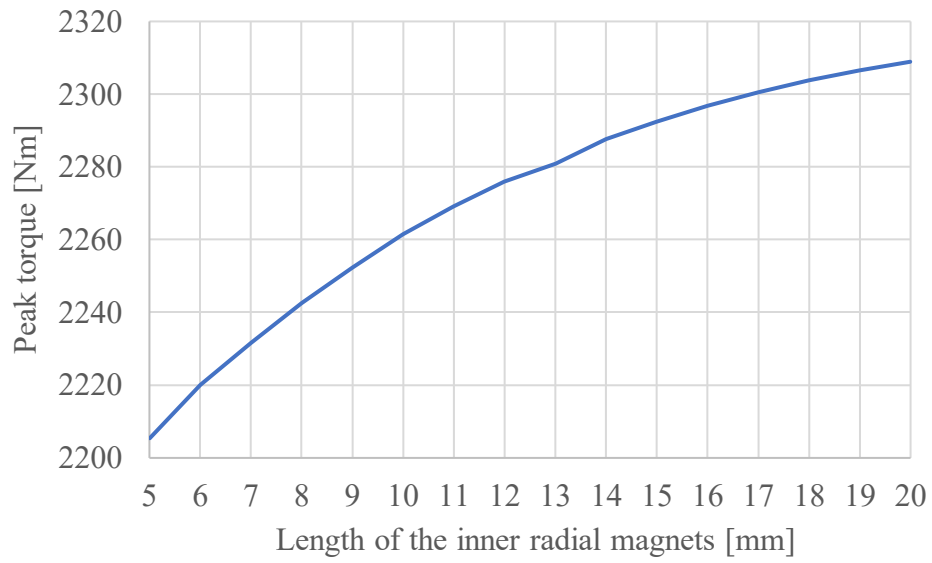


Figure 8-7. Peak torque plot with different values of the inner radial magnets.

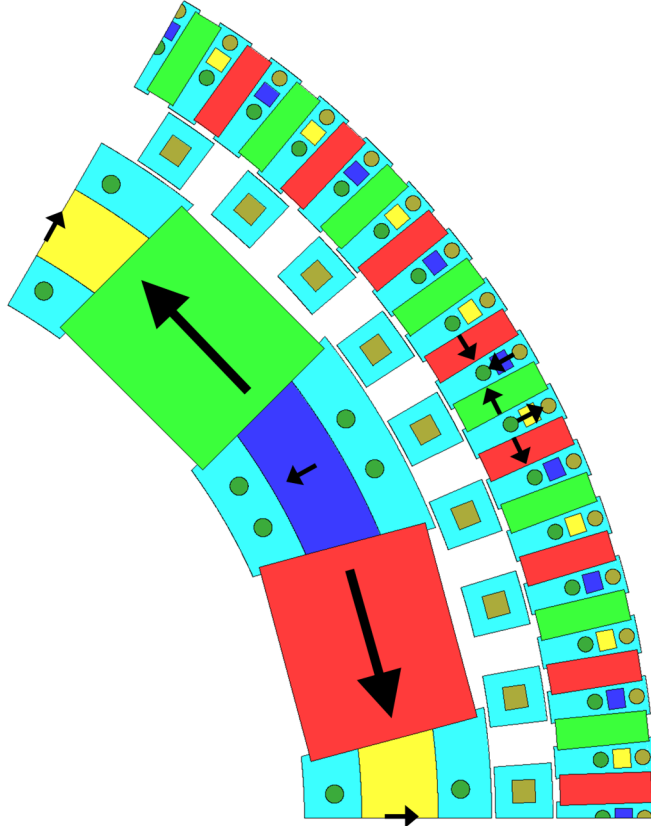
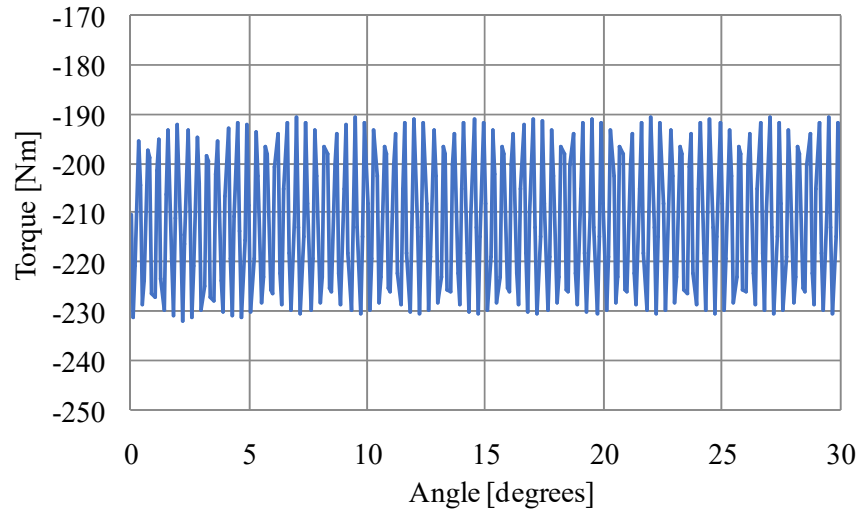


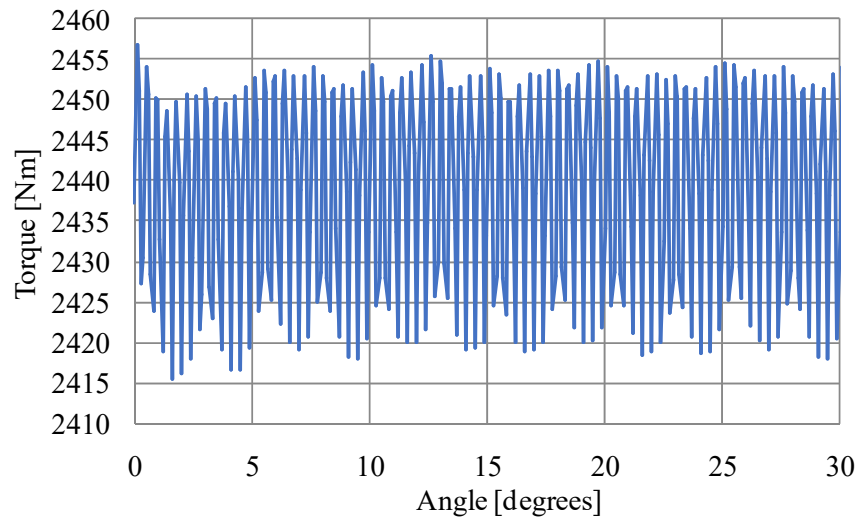
Figure 8-8. Stage 2 MG with radial magnets on the outer rotor.

Table 8-II. Modified geometry parameters of stage 2 MG.

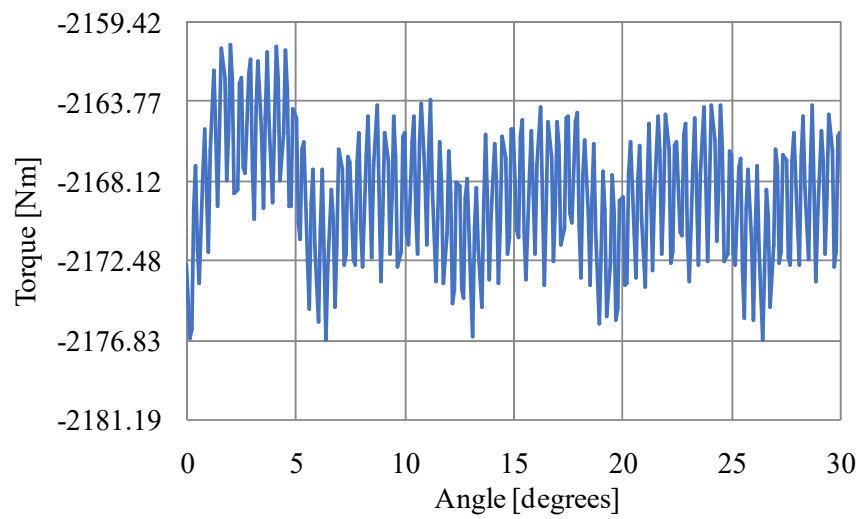
Description		Unit	
Inner rotor	Inner radius, $r_{i4}$	155	mm
	Outer radius, $r_{o4}$	204	mm
	Radial length of radial magnets	20	mm
	Pole pairs	6	-
Cage rotor	Inner radius, $r_{i5}$	205	mm
	Outer radius, $r_{o5}$	220	mm
	Pole pairs	54	-
Outer rotor	Inner radius, $r_{i6}$	221	mm
	Outer radius, $r_{o6}$	247	mm
	Radial length of radial magnets	4.5	mm
	Width of radial magnets	5	mm
	Pole pairs	48	-
Axial length, $d_2$		37.5	mm
Air gap, $g$		1	mm



(a)



(b)



(c)

Figure 8-9. Torque as a function of angle on the (a) inner rotor (b) cage rotor and (c) outer rotor.

The torque ripple on the inner rotor was very high which is shown in Figure 8-9. Therefore, the pole pair combination of stage 2 MG has been changed to 6-57-51 which gives a gear ratio of 9.5. The overall gear ratio of the multistage MG becomes 61.75:1 which is still close enough to 59:1. With this pole pair combination, a 1/3 model can be simulated. The parameter sweep analysis has been done for the design shown in Figure 8-10. The results are shown in Figure 8-11.

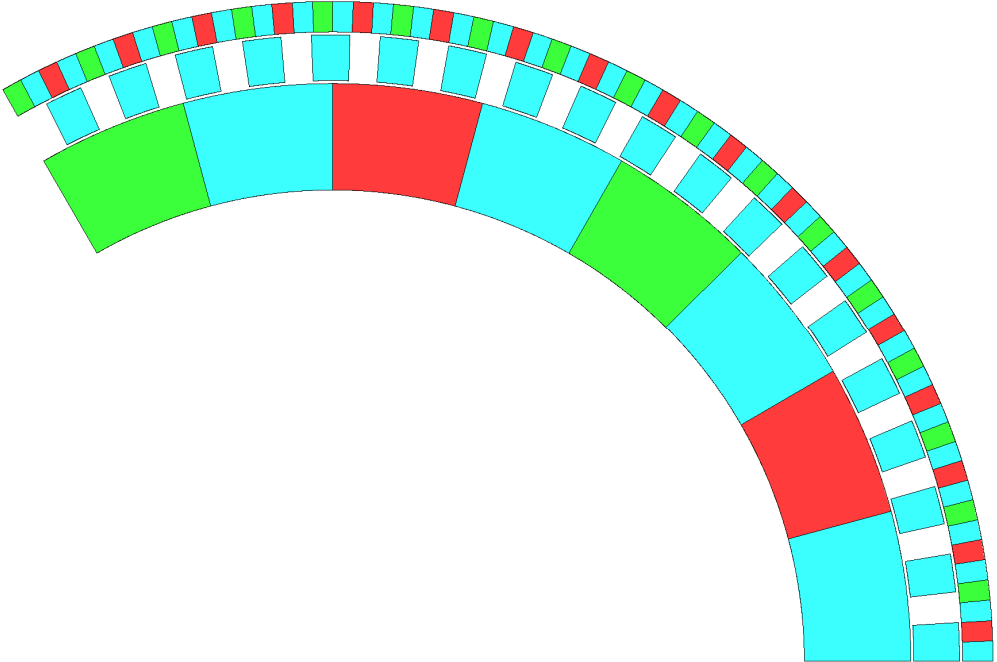


Figure 8-10. Stage 2 MG with a pole combination of 6-57-51.

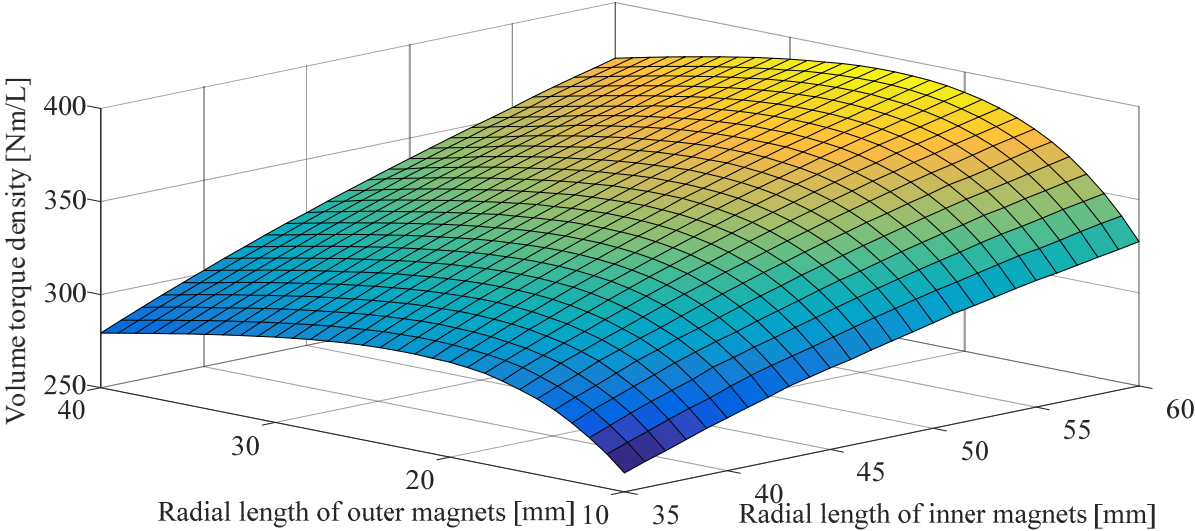


Figure 8-11. Parameter sweep analysis when the length of the outer and inner magnets was varied.

The geometry parameters were chosen to be the same used in Table 8-I considering the tradeoff between the size of the magnets and torque density which is shown in Figure 8-12. The corresponding torque and volume torque density is 2358.22 Nm and 344.64 Nm/L, respectively. The torque values on the inner, cage and outer rotors are shown in Figure 8-13

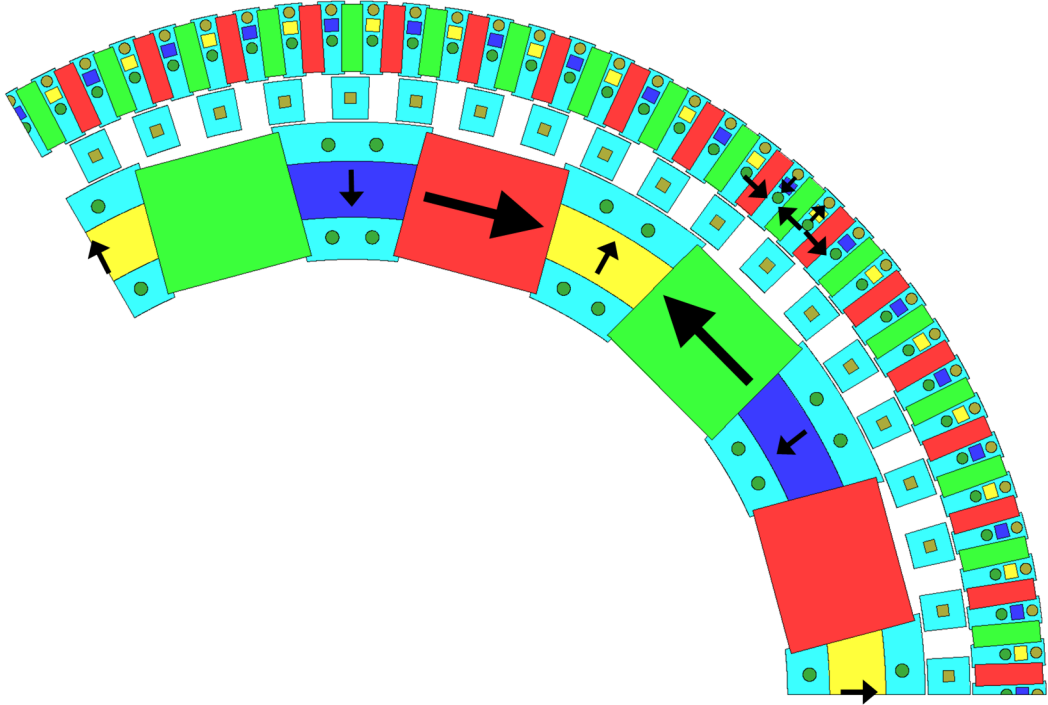
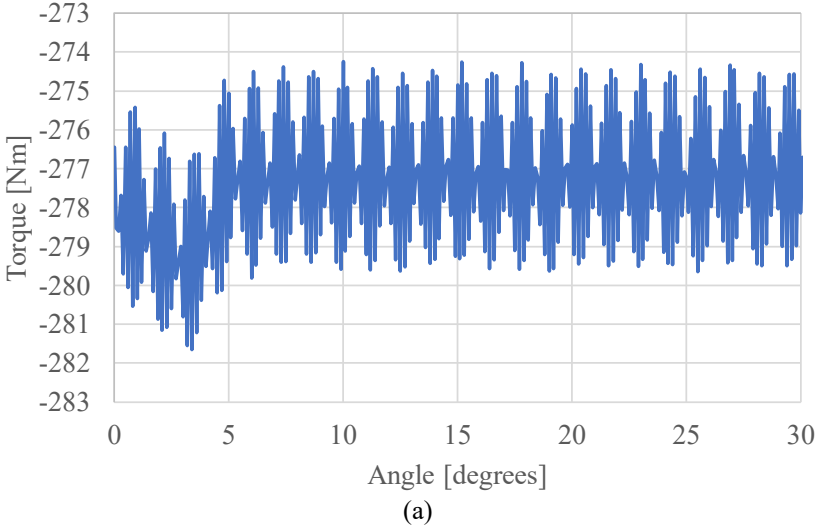
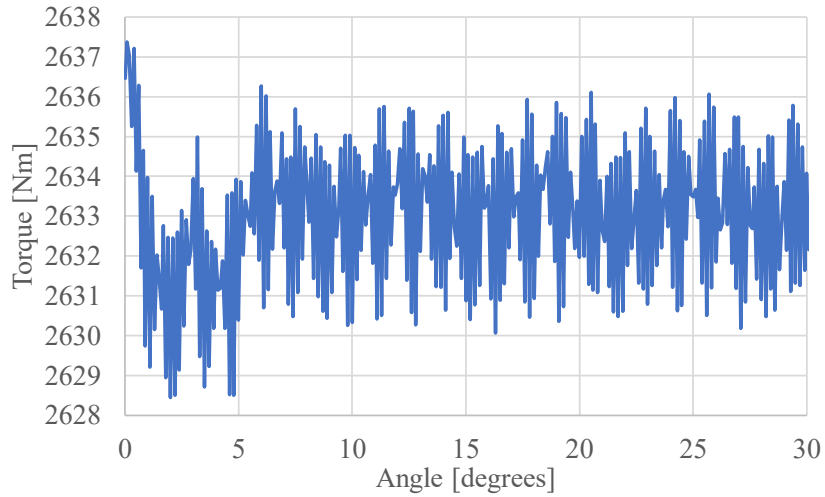
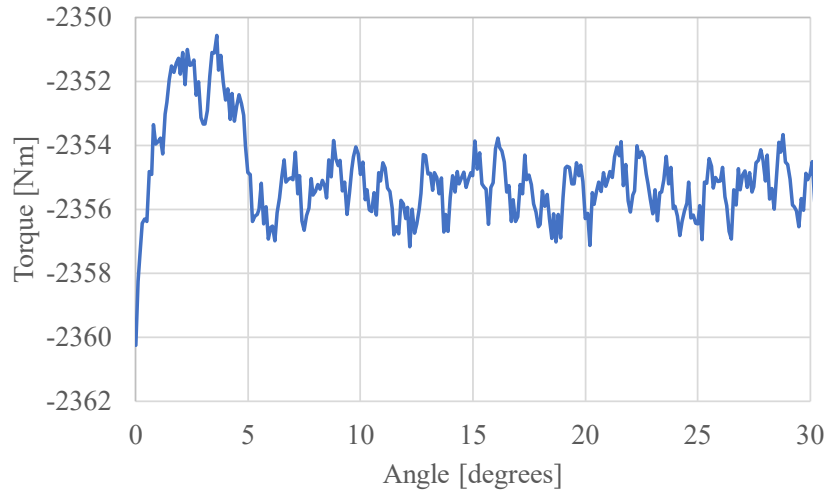


Figure 8-12. Final design of stage 2 MG.





(b)



(c)

**Figure 8-13. Torque on the (a) inner rotor (b) cage rotor and (c) outer rotor.**

### 8.1.1 Force and deflection analysis

The radial and tangential forces on each lamination have been calculated as shown in Figure 8-14. Based on the magnetic force values, the mechanical deflection of the rods have been calculated and is shown in Figure 8-15-Figure 8-17. The inner and half of the outer rods are steel material. The cage and half of the outer rods are carbon fiber material. It can be seen that the deflection of the rods is very small compare to the 1 mm air gap. Therefore, the deflection caused by the magnetic forces will not be a concern.

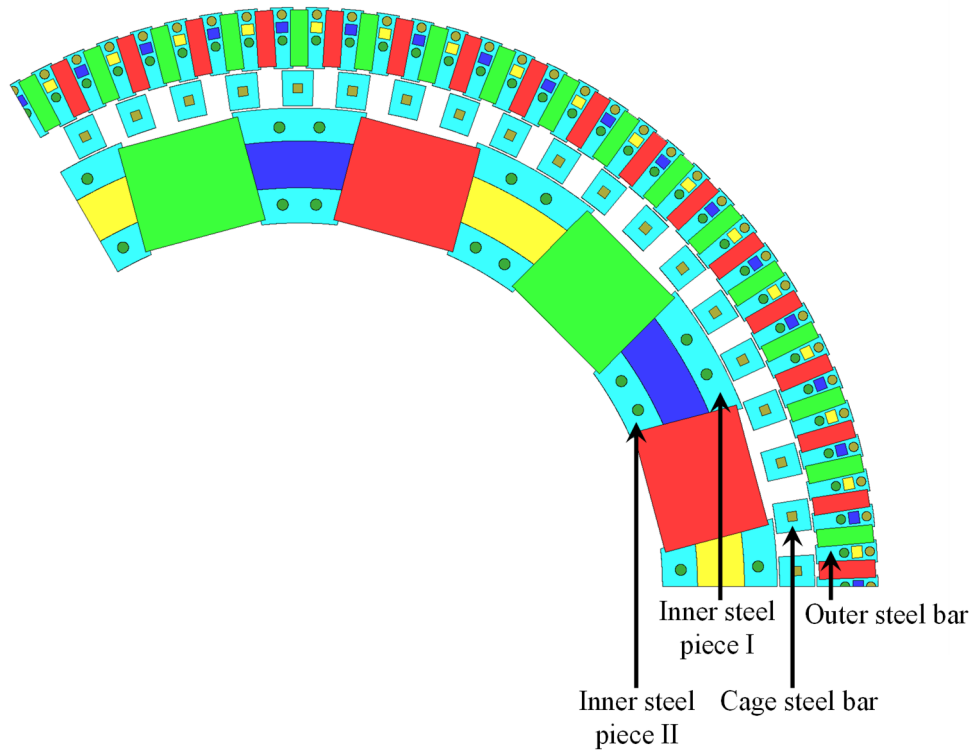


Figure 8-14. Forces to be calculated on each part.

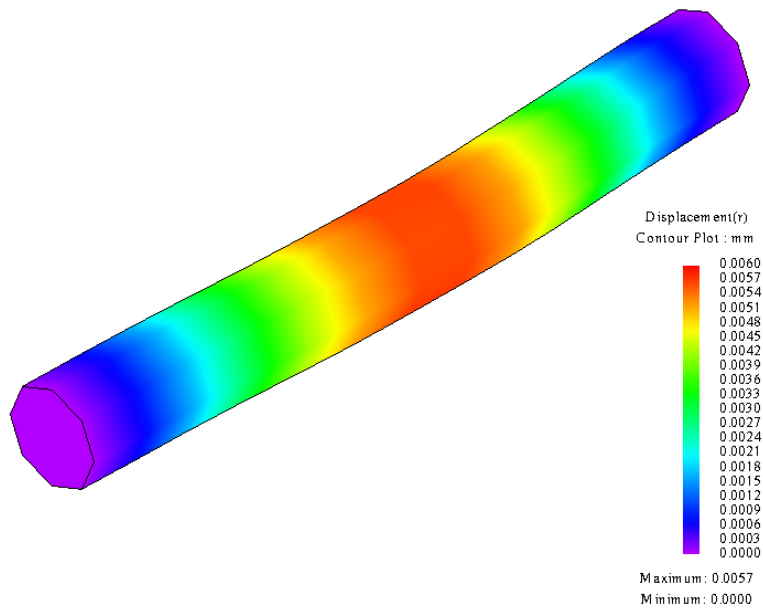
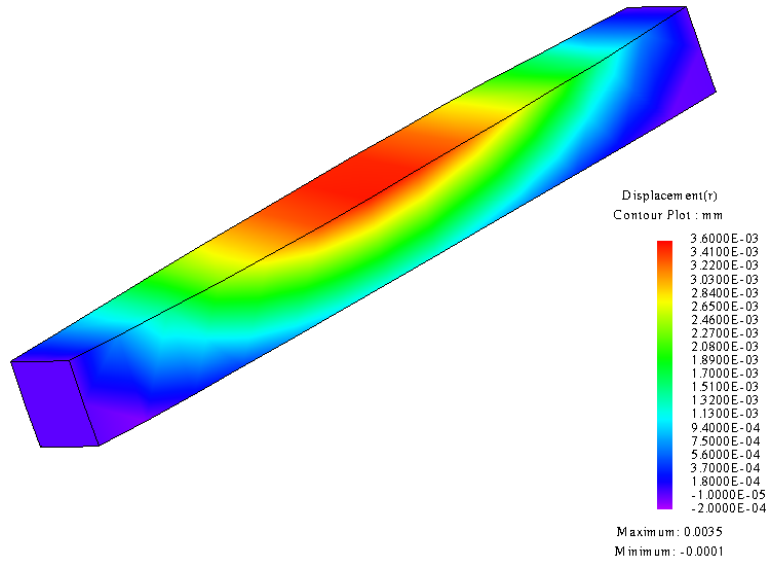
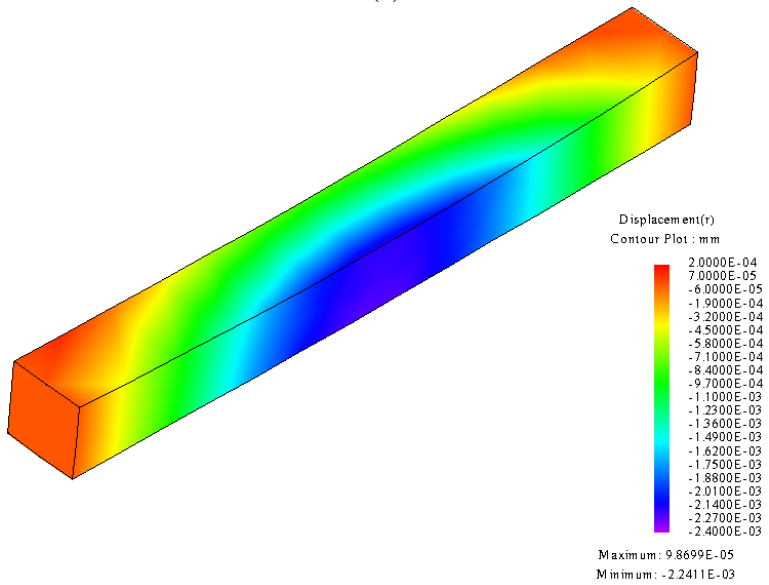


Figure 8-15. Deflection of the inner rod.



(a)



(b)

Figure 8-16. Deflection of the cage rod (a) deflected outward and (b) deflected inward.

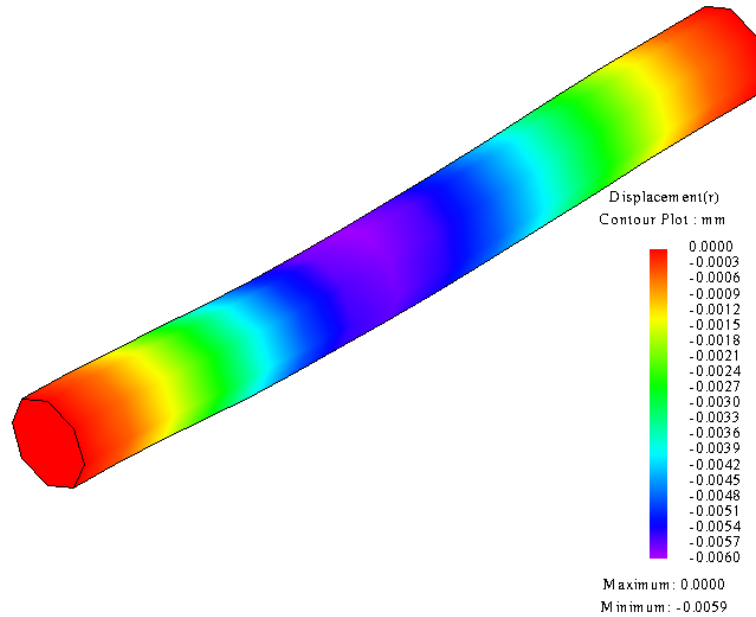


Figure 8-17. Deflection of the outer rod.

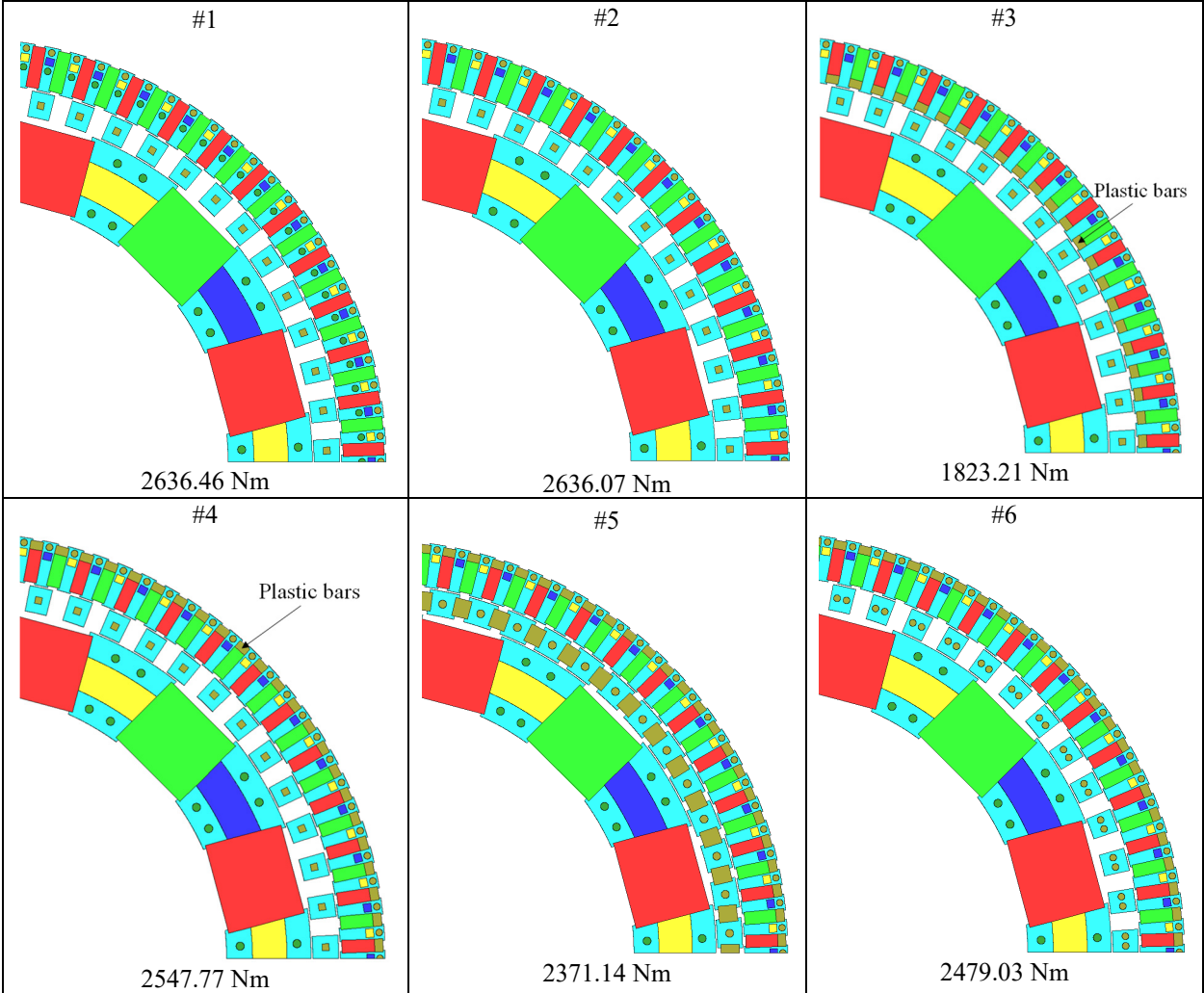
### 8.1.2 Loss analysis

The efficiency of the above design will be low with a high rotational speed as the number of pole pairs on the outer rotor is very high. The frequency of the outer rotor is high and therefore, the losses on the outer steel rods are high. There will be a lot of losses on the outer steel rods. Therefore, the outer steel rods have been removed to reduce the losses. The cage rotor has also been slightly modified so that there will not be any tolerance issue during assembly. The comparison of different designs is shown in Final design of the stage 1 magnetic gear

. Design #1 is the original design. Design #2 has no outer steel rods and the plastic rods will not be strong enough to hold the outer lamination bars in place. In design #3, plastic bars have been added. However, the torque is decreased a lot. Therefore, the plastic bars have been moved to the outside of the outer rotor as shown in design #4. In design #5, each cage lamination bar has one single rod and there is rectangular plastic bar between each cage lamination piece. The cage plastic bars can provide a lot of support for the cage rotor. The cage rods have also been changed to be round which can have a higher tolerance than square ones. Design #6 is chosen to be the final design as the torque is higher than design #5 and also it has enough support for prevent deflection. Plastic rectangular bars have been used on the outer rotor and the two ends of the plastic bars will be fixed on the two end plates. Therefore, the outer lamination bars can rest on both of the rods and the plastic bars. The loss was calculated when the cage rotor was rotating with an angular speed of 520 RPM which is shown in Figure 8-18 and the calculated efficiency was calculated to

be 89%. Figure 8-19 shows the current density plot and the loss density plot. It clearly shows that most of the losses were produced by the outer magnets

Table 8-III. Comparison of different designs.



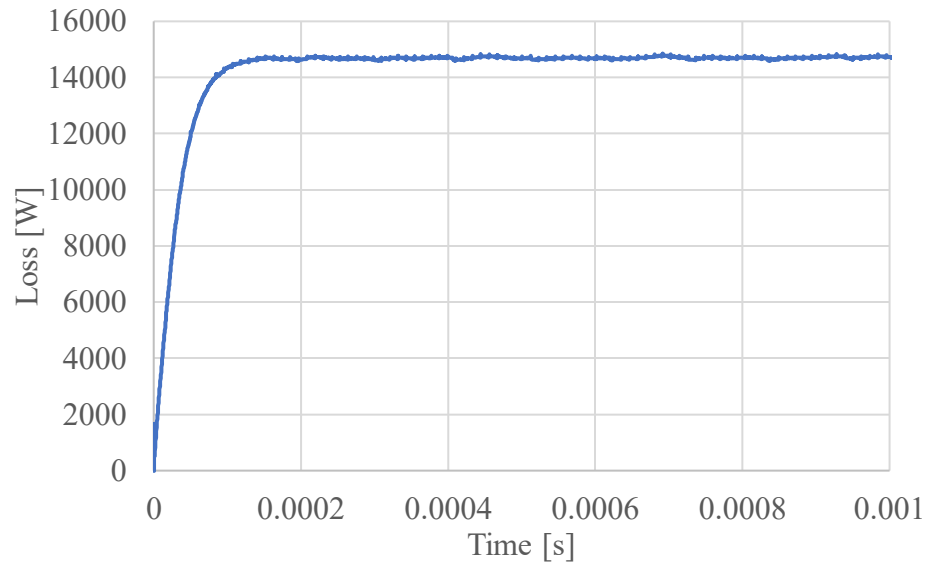
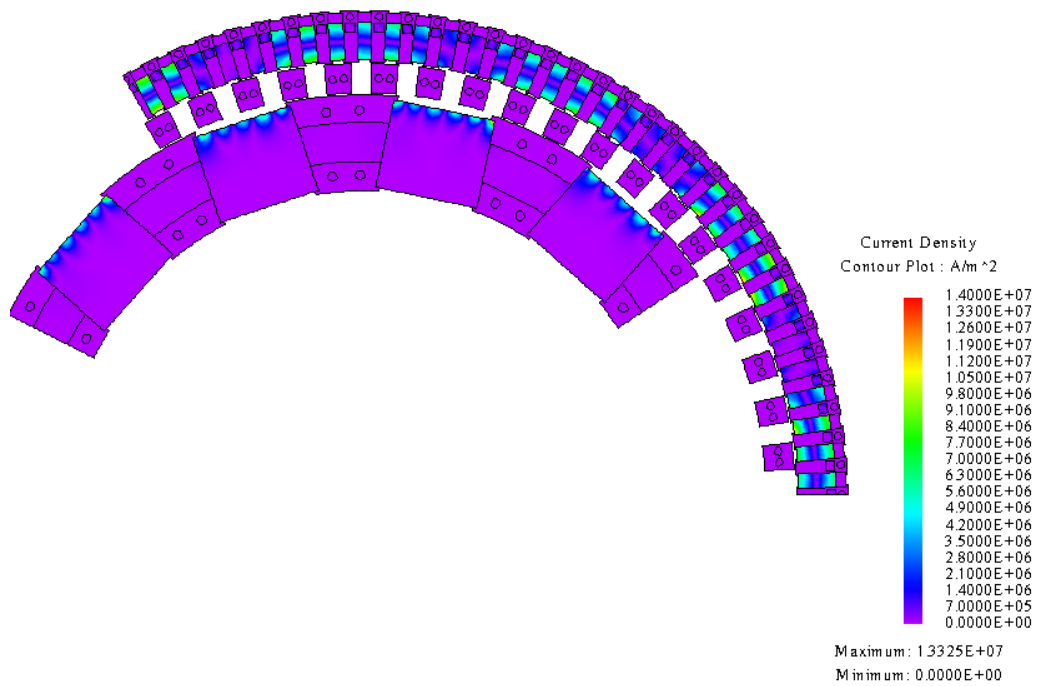
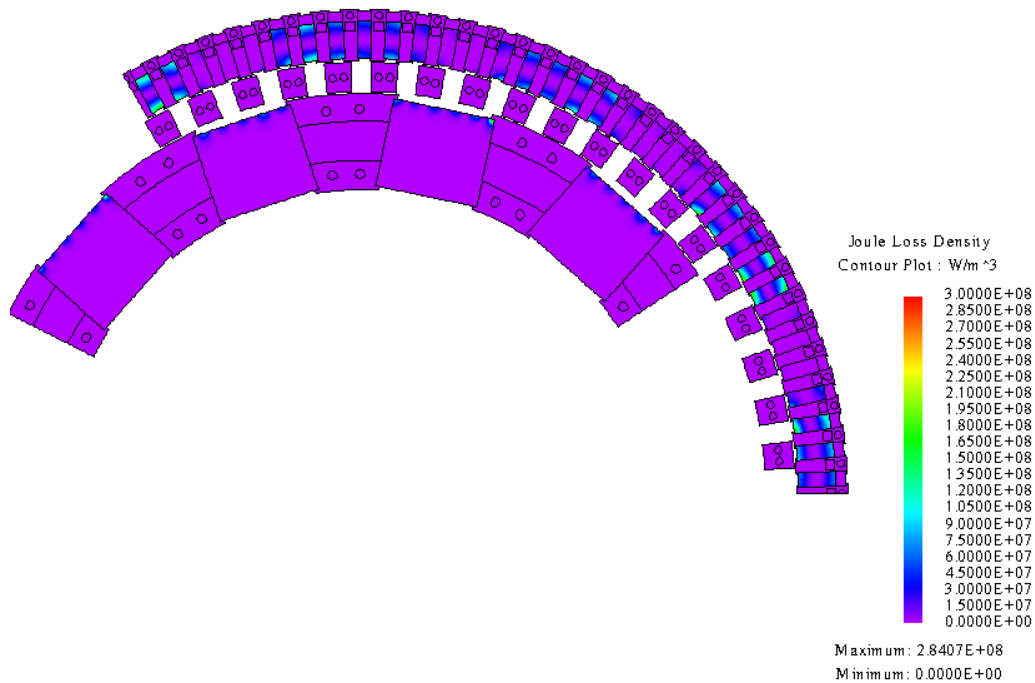


Figure 8-18. Eddy current loss when the cage rotor was rotating at an angular speed of 520 RPM.



(a)

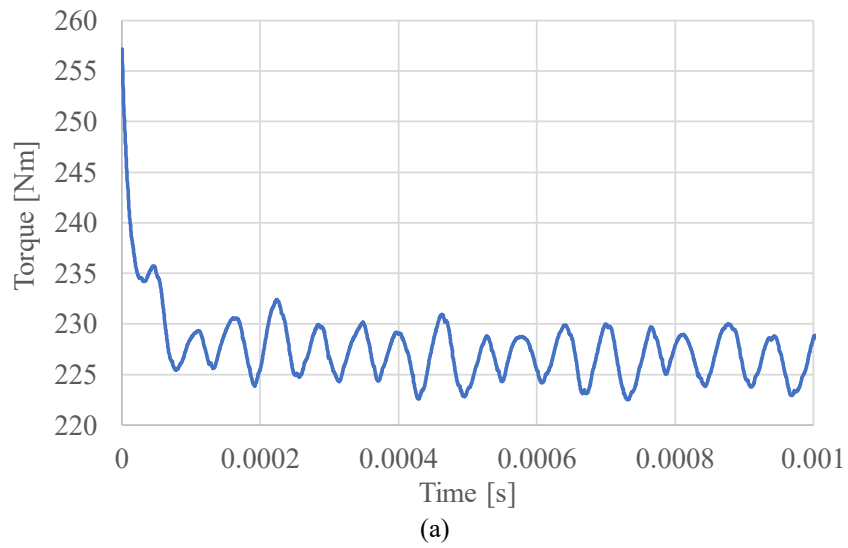


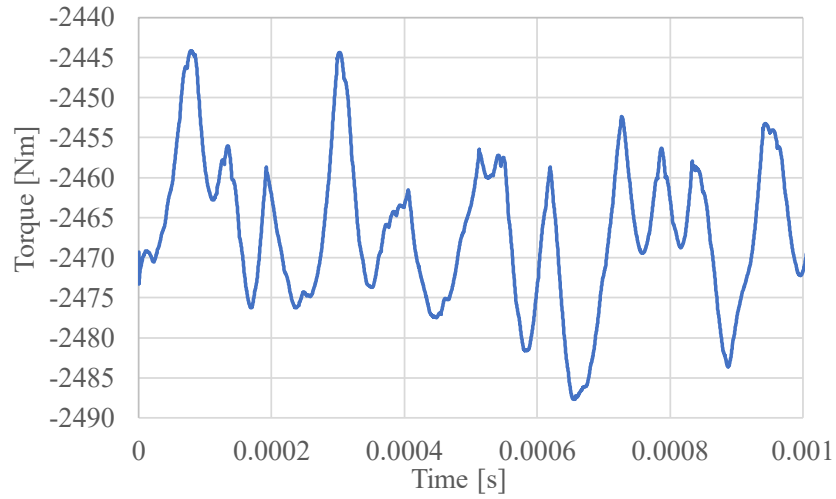
(b)

Figure 8-19. (a) Current density and (b) loss density.

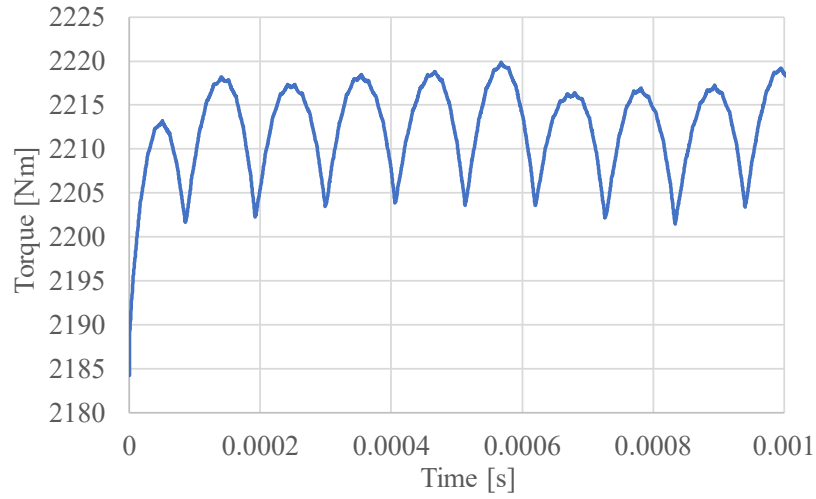
## 8.2 Final design of the stage 1 magnetic gear

The torque plots are present in Figure 8-20 which give low torque ripples. The calculated volume torque density is 344.91 Nm/L and the final parameters are shown in Table 8-IV.





(b)



(c)

Figure 8-20. Torque on the (a) inner rotor (b) cage rotor and (c) outer rotor.

Table 8-IV. Final Geometry parameters of the stage 2 MG.

Description			Unit
Inner rotor	Inner radius, $r_{i4}$	155	mm
	Outer radius, $r_{o4}$	204	mm
	Radial length of radial magnets	20	mm
	Pole pairs	6	-
Cage rotor	Inner radius, $r_{i5}$	205	mm
	Outer radius, $r_{o5}$	220	mm
	Pole pairs	57	-
Outer rotor	Inner radius, $r_{i6}$	221	mm
	Outer radius, $r_{o6}$	247	mm
	Radial length of radial magnets	4.5	mm
	Width of radial magnets	5	mm
	Pole pairs	51	-
Axial length, $d_2$		37.5	mm
Air gap, $g$		1	mm

### 8.2.1 Force and deflection analysis

The radial and tangential forces have been calculated on the inner, cage and outer steel pieces as shown in Figure 8-21. Based on those magnetic forces, the mechanical deflection of the rods has been calculated. The radial and tangential force values are shown in Figure 8-22-Figure 8-25.

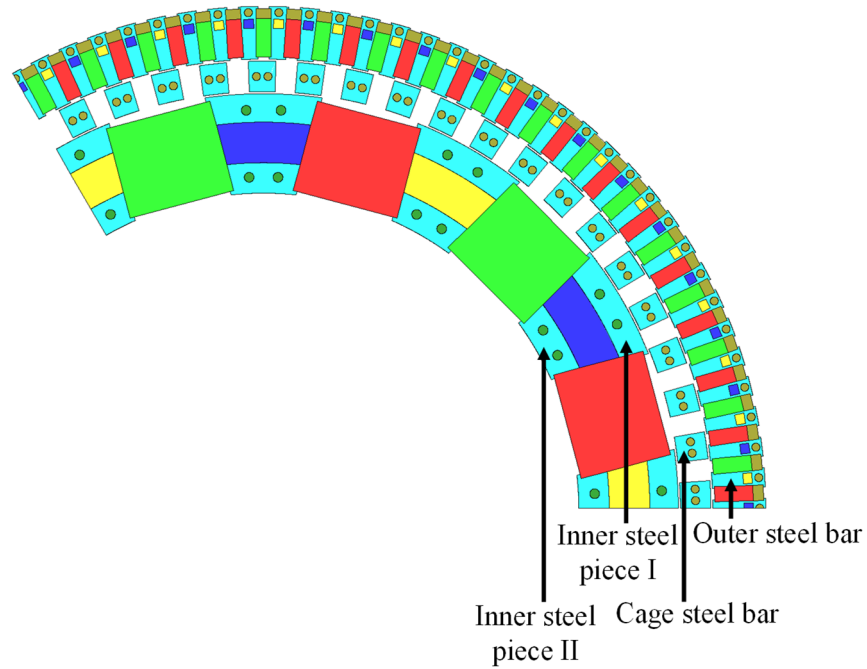
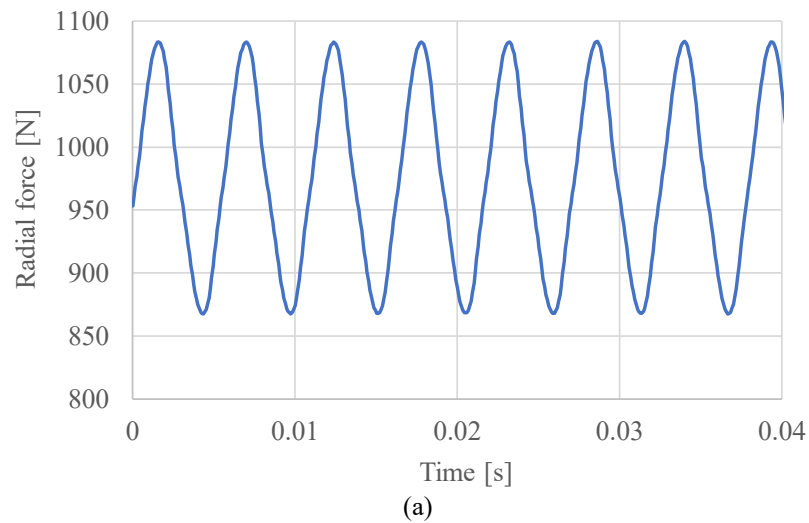
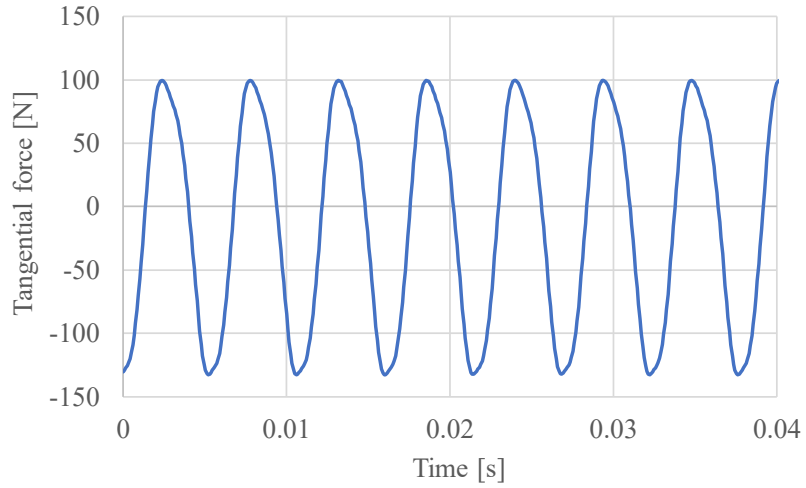


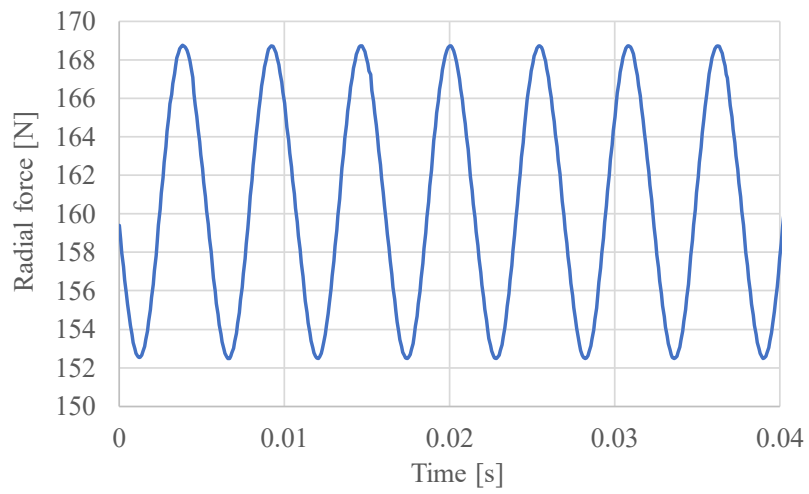
Figure 8-21. Magnetic forces on steel pieces.



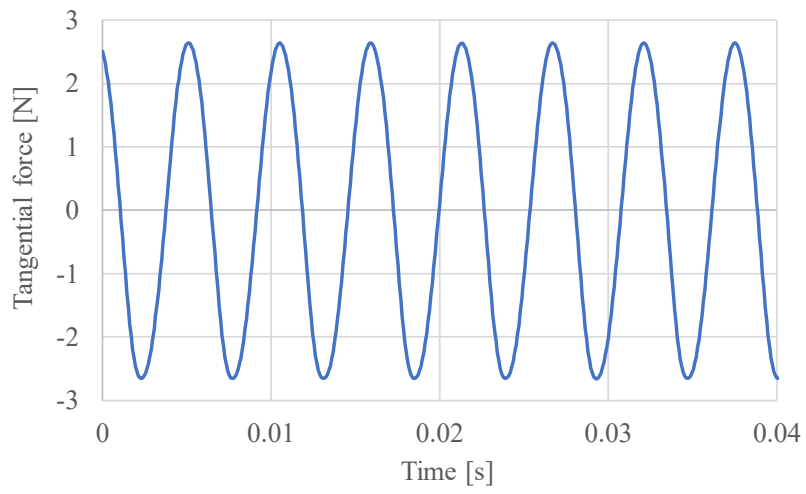


(b)

Figure 8-22. (a) Radial and (b) tangential forces on inner steel piece I.

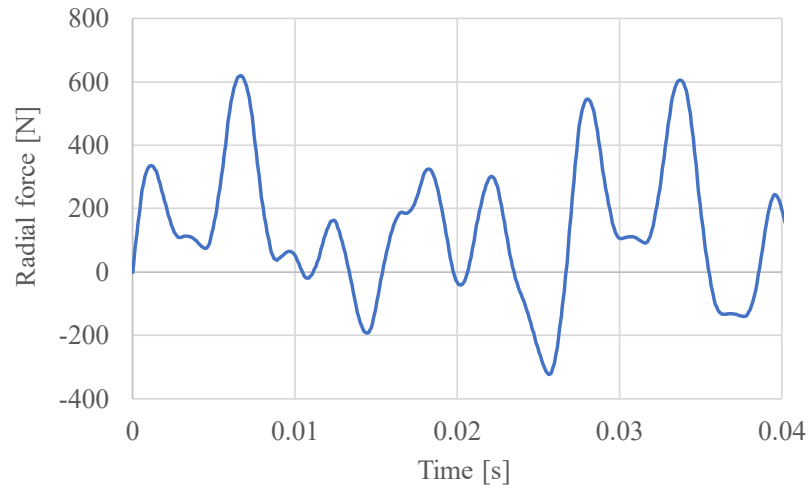


(a)

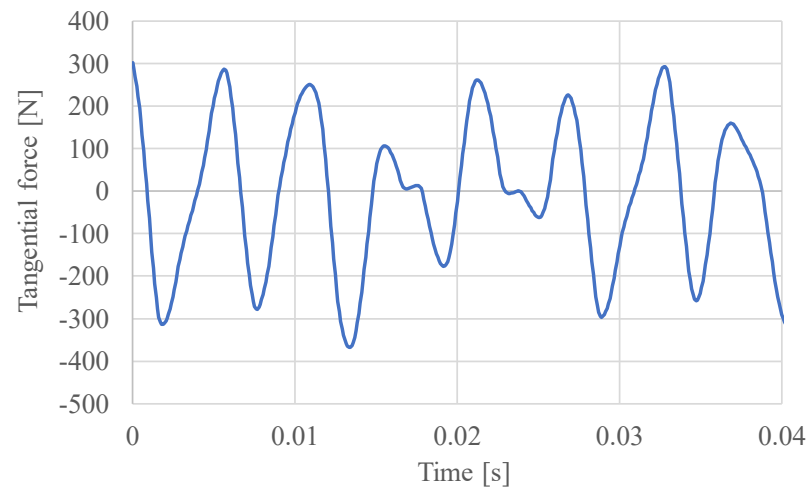


(b)

Figure 8-23. (a) Radial and (b) tangential forces on inner steel piece II.

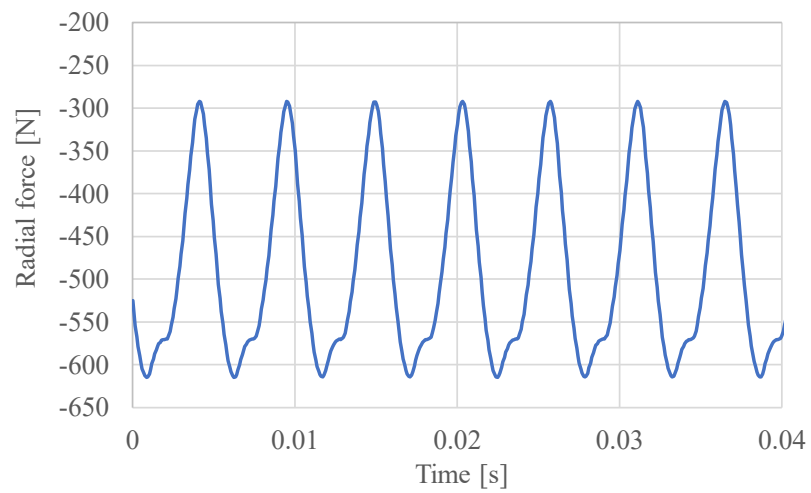


(a)

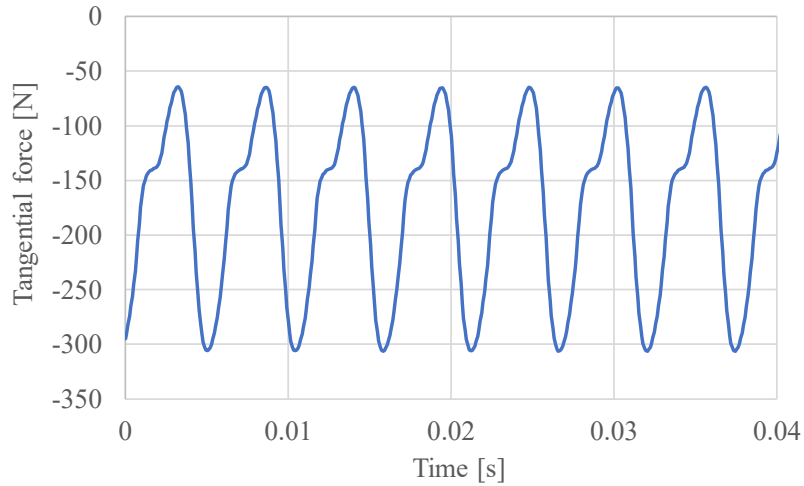


(b)

Figure 8-24. (a) Radial and (b) tangential forces on cage steel bar.



(a)



(b)  
**Figure 8-25. (a) Radial and (b) tangential forces on outer steel bar.**

Using these magnetic forces, the mechanical deflection of the rods is calculated again like what is done for the previous design. From the results shown in Figure 8-26-Figure 8-28, the maximum deflection of those rods is 0.0093 mm which is very small compared to the 1 mm air gap.

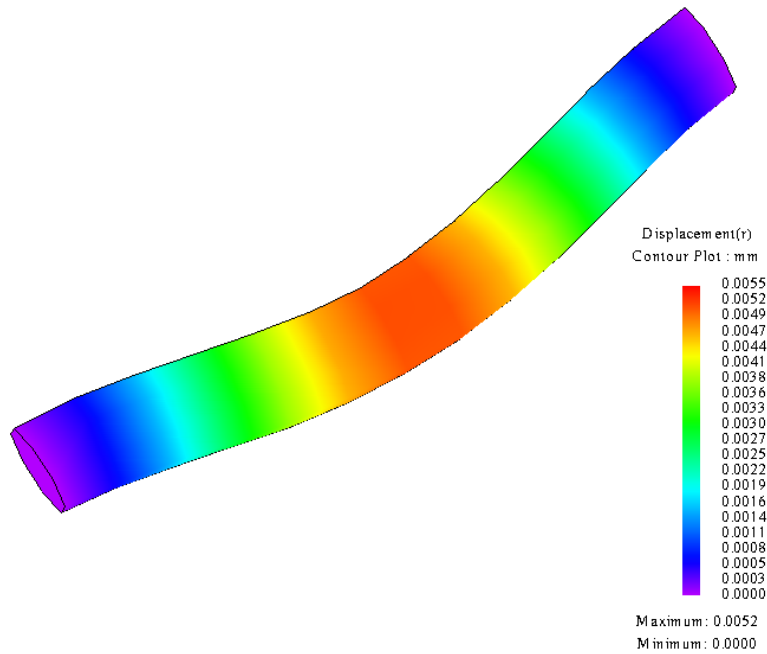
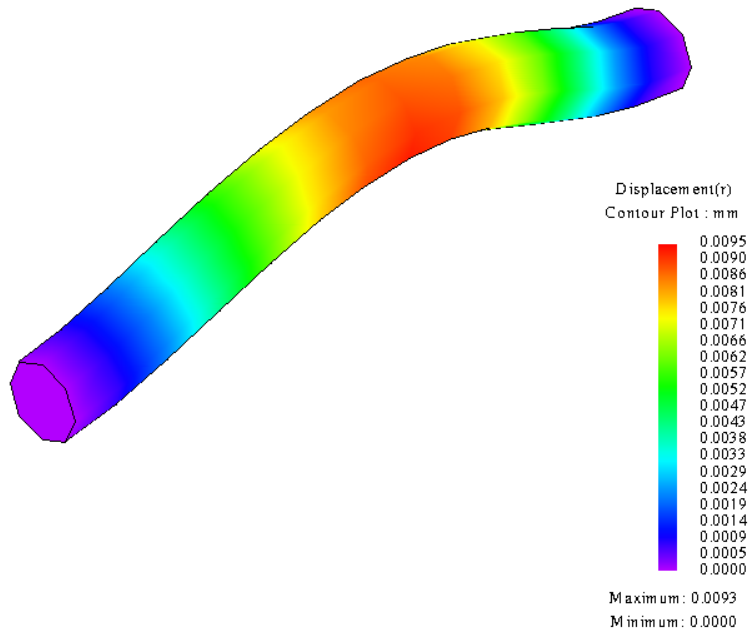
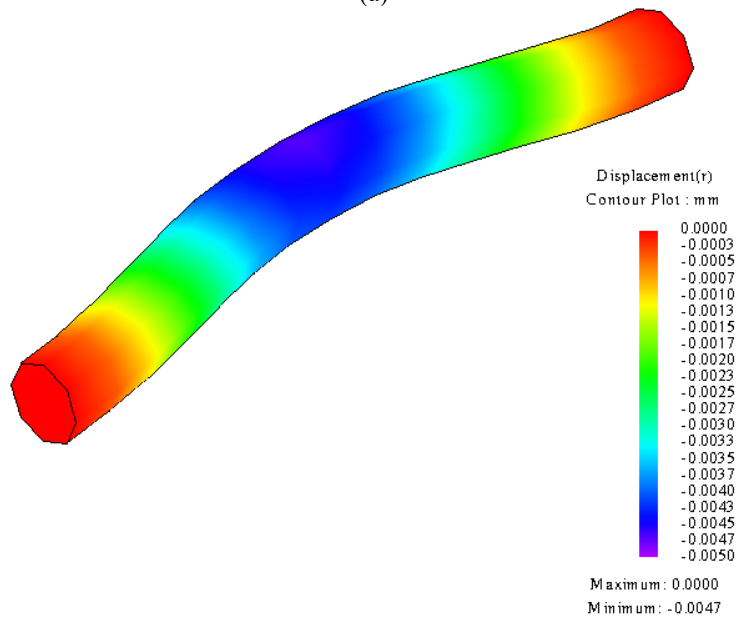


**Figure 8-26. Deflection of the inner rod.**



(a)



(b)

Figure 8-27. Deflection of the cage rod when (a) deflected outward and (b) deflected inward.

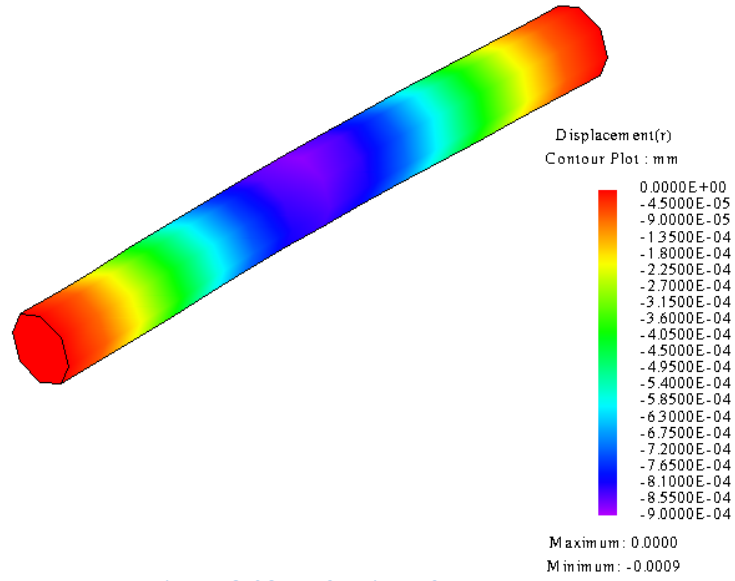


Figure 8-28. Deflection of the outer rod.

## 9. Stage 2 MG Design with Stator

### 9.1 Fractional winding design for different number of slots

A stator has been added inside the inner rotor of the stage 2 MG. In this way, it will work as a magnetically geared generator (MGG). The stator has to be able to create 12 poles (6 pole pairs) so that it can generate a constant torque. At first, a 45-slot stator was designed which is shown in Figure 9-1. The distribution of the three-phase distributed winding (phase U, phase W and phase V) is also shown in Figure 9-1. The phase of the winding was chosen to achieve the highest torque and the corresponding torque on the inner rotor was plotted in Figure 9-2. The parameters of the stator are described in Table 9-I.

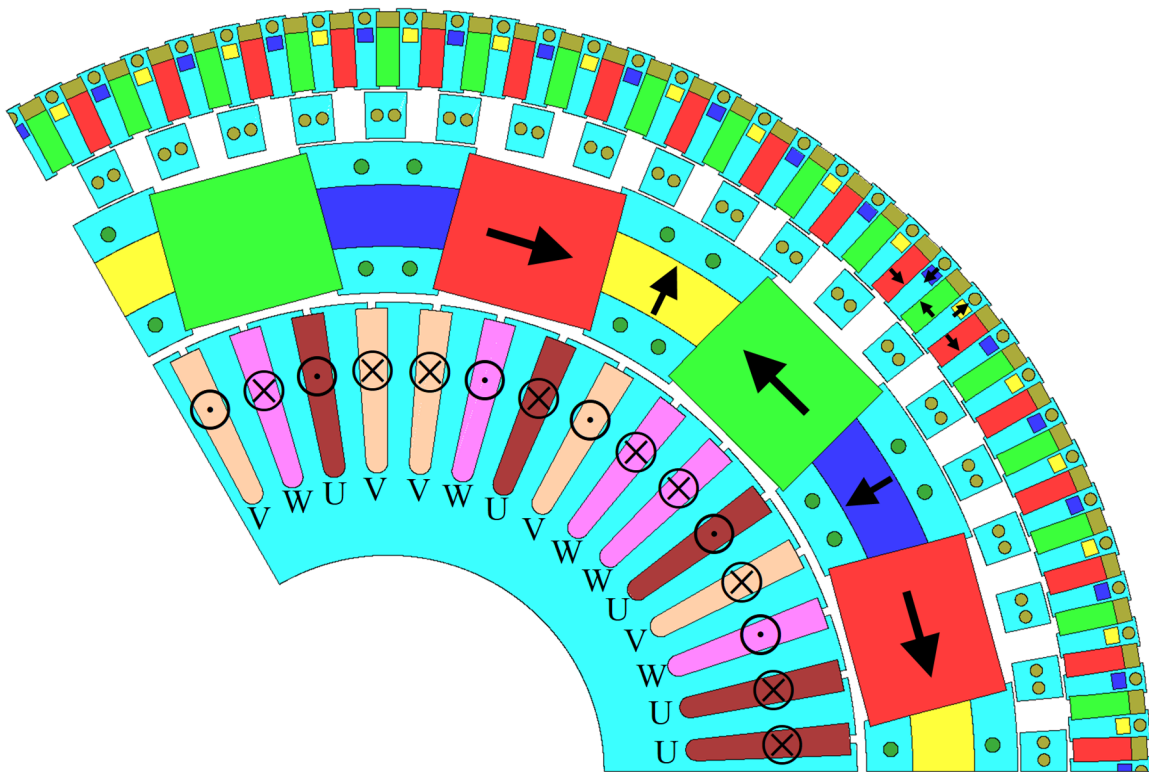
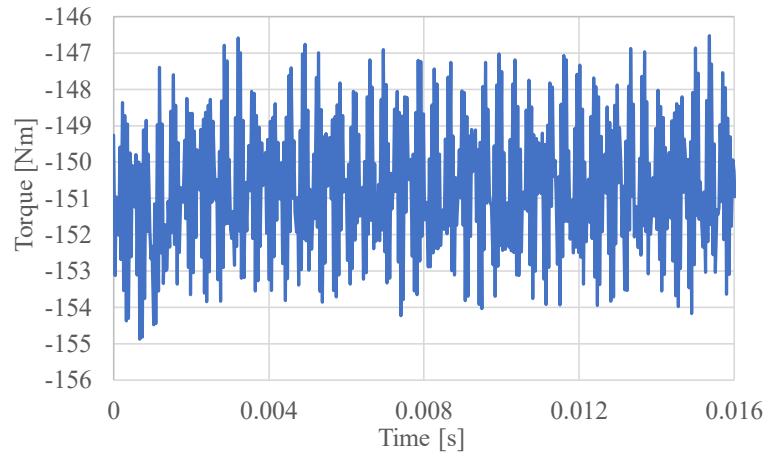


Figure 9-1. Stage 2 MG with stator which has 45 slots.



**Figure 9-2. Torque on the inner rotor.**

**Table 9-I. Parameters of the stator.**

Parameter	Value	Unit
Outer radius, $r_{so}$	152	mm
Inner radius, $r_{si}$	70	mm
Air gap	3	mm
Axial length	37.5	mm
Maximum current density	3.5	A/mm <sup>2</sup>
Winding fill factor	0.5	-

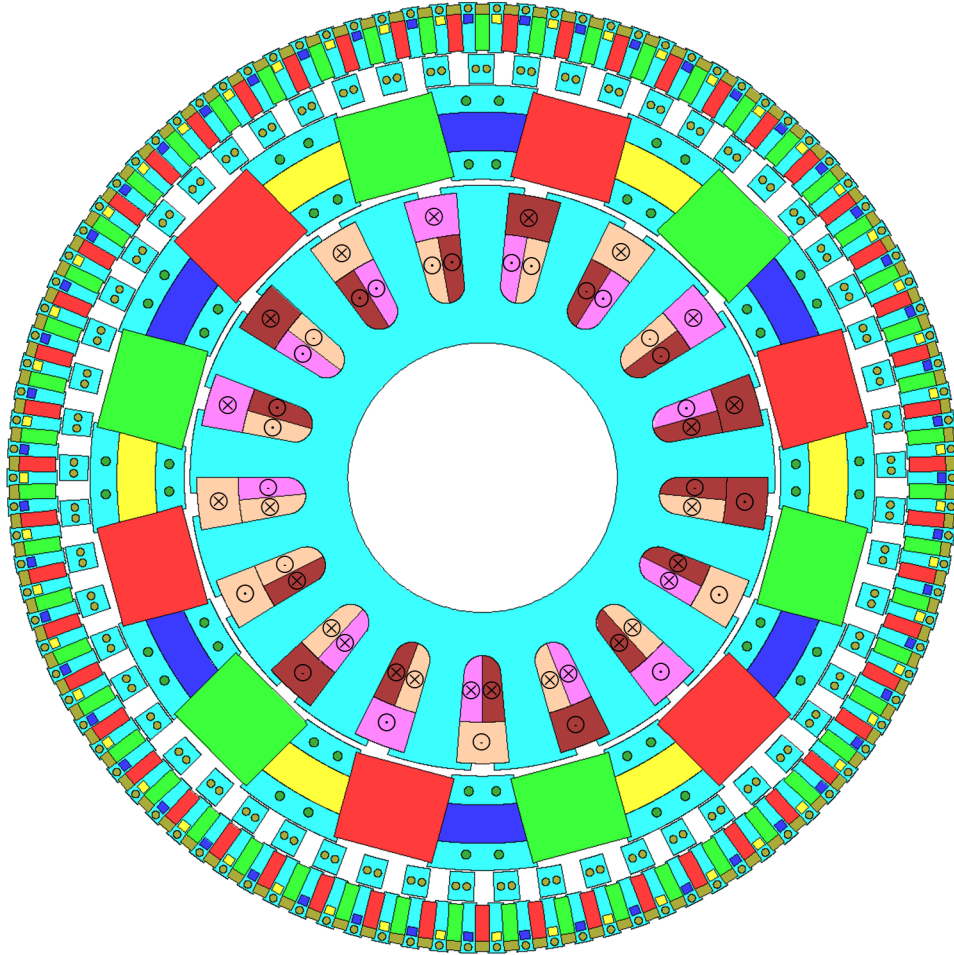


Figure 9-3. Stage 2 MG with stator which has 17 slots.

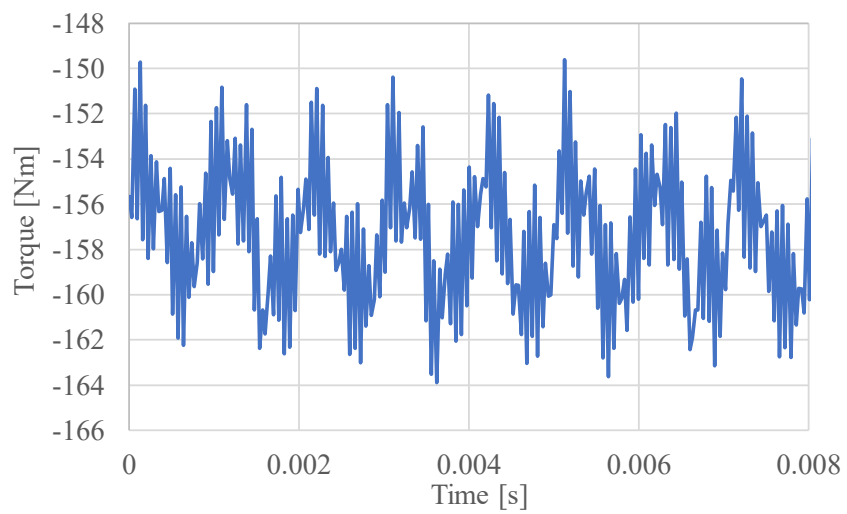


Figure 9-4. Torque on the inner rotor.

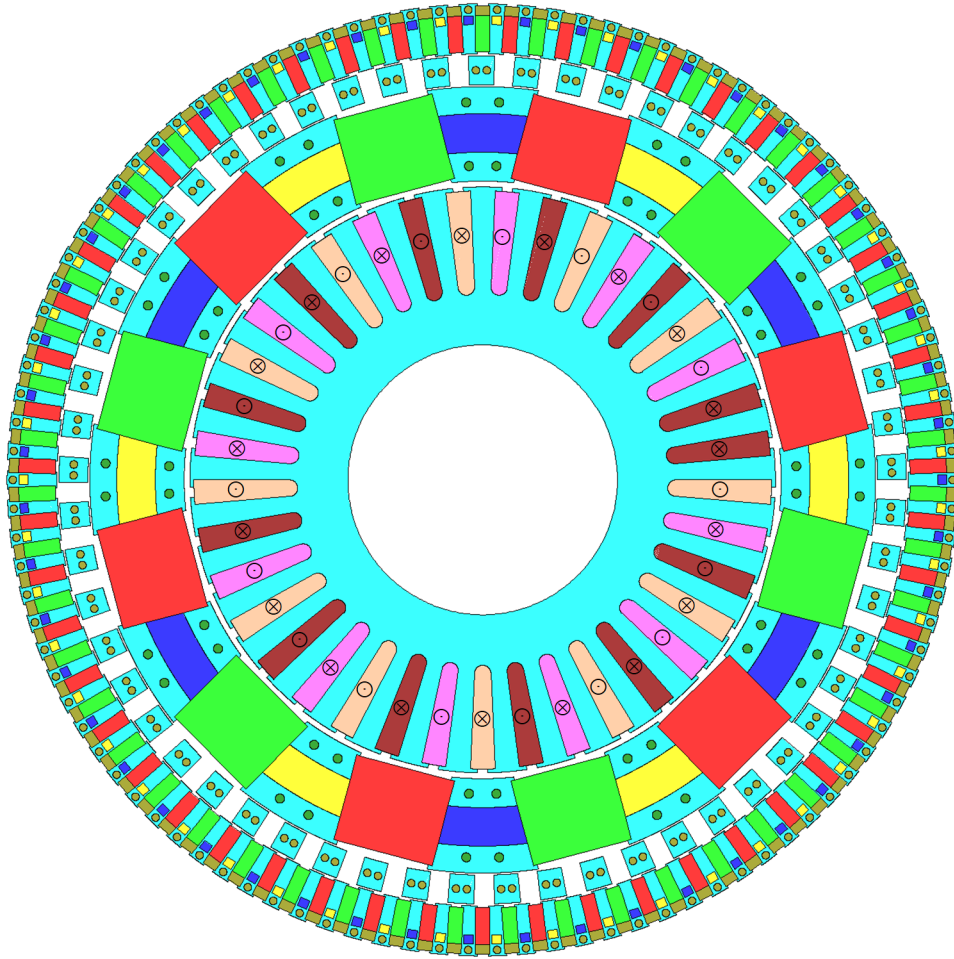


Figure 9-5. Stage 2 MG with stator which has 37 slots.

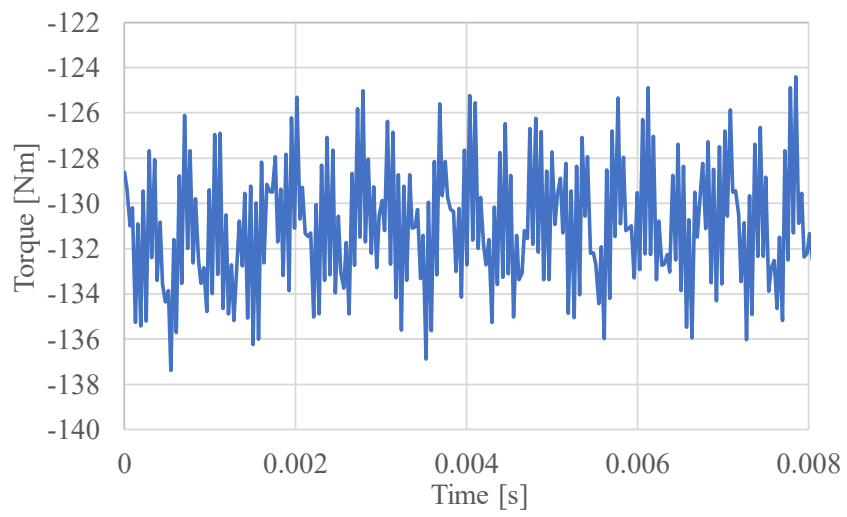


Figure 9-6. Torque on the inner rotor.

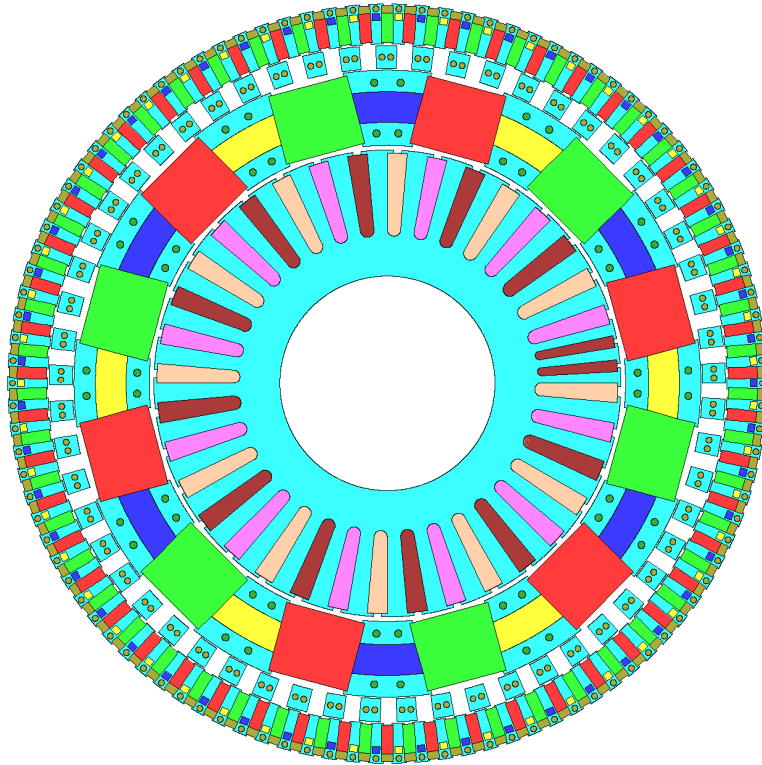


Figure 9-7. Stage 2 MG with stator which has 37 slots (ununiform teeth).

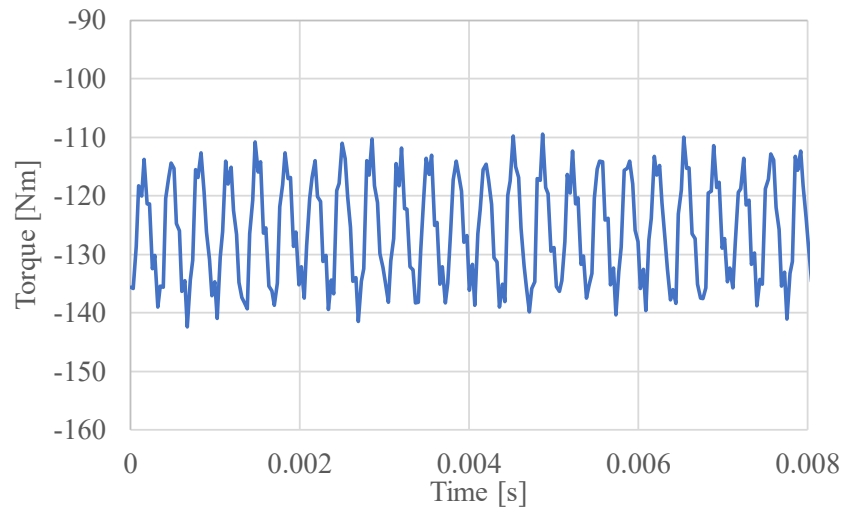


Figure 9-8. Torque on the inner rotor.

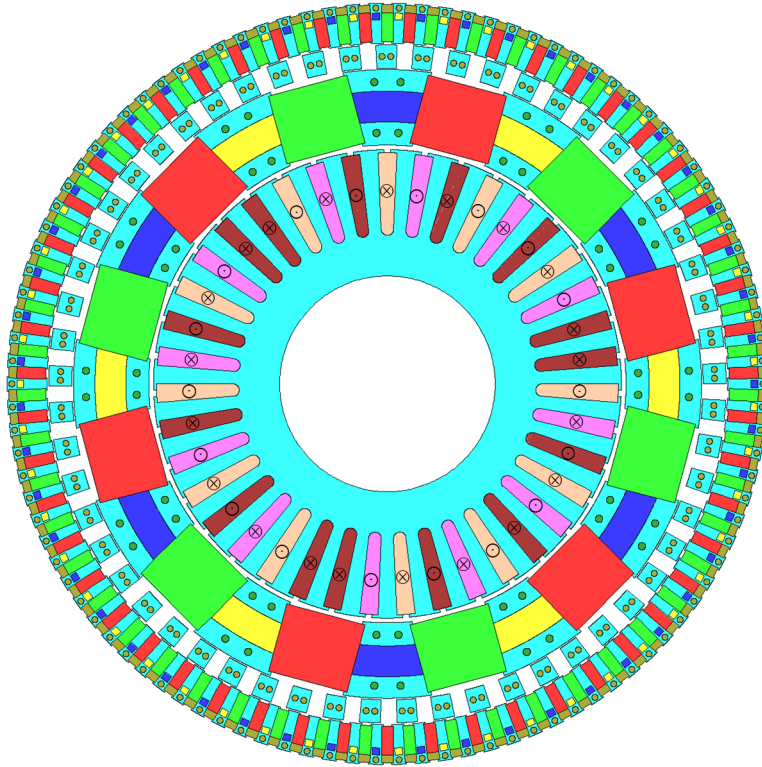


Figure 9-9. Stage 2 MG with stator which has 39 slots.

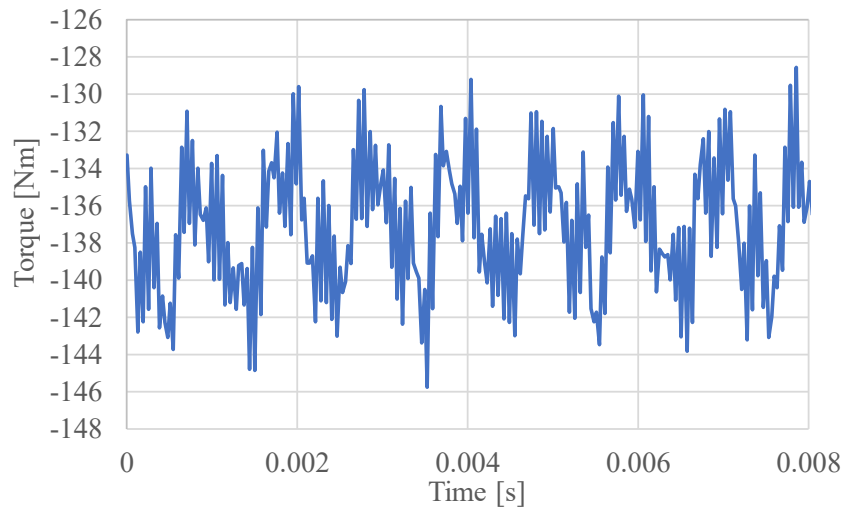


Figure 9-10. Torque on the inner rotor.

## 9.2 Winding function

The number of turns in each coil is  $N_l$  and the turns function is  $n(\theta)$  which gives the total number of turns in a span of  $\theta$  (starting from 0 degree). The winding function  $N(\theta)$ , is related to the turns function by

$$N(\theta) = n(\theta) - \langle n(\theta) \rangle \quad (2.2)$$

where  $\langle n(\theta) \rangle$  is the average of the turns function. The turns functions for the 45-slot design are shown in Figure 9-11-Figure 9-13. The winding functions are shown in Figure 9-14-Figure 9-16. When  $I_W = I_V = -0.5I_U$ , the combined winding function is shown in Figure 9-17. It can be clearly seen that 12 poles (6 pole pairs) is created by this winding distribution. Similarly, the combined winding functions for 17 slots, 37 slots and 39 slots are shown in Figure 9-18-Figure 9-20. For the 17-slot design, the combined winding function is not so sinusoidal which explains that it has the highest torque ripple.

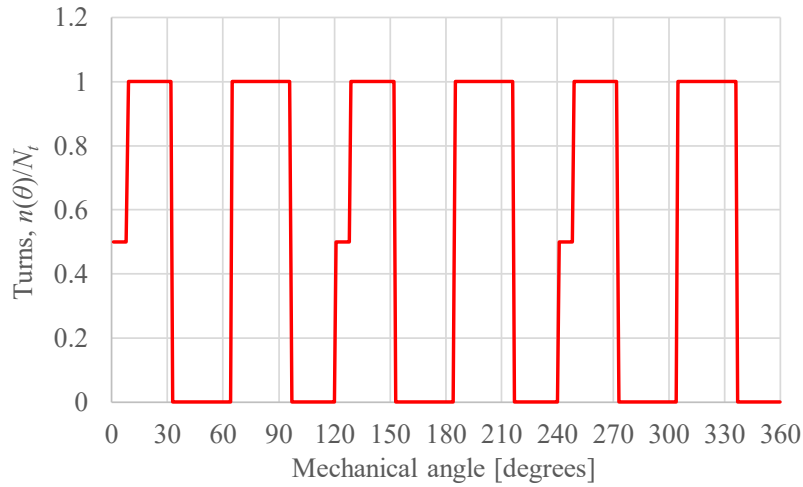


**Figure 9-11. The turns function for phase U with 45 slots.**

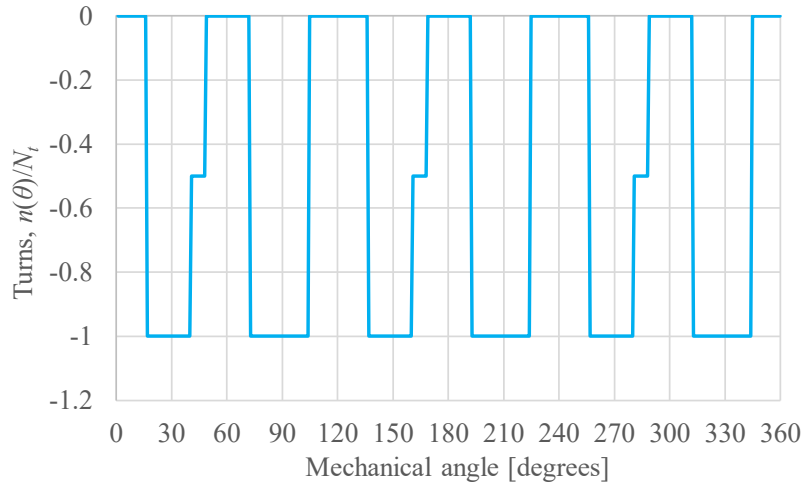


**Figure 9-12. The turns function for phase W with 45 slots.**

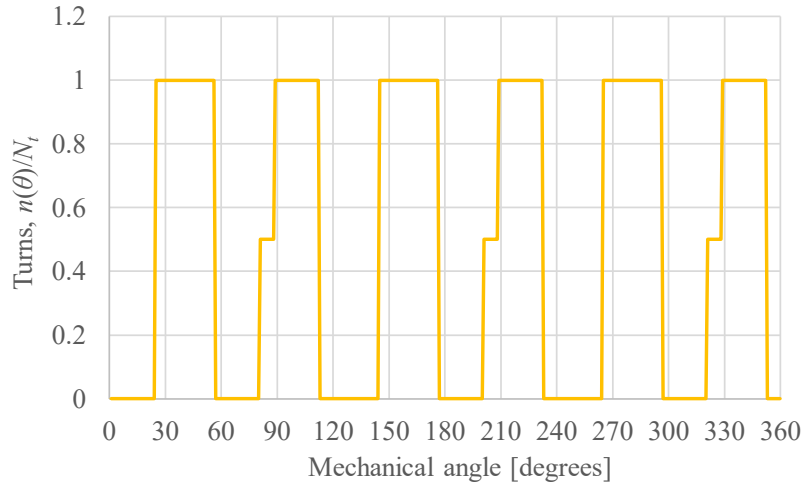


**Figure 9-13. The turns function for phase V with 45 slots.**

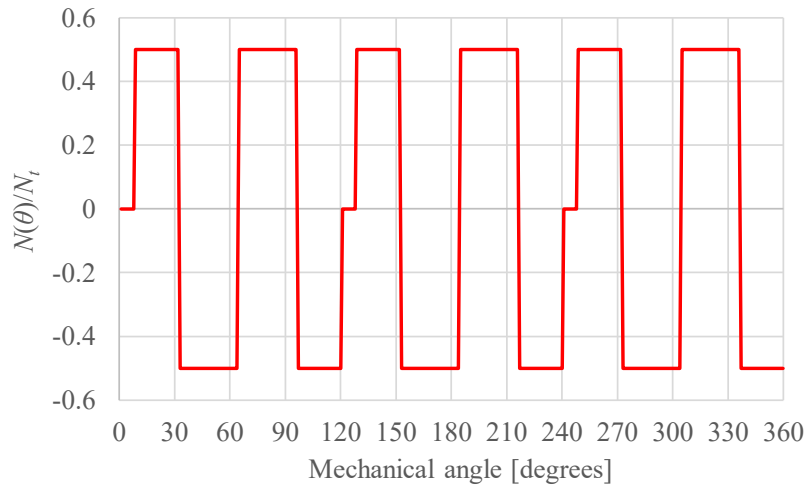


**Figure 9-14. The winding function for phase U with 45 slots.**

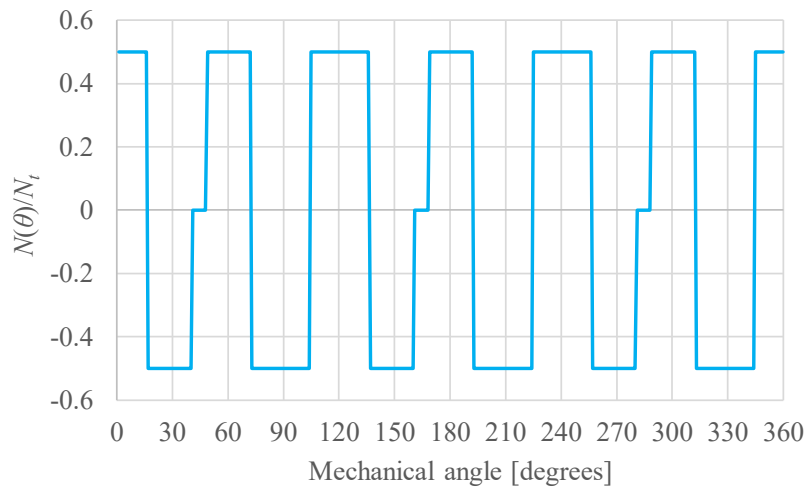


**Figure 9-15. The winding function for phase W with 45 slots.**

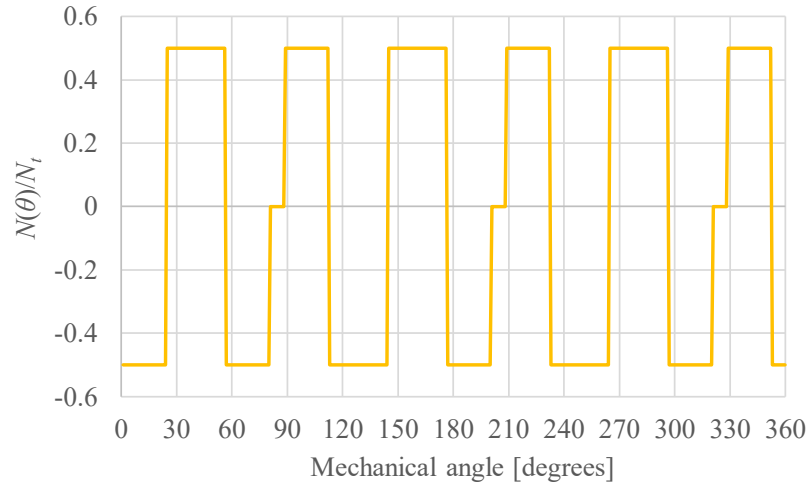


**Figure 9-16. The winding function for phase V with 45 slots.**

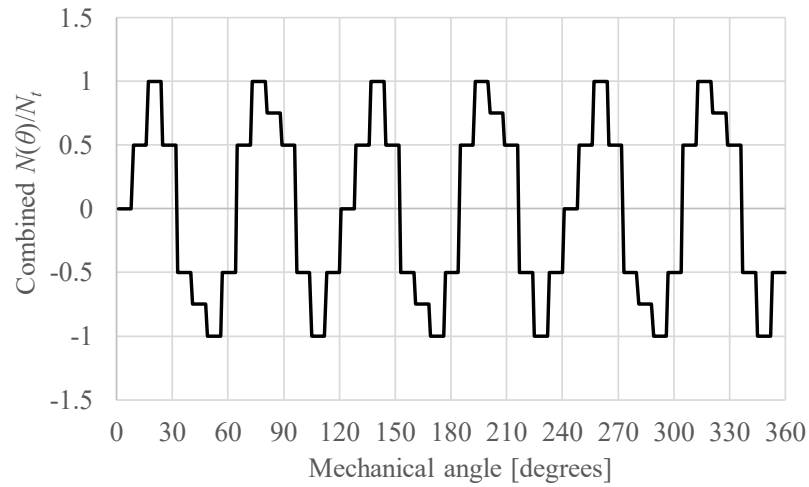


**Figure 9-17. The combined winding function with 45 slots.**

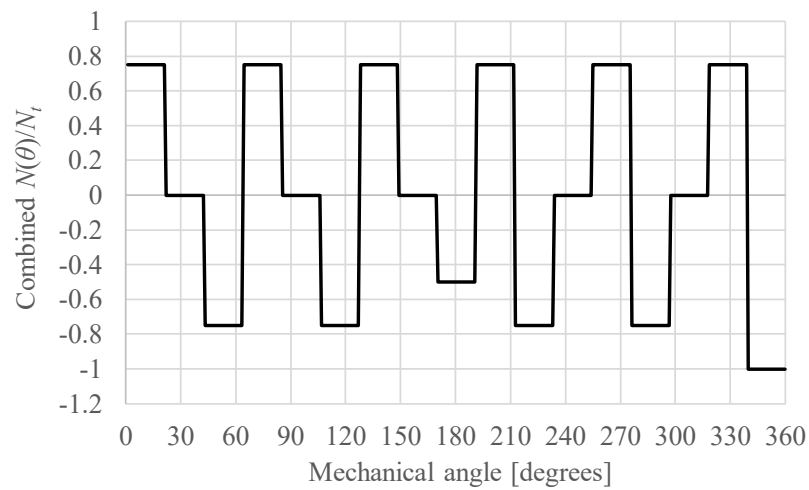


**Figure 9-18. The combined winding function with 17 slots.**

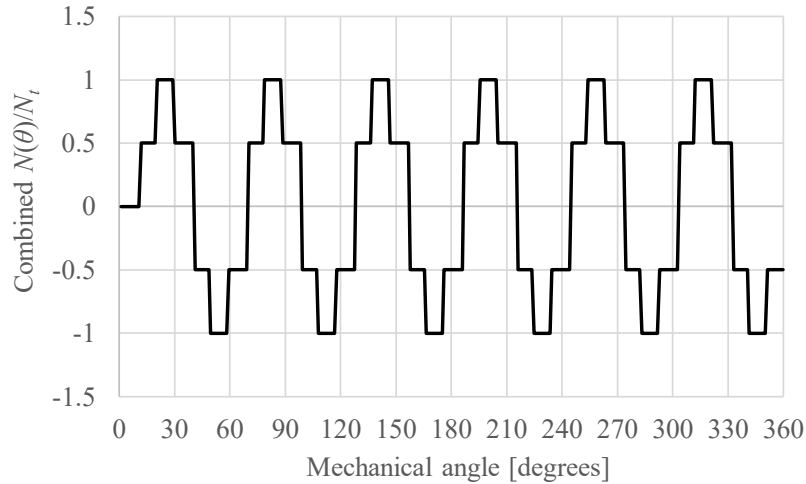


**Figure 9-19. The combined winding function with 37 slots.**

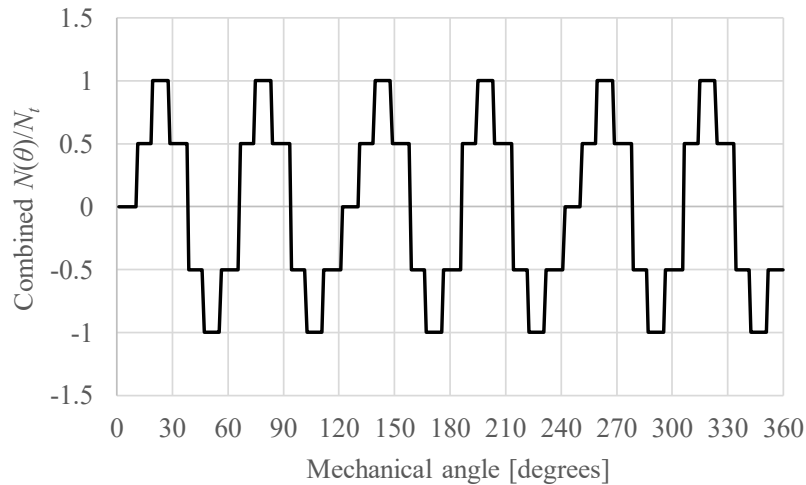


**Figure 9-20. The combined winding function with 39 slots.**

### 9.3 Performance comparison between different stator designs

The performance of different designs of stator has been summarized in Table 9-II. Stator with 37 slots can create the highest torque while stator with 45 slots has the lowest torque ripple on the inner rotor. The 45-slot design has been chosen because of the low torque ripple and as it is the only design which has a symmetric winding distribution. The span of the stator teeth lips,  $\theta_s$  has been varied to evaluate the torque and torque ripple variation. It is illustrated in Figure 9-21 and the results are shown in Table 9-III. There is no significant difference for the torque and torque ripple values. Therefore, the value of  $\theta_s$  is kept as 1.5 degrees.

**Table 9-II. Comparison of different designs of stator.**

Number of slots	Peak torque created by stator [Nm]	Torque ripple on the inner rotor [%]
45	95.4	5.55
17	92.5	9.06
37	117.2	9.92
37 (ununiform teeth)	133.1	25.5
39	113.4	12.52

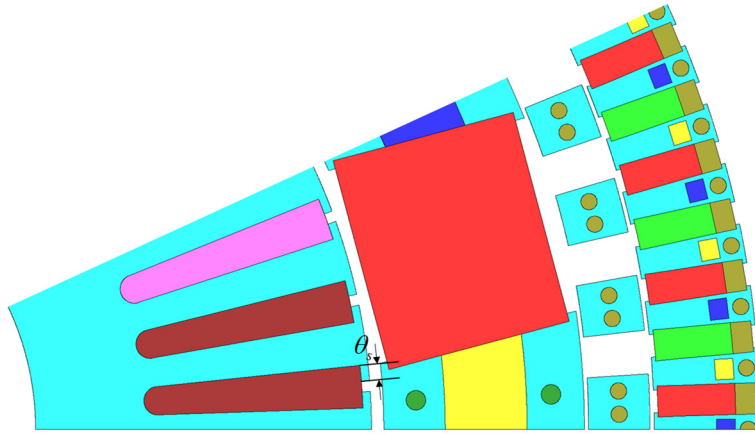


**Figure 9-21. Variation of the lips of the stator teeth.**

**Table 9-III. Performance comparison with different values of  $\theta_s$ .**

$\theta_s$ [degrees]	Peak torque created by stator [Nm]	Torque ripple on the inner rotor [%]
1.8	94.6	6.45
1.5 (original)	95.4	5.55
1.2	97.5	5.29
0.9	97.3	5.15
0.6	96.0	4.95

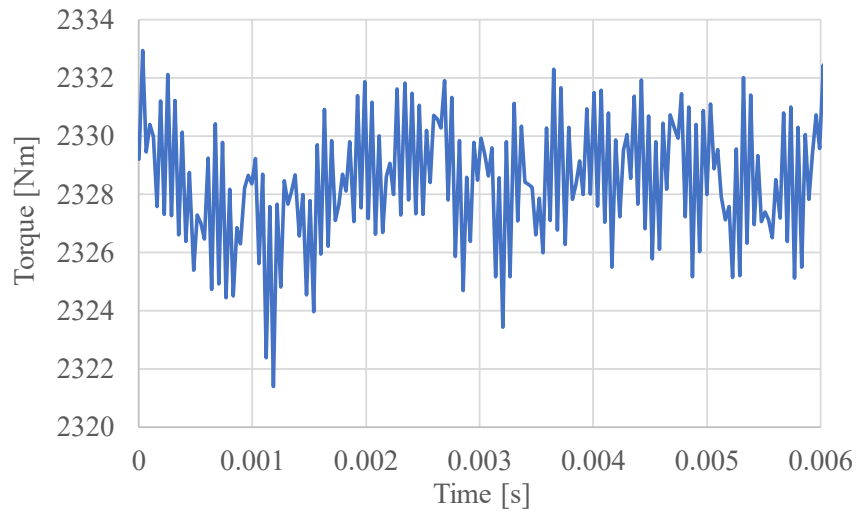


**Figure 9-22. Torque on the cage rotor.**

## 10. Cost of the Multistage Magnetic Gear

The mass of the stage 1 MG, stage 2 MG and MSMG have been estimated and the details are shown in Table 10-I.

**Table 10-I. Mass of the MSMG.**

Stage 1 MG		Value [kg]
Inner rotor	Lamination	14.14
	Magnets	28.55
	Rods	0.99
Cage rotor	Lamination	6.95
	Rods	0.14
Outer rotor	Lamination	7.38
	Magnets	8.31
	Rods	1.07
Total mass (stage 1)		67.53
Stage 2 MG		
Stator	Lamination	10.75
	Winding	6.86
Inner rotor	Lamination	3.99
	Magnets	11.03
	Rods	0.25
Cage rotor	Lamination	2.88
	Rods	0.05
Outer rotor	Lamination	4.41
	Magnets	4.84
	Rods	0.19
Total mass (stage 2)		45.25
Total mass (MSMG)		112.78

The estimated cost of the MSMG is summarized in Table 10-II and Figure 10-1. Most of the cost is from the lamination and the mechanical assembling parts.

**Table 10-II. Estimated cost of the MSMG.**

		Cost [\$]
Stage 1 MG	Magnets	3,500
	Lamination	29,000
	Endplates and rings	25,000
	Steel rods	3,600
	Plastic rods	900
Stage 2 MG	Magnets	1,500
	Lamination	20,000
	Endplates and rings	19,000
	Steel rods	1,000
	Plastic rods	900
Total		104,400

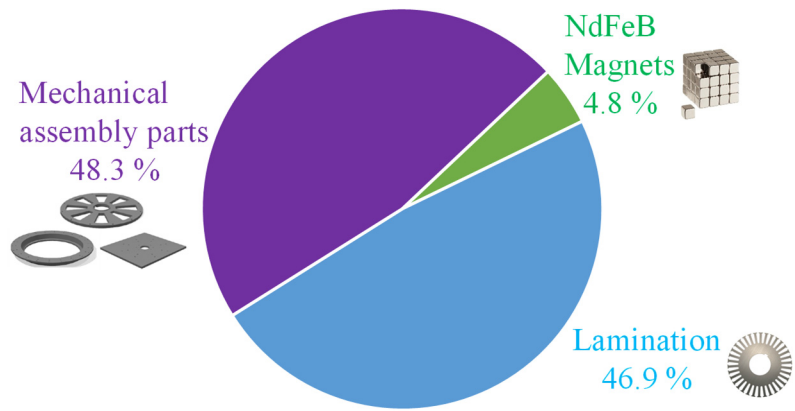


Figure 10-1. Cost of the MSMG.

## 11. Scaling Analysis

The performance of magnetic gearboxes has been compared with the mechanical 59:1 Sumitomo gearbox which is shown in Figure 11-1. The magnetic gear is competitive with a similar size mechanical gearbox.

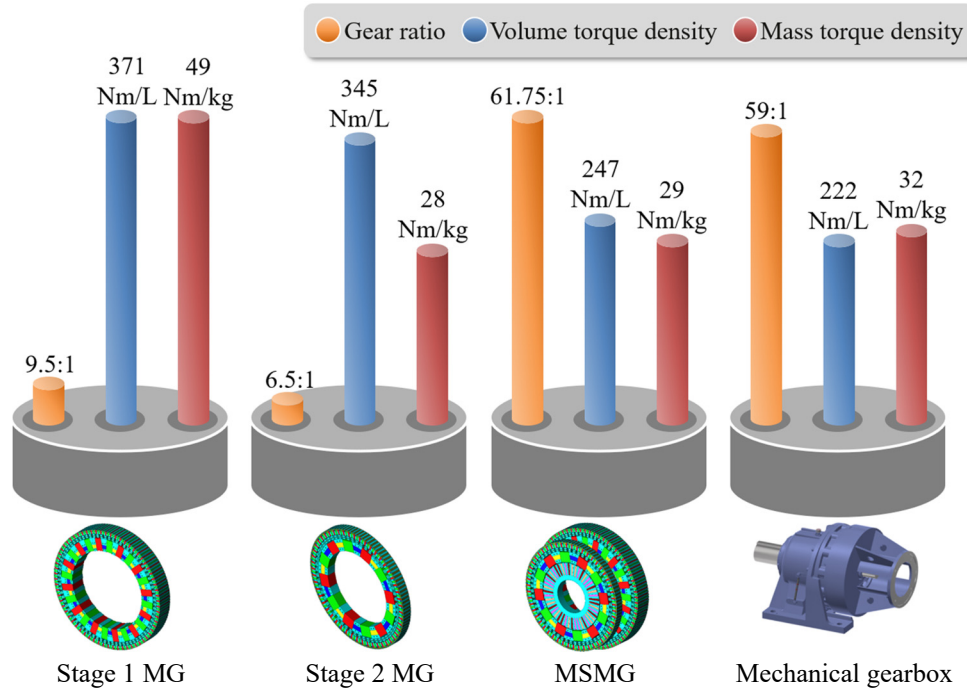


Figure 11-1. Comparison between the magnetic gearboxes and mechanical gearbox.

The scaling analysis has been done to evaluate the possibility to scale up to MW size. In this analysis, the number of pole pairs has been kept the same and the sizes of the rotors and the air gap have been scaled up by a scaling factor  $\gamma$ . The power is calculated when the cage rotor has a speed of 80 RPM and the results are given in Table 11-I and Figure 11-2. The MG is capable of achieving more than 3.5 MW when the outer radius is larger than 1.1 m. The volume torque density is almost the same with different scaling factor which means the power and torque are proportional of  $\gamma^3$ .

Table 11-I. Scaling analysis of stage 1 MG.

$\gamma$	Outer radius $r_{o3}$ [mm]	Axial length $d_1$ [mm]	Air gap $g$ [mm]	Torque [Nm]	Torque density [Nm/L]	Power [kW]
1 (original)	274	75	1	6560	371	55
1.1	301.4	82.5	1.1	8755	372	73
1.2	328.8	90	1.2	11324	370	95
1.3	356.2	97.5	1.3	14380	370	120
1.4	383.6	105	1.4	17979	370	151
1.5	411	112.5	1.5	22121	371	185
2	548	150	2	52349	370	439
3	822	225	3	176944	370	1482
4	1096	300	4	419878	371	3518

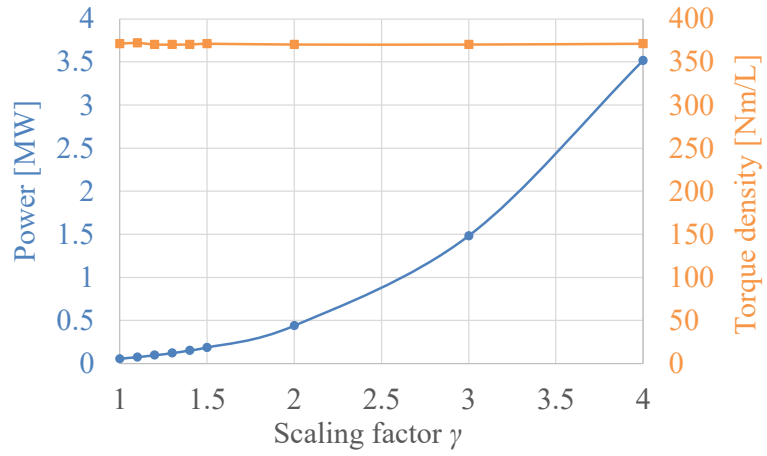


Figure 11-2. Scaling analysis of the stage 1 MG.

## **12. Summary and Future Work**

In this project, a MSMG with a gear ratio of 59:1 has been designed which can achieve a high torque and a high torque density. The magnetic gearbox also has the potential to achieve the MW size after conducting the scaling analysis. the overall performance is competitive with the conventional mechanical gearbox.

More research should be done before the MGs can be commercialized. The thermal analysis needs to be done to check the temperature of the magnets when rotating at a high speed. The material properties of different steels and magnets should be investigated when operating at high temperature conditions.